arXiv:1102.5300v2 [hep-lat] 22 Sep 2011

DESY 11-030
Edinburgh 2011/09
LTH 909
September 22, 2011

Flavour blindness and patterns of flavour symmetry breaking in lattice simulations of up, down and strange quarks

W. Bietenholz[a], V. Bornyakov[b], M. Göckeler[c], R. Horsley[d], W. G. Lockhart[e], Y. Nakamura[f], H. Perlt[g], D. Pleiter[h], P. E. L. Rakow[e], G. Schierholz[ci], A. Schiller[g], T. Streuer[c], H. Stüben[j], F. Winter[d] and J. M. Zanotti[d]

– QCDSF-UKQCD Collaboration –

[a] Instituto de Ciencias Nucleares, Universidad Autónoma de México, A.P. 70-543, C.P. 04510 Distrito Federal, Mexico

[b] Institute for High Energy Physics, 142281 Protovino, Russia and Institute of Theoretical and Experimental Physics, 117259 Moscow, Russia

[c] Institut für Theoretische Physik, Universität Regensburg, 93040 Regensburg, Germany

[d] School of Physics and Astronomy, University of Edinburgh, Edinburgh EH9 3JZ, UK

[e] Theoretical Physics Division, Department of Mathematical Sciences, University of Liverpool, Liverpool L69 3BX, UK

[f] RIKEN Advanced Institute for Computational Science, Kobe, Hyogo 650-0047, Japan

[g] Institut für Theoretische Physik, Universität Leipzig, 04109 Leipzig, Germany

[h] Deutsches Elektronen-Synchrotron DESY, 15738 Zeuthen, Germany

[i] Deutsches Elektronen-Synchrotron DESY, 22603 Hamburg, Germany

[j] Konrad-Zuse-Zentrum für Informationstechnik Berlin, 14195 Berlin, Germany

Abstract

QCD lattice simulations with 2+1 flavours (when two quark flavours are mass degenerate) typically start at rather large up-down and strange quark masses and extrapolate first the strange quark mass and then the up-down quark mass to its respective physical value. Here we discuss an alternative method of tuning the quark masses, in which the singlet quark mass is kept fixed. Using group theory the possible quark mass polynomials for a Taylor expansion about the flavour symmetric line are found, first for the general $1 + 1 + 1$ flavour case and then for the $2 + 1$ flavour case. This ensures that the kaon always has mass less than the physical kaon mass. This method of tuning quark masses then enables highly constrained polynomial fits to be used in the extrapolation of hadron masses to their physical values. Numerical results for the $2 + 1$ flavour case confirm the usefulness of this expansion and an extrapolation to the physical pion mass gives hadron mass values to within a few percent of their experimental values. Singlet quantities remain constant which allows the lattice spacing to be determined from hadron masses (without necessarily being at the physical point). Furthermore an extension of this programme to include partially quenched results is given.

Contents

1 Introduction **5**

2 Theory for $1+1+1$ flavours **6**
- 2.1 Singlet and non-singlet renormalisation . . . 7
- 2.2 General strategy . . . 8
- 2.3 Taylor expansion . . . 12
- 2.4 $\mathbf{O(a)}$ improvement of quark masses . . . 14
- 2.5 $\mathbf{SU(3)}$ and $\mathbf{S_3}$ classification of hadron mass matrices . . . 17
  - 2.5.1 The decuplet mass matrix . . . 18
  - 2.5.2 The octet mass matrix . . . 21

3 Theory for $2+1$ flavours **23**

4 Partial quenching **28**
- 4.1 PQ decuplet baryons . . . 29
- 4.2 PQ octet mesons . . . 32
- 4.3 PQ octet baryons . . . 33
- 4.4 Generalising a constant $\overline{\mathbf{m}}$ formula . . . 35
- 4.5 The usefulness of PQ . . . 35

5 Applications to chiral perturbation theory **37**
- 5.1 Decuplet baryon masses at $\mathbf{O(m_q^{3/2})}$ . . . 37
- 5.2 Relationships between expansion coefficients . . . 38
- 5.3 Chiral non-analytic behaviour . . . 39

6 The path to the physical point **40**

7 The lattice – generalities **41**
- 7.1 Lattice simulations . . . 41
- 7.2 $\mathbf{O(a)}$ improvement of the coupling constant . . . 43
- 7.3 Hadron 'sources' and 'sinks' . . . 43

8 The lattice – results **45**
- 8.1 Locating $\kappa_{\mathbf{0}}$ and the $\mathbf{m_s^R}$–$\mathbf{m_l^R}$ plane . . . 45
- 8.2 Determination of $\kappa_{\mathbf{0;c}}$, $\alpha_{\mathbf{Z}}$ . . . 47
- 8.3 Singlet quantities and the scale . . . 48
  - 8.3.1 Finite size effects . . . 49
  - 8.3.2 Scale estimation . . . 51

9 Spectrum results for $2+1$ flavours **53**
- 9.1 Experimental values . . . 53
- 9.2 Mass hierarchy . . . 54

9.3 'Fan' plots 54
9.4 Partially quenched results 59

10 Conclusions **61**

A The permutation group $\mathbf{S_3}$ **65**
A.1 Singlet representation $\mathbf{A_1}$ 65
A.2 Singlet representation $\mathbf{A_2}$ 66
A.3 Doublet representation $\mathbf{E}$ 66

B Some group theory **67**
B.1 Flavour permutations, $\mathbf{S_3}$, as a subgroup of $\mathbf{SU(3)}$ 68
B.2 Group classification of quark mass polynomials 69
B.3 Matrix representations of $\mathbf{SU(3)}$ 72
B.4 Hadron mass matrices 74

C Coordinate choice for partially quenched formulae **76**

D The action **78**

E Hadron masses **80**

1 Introduction

The QCD interaction is flavour blind. Neglecting electromagnetic and weak interactions, the only difference between quark flavours comes from the quark mass matrix, which originates from the coupling to the Higgs field. We investigate here how flavour blindness constrains hadron masses after flavour $SU(3)$ symmetry is broken by the mass difference between the strange and light quarks. The flavour structure illuminates the pattern of symmetry breaking in the hadron spectrum and helps us extrapolate $2+1$ flavour lattice data to the physical point. (By $2+1$ we mean that the u and d quarks are mass degenerate.)

We have our best theoretical understanding when all 3 quark flavours have the same masses (because we can use the full power of flavour $SU(3)$ symmetry); nature presents us with just one instance of the theory, with $m_s^R/m_l^R \approx 25$ (where the superscript ^{R} denotes the renormalised mass). We are interested in interpolating between these two cases. We consider possible behaviours near the symmetric point, and find that flavour blindness is particularly helpful if we approach the physical point, denoted by (m_l^{R*}, m_s^{R*}), along a path in the m_l^R–m_s^R plane starting at a point on the $SU(3)$ flavour symmetric line $(m_l^R = m_s^R = m_0^R)$ and holding the sum of the quark masses $\overline{m}^R = \frac{1}{3}(m_u^R + m_d^R + m_s^R) \equiv \frac{1}{3}(2m_l^R + m_s^R)$ constant [1], at the value m_0^R as sketched in Fig. 1. The usual procedure (path)

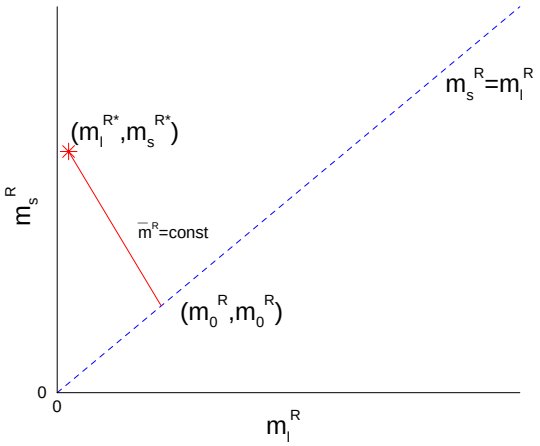


Figure 1: Sketch of the path (red, solid line) in the m_l^R–m_s^R plane to the physical point denoted by (m_l^{R*}, m_s^{R*}). The dashed diagonal line is the $SU(3)$-symmetric line.

is to estimate the physical strange quark mass and then try to keep it fixed, i.e. m_s^R = constant, as the light quark mass is reduced towards its physical value. However on that path the problem is that the kaon mass[1] is always larger than its physical value. Choosing instead a path such that the singlet quark mass is

[1]In this article quark masses will be denoted by m, and hadron masses by M.

kept fixed has the advantage that we can vary both quark masses over a wide range, with the kaon mass always being lighter than its physical value along the entire trajectory. Starting from the symmetric point when masses are degenerate is particularly useful for strange quark physics as we can track the development of the strange quark mass. Also if we extend our measurements beyond the symmetric point we can investigate a world with heavy up-down quarks and a lighter strange quark.

The plan of this article is as follows. Before considering the $2+1$ quark flavour case, we consider the more general $1+1+1$ case in section 2. This also includes a discussion of the renormalisation of quark masses for non-chiral fermions. Keeping the singlet quark mass constant constrains the extrapolation and in particular it is shown in this section that flavour singlet quantities remain constant to leading order when extrapolating from a flavour symmetric point. This motivates investigating possible quark mass polynomials – we are able to classify them here to third order in the quark masses under the $SU(3)$ and S_3 (flavour) groups. In section 3 we specialise to $2+1$ flavours and give quark mass expansions to second order for the pseudoscalar and vector meson octets and baryon octet and decuplet. (The relation of this expansion to chiral perturbation theory is discussed later in section 5.) In section 4 we extend the formalism to the partially quenched case (when the valence quarks of a hadron do not have to have the same mass as the sea quarks). This is potentially useful as the same expansion coefficients occur, which could allow a cheaper determination of them. We then turn to more specific lattice considerations in sections 6, 7 with emphasis on clover fermions (i.e. non-chiral fermions) used here. This is followed by section 8, which first gives numerical results for the constant singlet quark mass results used here. Flavour singlet quantities prove to be a good way of defining the scale and the consistency of some choices is discussed. We also investigate possible finite size effects. Finally in section 9 the numerical results for the hadron mass spectrum are presented in the form of a series of 'fan' plots where the various masses fan out from their common value at the symmetric point. Our conclusions are given in section 10. Several Appendices provide some group theory background for this article, discuss the action used here and give tables of the hadron masses found.

Mostly we restrict ourselves to the constant surface. However, in a few sections, we also consider variations in $\overline{m}^R$ (for example in the derivation of the quark mass expansion polynomials, section 2.3, the discussion of $O(a)$ improvement in section 2.4, and in section 4.4 where we generalise a constant $\overline{m}^R$ formula).

2 Theory for $1+1+1$ flavours

Our strategy is to start from a point with all three sea quark masses equal,

$$m_u^R = m_d^R = m_s^R \equiv m_0^R \,, \tag{1}$$

and extrapolate towards the physical point, $(m_u^{R*}, m_d^{R*}, m_s^{R*})$, keeping the average sea quark mass

$$\overline{m}^R = \tfrac{1}{3}(m_u^R + m_d^R + m_s^R)\,, \tag{2}$$

constant at the value m_0^R. For this trajectory to reach the physical point we have to start at a point where $m_0^R \approx \frac{1}{3} m_s^{R*}$. As we approach the physical point, the u and d quarks become lighter, but the s quark becomes heavier. Pions are decreasing in mass, but K and η increase in mass as we approach the physical point.

2.1 Singlet and non-singlet renormalisation

Before developing the theory, we first briefly comment on the renormalisation of the quark mass. While for chiral fermions the renormalised quark mass is directly proportional to the bare quark mass, $m_q^R = Z_m m_q$, the problem, at least for Wilson-like fermions which have no chiral symmetry, is that singlet and non-singlet quark mass can renormalise differently [2, 3][2]

$$m_q^R = Z_m^{NS}(m_q - \overline{m}) + Z_m^S \overline{m}\,, \qquad q = u, d, s\,, \tag{3}$$

where m_q are the bare quark masses,

$$\overline{m} = \tfrac{1}{3}(m_u + m_d + m_s)\,, \tag{4}$$

Z_m^{NS} is the non-singlet renormalisation constant, and Z_m^S is the singlet renormalisation constant (both in scheme R). It is often convenient to re-write eq. (3) as

$$m_q^R = Z_m^{NS}(m_q + \alpha_Z \overline{m})\,, \tag{5}$$

where

$$\alpha_Z = r_m - 1\,, \quad r_m = \frac{Z_m^S}{Z_m^{NS}}\,, \tag{6}$$

represents the fractional difference between the renormalisation constants. (Numerically we will later see that this factor α_Z is $\sim O(1)$, and is thus non-negligible at our coupling.) This then gives

$$\overline{m}^R = Z_m^{NS}(1 + \alpha_Z)\overline{m}\,. \tag{7}$$

This means that even for Wilson-type actions it does not matter whether we keep the bare or renormalised average sea quark mass constant. Obviously eq. (7) also holds for a reference point (m_0, m_0, m_0) on the flavour symmetric line, i.e.

$$m_0^R = Z_m^S m_0 = Z_m^{NS}(1 + \alpha_Z) m_0\,. \tag{8}$$

[2] Perturbative computations showing this effect, which starts at the two-loop order, are given in [4, 5].

Furthermore introducing the notation

$$\delta m_q^R \equiv m_q^R - \overline{m}^R\,, \qquad \delta m_q \equiv m_q - \overline{m}\,, \qquad q = u, d, s\,, \tag{9}$$

for both renormalised and bare quark masses, we find that

$$\delta m_q^R = Z_m^{NS}\,\delta m_q\,. \tag{10}$$

So by keeping the singlet mass constant we avoid the need to use two different Zs and as we will be considering expansions about a flavour symmetric point, they will be similar using either the renormalised or bare quark masses. (Of course the value of the expansion parameters will be different, but the structure of the expansion will be the same.) We shall discuss this point a little further in section 2.4.

So in the following we need not usually distinguish between bare and renormalised quark masses.

Note that it follows from the definition that

$$\delta m_u + \delta m_d + \delta m_s = 0\,, \tag{11}$$

so we could eliminate one of these symbols. However we shall keep all three symbols as we can then write some expressions in a more obviously symmetrical form.

2.2 General strategy

With this notation, the quark mass matrix is

$$\begin{aligned}
\mathcal{M} &= \begin{pmatrix} m_u & 0 & 0 \\ 0 & m_d & 0 \\ 0 & 0 & m_s \end{pmatrix} \\
&= \overline{m} \begin{pmatrix} 1 & 0 & 0 \\ 0 & 1 & 0 \\ 0 & 0 & 1 \end{pmatrix} \\
&\quad + \tfrac{1}{2}(\delta m_u - \delta m_d) \begin{pmatrix} 1 & 0 & 0 \\ 0 & -1 & 0 \\ 0 & 0 & 0 \end{pmatrix} + \tfrac{1}{2}\delta m_s \begin{pmatrix} -1 & 0 & 0 \\ 0 & -1 & 0 \\ 0 & 0 & 2 \end{pmatrix}\,.
\end{aligned} \tag{12}$$

The mass matrix $\mathcal{M}$ has a singlet part (proportional to I) and an octet part, proportional to λ_3, λ_8. We argue here that the theoretically cleanest way to approach the physical point is to keep the singlet part of $\mathcal{M}$ constant, and vary only the non-singlet parts.

An important advantage of our strategy is that it strongly constrains the possible mass dependence of physical quantities, and so simplifies the extrapolation towards the physical point. Consider a flavour singlet quantity, which we

shall denote by X_S, at a symmetric point (m_0, m_0, m_0). Examples are the scale[3] $X_r = r_0^{-1}$, or the plaquette P (this will soon be generalised to other singlet quantities). If we make small changes in the quark masses, symmetry requires that the derivatives at the symmetric point are equal

$$\frac{\partial X_S}{\partial m_u} = \frac{\partial X_S}{\partial m_d} = \frac{\partial X_S}{\partial m_s}\,. \tag{13}$$

So if we keep $m_u + m_d + m_s$ constant, then any arbitrary small changes in the quark masses mean that $\Delta m_s + \Delta m_u + \Delta m_d = 0$ so

$$\Delta X_S = \frac{\partial X_S}{\partial m_u}\Delta m_u + \frac{\partial X_S}{\partial m_d}\Delta m_d + \frac{\partial X_S}{\partial m_s}\Delta m_s = 0\,. \tag{14}$$

The effect of making the strange quark heavier exactly cancels the effect of making the light quarks lighter, so we know that X_S must be stationary at the symmetrical point. This makes extrapolations towards the physical point much easier, especially since we find that in practice quadratic terms in the quark mass expansion are very small. Any permutation of the quarks, such as an interchange $u \leftrightarrow s$, or a cyclic permutation $u \to d \to s \to u$ does not change the physics, it just renames the quarks. Any quantity unchanged by all permutations will be flat at the symmetric point, like X_r.

We can also construct permutation-symmetric combinations of hadrons. For orientation in Fig. 2 we give the octet multiplets for spin 0 (pseudoscalar) and

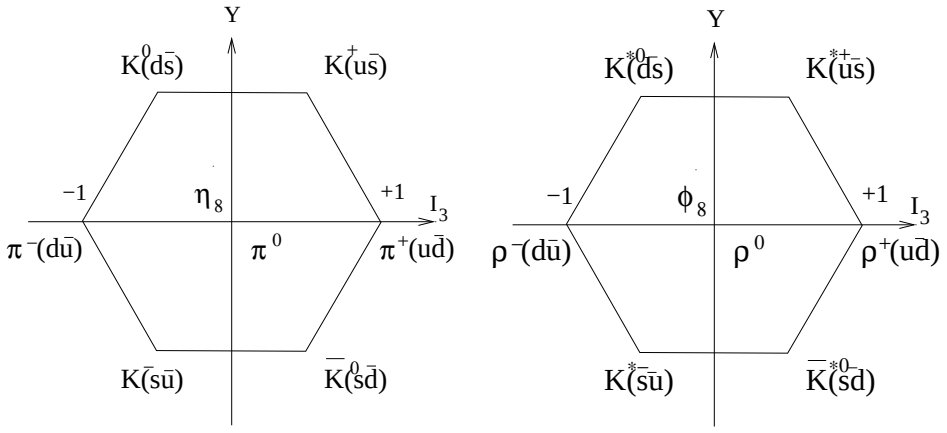


Figure 2: The octets for spin 0 (pseudoscalar) and spin 1 (vector) mesons (plotted in the I_3–Y plane). η_8 and ϕ_8 are pure octet states, ignoring any mixing with the singlet mesons.

spin 1 (vector) mesons and in Fig. 3 the lowest octet and decuplet multiplets for

[3]There is no significance here to using r_0 or r_0^{-1}; however defining $X_r = r_0^{-1}$ is more consistent with later definitions.

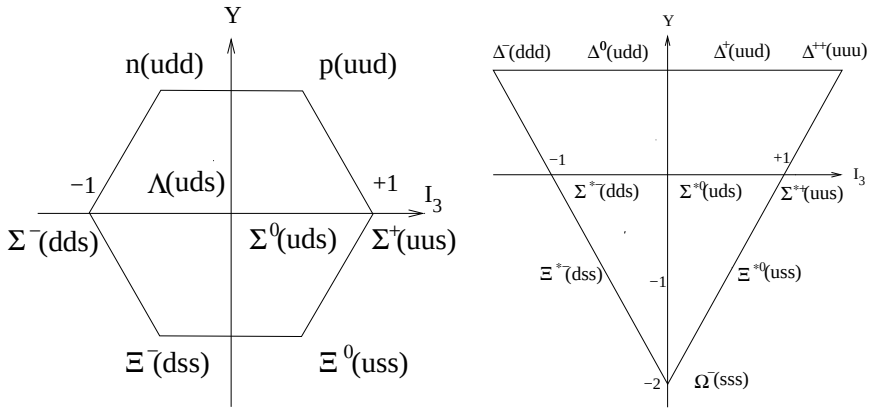


Figure 3: The lowest octet and decuplet for the spin $\frac{1}{2}$ and for the spin $\frac{3}{2}$ baryons.

the spin $\frac{1}{2}$ and for the spin $\frac{3}{2}$ baryons (all plotted in the I_3–Y plane).

For example, for the decuplet, any permutation of the quark labels will leave the $\Sigma^{*0}(uds)$ unchanged, so the Σ^{*0} is shown by a single black (square) point in Fig. 4. On the other hand, a permutation (such as $u \to d \to s$) can change a

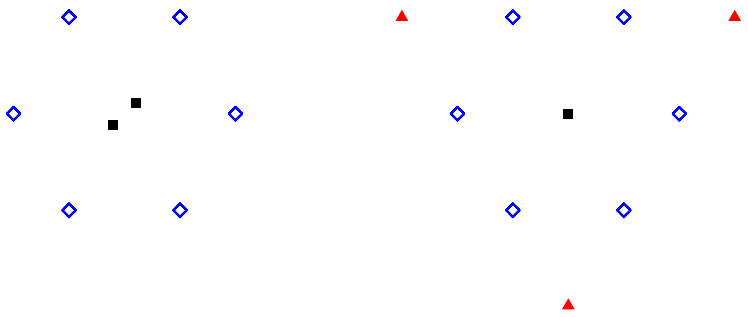


Figure 4: The behaviour of the octet and decuplet under the permutation group S_3. The colours denote sets of particles which are invariant under permutations of the quark flavours (red or filled triangles, blue or open diamonds and black or filled squares).

$\Delta^{++}(uuu)$ into a $\Delta^{-}(ddd)$ or (if repeated) into an $\Omega^{-}(sss)$, so these three particles form a set of baryons which is closed under quark permutations, and are all given the same colour red (triangle) in Fig. 4. Finally the 6 baryons containing two quarks of one flavour, and one quark of a different flavour, form an invariant set, shown in blue (diamond) in Fig. 4.

If we sum the masses in any of these sets, we get a flavour symmetric quantity, which will obey the same argument we gave in eq. (14) for the quark mass (in)dependence of the scale r_0. We therefore expect that the Σ^{*0} mass must be flat at the symmetric point, and furthermore that the combinations

$(M_{\Delta^{++}} + M_{\Delta^-} + M_{\Omega^-})$ and $(M_{\Delta^+} + M_{\Delta^0} + M_{\Sigma^{*+}} + M_{\Sigma^{*-}} + M_{\Xi^{*0}} + M_{\Xi^{*-}})$ will also be flat. Technically these symmetrical combinations are in the A_1 singlet representation of the permutation group S_3. This is the symmetry group of an equilateral triangle, C_{3v}. This group has 3 irreducible representations, [6], two different singlets, A_1 and A_2 and a doublet E, with elements E^+ and E^-. Some details of this group and its representations are given in Appendix A, while Table 1 gives a summary of the transformations.

	A_1	E		A_2
Operation		E^+	E^-	
Identity	+	+	+	+
$u \leftrightarrow d$	+	+	−	−
$u \leftrightarrow s$	+	mix		−
$d \leftrightarrow s$	+	mix		−
$u \to d \to s \to u$	+	mix		+
$u \to s \to d \to u$	+	mix		+

Table 1: A simplified table showing how the group operations of S_3 act in the different representations: + refers to unchanged; − refers to states that are odd under the group operation.

We list some of these invariant mass combinations in Table 2. The permuta-

Pseudoscalar	$X_\pi^2 = \frac{1}{6}(M_{K^+}^2 + M_{K^0}^2 + M_{\pi^+}^2 + M_{\pi^-}^2 + M_{\overline{K}^0}^2 + M_{K^-}^2)$	blue
mesons	$X_{\eta_8}^2 = \frac{1}{2}(M_{\pi^0}^2 + M_{\eta_8}^2)$	black
Vector	$X_\rho = \frac{1}{6}(M_{K^{*+}} + M_{K^{*0}} + M_{\rho^+} + M_{\rho^-} + M_{\overline{K}^{*0}} + M_{K^{*-}})$	blue
mesons	$X_{\phi_8} = \frac{1}{2}(M_{\rho^0} + M_{\phi_8})$	black
	$X_{\phi_s} = \frac{1}{3}(2M_{\rho^0} + M_{\phi_s})$	
Octet	$X_N = \frac{1}{6}(M_p + M_n + M_{\Sigma^+} + M_{\Sigma^-} + M_{\Xi^0} + M_{\Xi^-})$	blue
baryons	$X_\Lambda = \frac{1}{2}(M_\Lambda + M_{\Sigma^0})$	black
Decuplet	$X_\Delta = \frac{1}{3}(M_{\Delta^{++}} + M_{\Delta^-} + M_{\Omega^-})$	red
baryons	$X_{\Xi^*} = \frac{1}{6}(M_{\Delta^+} + M_{\Delta^0} + M_{\Sigma^{*+}} + M_{\Sigma^{*-}} + M_{\Xi^{*0}} + M_{\Xi^{*-}})$	blue
	$X_{\Sigma^*} = M_{\Sigma^{*0}}$	black

Table 2: Permutation invariant mass combinations, see Fig. 4. ϕ_s is a fictitious $s\overline{s}$ particle; η_8 and ϕ_8 are pure octet mesons. The colours in the third column correspond to Fig. 4.

tion group S_3 yields a lot of useful relations, but cannot capture the entire structure. For example, there is no way to make a connection between the $\Delta^{++}(uuu)$ and the $\Delta^+(uud)$ by permuting quarks. To go further, we need to classify phys-

ical quantities by $SU(3)$ (containing the permutation group S_3 as a subgroup), which we shall consider now.

2.3 Taylor expansion

We want to describe how physical quantities depend on the quark masses. To do this we will Taylor expand about a symmetric reference point

$$(m_u, m_d, m_s) = (m_0, m_0, m_0)\,. \tag{15}$$

Our results will be polynomials in the quark masses, we will express them in terms of $\overline{m}$ and δm_q of eq. (9). The main idea is to classify all possible mass polynomials by their transformation properties under the permutation group S_3 and under the full flavour group $SU(3)$, and classify hadronic observables in the same way. $\overline{m}$ and δm_q are a natural basis to choose as $\overline{m}$ is purely singlet and δm_q is non-singlet. The alternative $m_q - m_0$ would be less useful as it contains a mixture of singlet and non-singlet quantities.

The Taylor expansion of a given observable can only include the polynomials of the same symmetry as the observable. The Taylor expansions of hadronic quantities in the same $SU(3)$ multiplet but in different S_3 representations will have related expansion coefficients. (We will show examples of the latter, e.g. in eqs. (31)–(33).)

While we can always arrange polynomials to be in definite permutation group states, when we get to polynomials of $O(\delta m_q^2)$ we find that a polynomial may be a mixture of several $SU(3)$ representations, but the classification is still useful. In Table 3 we classify all the polynomials which could occur in a Taylor expansion about the symmetric point, eq. (15), up to $O(\delta m_q^3)$.

Many of the polynomials in the table have factors of $(\overline{m} - m_0)$. These polynomials drop out if we restrict ourselves to the surface of constant $\overline{m} = m_0$, leaving only the polynomials marked with a tick (✓) in Table 3. At $O(m_q^k)$ there are $k+1$ independent polynomials needed to describe functions on the constant $\overline{m}$ surface (the polynomials with the ticks), but $\frac{1}{2}(k+1)(k+2)$ polynomials needed if the constraint $\overline{m}$ = constant is dropped (all polynomials, with and without ticks). Thus the advantage of working in the constant $\overline{m}$ surface increases as we proceed to higher order in m_q.

Since we are keeping $\overline{m}$ constant, we are only changing the octet part of the mass matrix in eq. (12). Therefore, to first order in the mass change, only octet quantities can be affected. $SU(3)$ singlets have no linear dependence on the quark mass, as we have already seen by the symmetry argument eq. (14), but we now see that all quantities in $SU(3)$ multiplets higher than the octet cannot have linear terms. This provides a constraint on the hadron masses within a multiplet and leads (as we shall see) to the Gell-Mann–Okubo mass relations [7, 8].

When we proceed to quadratic polynomials we can construct polynomials which transform like mixtures of the 1, 8 and 27 multiplets of $SU(3)$, see Table 3.

Polynomial		S_3	$SU(3)$				
1	✓	A_1	1				
$(\overline{m} - m_0)$		A_1	1				
δm_s	✓	E^+		8			
$(\delta m_u - \delta m_d)$	✓	E^-		8			
$(\overline{m} - m_0)^2$		A_1	1				
$(\overline{m} - m_0)\delta m_s$		E^+		8			
$(\overline{m} - m_0)(\delta m_u - \delta m_d)$		E^-		8			
$\delta m_u^2 + \delta m_d^2 + \delta m_s^2$	✓	A_1	1			27	
$3\delta m_s^2 - (\delta m_u - \delta m_d)^2$	✓	E^+		8		27	
$\delta m_s(\delta m_d - \delta m_u)$	✓	E^-		8		27	
$(\overline{m} - m_0)^3$		A_1	1				
$(\overline{m} - m_0)^2\delta m_s$		E^+		8			
$(\overline{m} - m_0)^2(\delta m_u - \delta m_d)$		E^-		8			
$(\overline{m} - m_0)(\delta m_u^2 + \delta m_d^2 + \delta m_s^2)$		A_1	1			27	
$(\overline{m} - m_0)\left[3\delta m_s^2 - (\delta m_u - \delta m_d)^2\right]$		E^+		8		27	
$(\overline{m} - m_0)\delta m_s(\delta m_d - \delta m_u)$		E^-		8		27	
$\delta m_u \delta m_d \delta m_s$	✓	A_1	1			27	64
$\delta m_s(\delta m_u^2 + \delta m_d^2 + \delta m_s^2)$	✓	E^+		8		27	64
$(\delta m_u - \delta m_d)(\delta m_u^2 + \delta m_d^2 + \delta m_s^2)$	✓	E^-		8		27	64
$(\delta m_s - \delta m_u)(\delta m_s - \delta m_d)(\delta m_u - \delta m_d)$	✓	A_2		10	$\overline{10}$		64

Table 3: All the quark-mass polynomials up to $O(m_q^3)$, classified by symmetry properties. A tick (✓) marks the polynomials relevant on a constant $\overline{m}$ surface. These polynomials are plotted in Fig. 6. If we want to make an expansion valid when $\overline{m}$ varies, then all the polynomials in the table (with and without ticks) are needed.

Further representations, namely the 10, $\overline{10}$ and 64, first occur when we look at cubic polynomials in the quark masses, see again Table 3.

In a little more detail, constructing polynomials with a definite S_3 classification is fairly straightforward, we have to see what happens to each polynomial under simple interchanges (e.g. $u \leftrightarrow d$) and cyclic permutations (e.g. $u \to s$, $s \to d$, $d \to u$). The S_3 column of Table 3 is easy to check by hand. The $SU(3)$ assignment of polynomials is less straightforward. Only the simplest polynomials belong purely to a single $SU(3)$ multiplet; most polynomials contain mixtures of several multiplets. The non-singlet mass is an octet of $SU(3)$, so quadratic polynomials in δm_q can contain representations which occur in $8 \otimes 8$, cubic polynomials representations which occur in $8 \otimes 8 \otimes 8$. We can find out which representations are present in a given polynomial by using the Casimir operators of $SU(3)$ [9, 10]. That operator was programmed in Mathematica, and used to analyse our polynomial basis. Some more details are presented in Appendix B

(in section B.2). The results of the calculation are recorded in the $SU(3)$ section of Table 3.

The allowed quark mass region on the $\overline{m}$ = constant surface is an equilateral triangle, as shown in Fig. 5. Plotting the polynomials of Table 3 across this triangular region then gives the plots in Fig. 6, where the colour coding indicates whether the polynomial is positive (red) or negative (blue).

As a first example of the use of these tables, consider the Taylor expansion for the scale r_0/a up to cubic order in the quark masses. As discussed previously, this is a gluonic quantity, blind to flavour, so it has symmetry A_1 under the S_3 permutation group. Therefore its Taylor expansion only contains polynomials of symmetry A_1. If we keep $\overline{m}$, the average quark mass, fixed, the expansion of r_0/a must take the form

$$\frac{r_0}{a} = \alpha + \beta(\delta m_u^2 + \delta m_d^2 + \delta m_s^2) + \gamma\, \delta m_u \delta m_d \delta m_s \,, \tag{16}$$

with just 3 coefficients. Interestingly, we could find all 3 coefficients from $2+1$ data, so we would be able to predict $1{+}1{+}1$ flavour results from fits to $2{+}1$ data. This is common. If we allow $\overline{m}$ to vary too, we would need 7 coefficients to give a cubic fit for r_0 (all the A_1 polynomials in Table 3 both ticked and unticked). This point is further discussed in section 4.4. If we did not have any information on the flavour symmetry of r_0 we would need all the polynomials in Table 3, which would require 20 coefficients.

2.4 O(a) improvement of quark masses

Before classifying the hadron mass matrix, we pause and consider the $O(a)$ improvement of quark masses. (If we are considering chiral fermions, we have 'automatic $O(a)$ improvement', see e.g. [11] for a discussion.) In writing down expressions for bare and improved quark masses, it is natural to expand about the chiral point, all three quarks massless, which means setting $m_0 = 0$ in the expressions in Table 3. Later, when we consider lattice results, we want to expand around a point where we can run simulations, so we will normally have a non-zero m_0.

Improving the quark masses requires us to add improvement terms of the type am_q^2 to the bare mass. We can add $SU(3)$-singlet improvement terms to the singlet quark mass, $SU(3)$-octet improvement terms to the non-singlet quark mass. We are led to the following expressions for the improved and renormalised quark masses

$$\begin{aligned} \overline{m}^R &= Z_m^S \left[\overline{m} + a\left\{b_1 \overline{m}^2 + b_2(\delta m_s^2 + \delta m_u^2 + \delta m_d^2)\right\}\right] \\ \delta m_s^R &= Z_m^{NS} \left[\delta m_s + a\left\{b_3 \overline{m}\delta m_s + b_4(3\delta m_s^2 - (\delta m_u - \delta m_d)^2)\right\}\right] \,, \end{aligned} \tag{17}$$

together with $Z_m^S = Z_m^{NS} r_m$, eqs. (5), (6). We have improved $\overline{m}^R$ by adding the two possible singlet terms from the quadratic section of Table 3, and improved

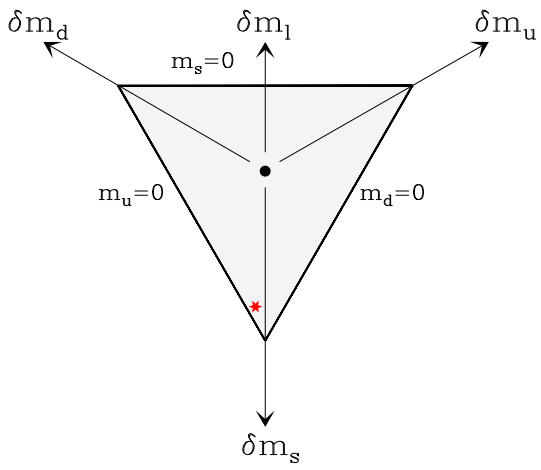


Figure 5: The allowed quark mass region on the $\overline{m}$ = constant surface is an equilateral triangle. The black point at the centre is the symmetric point, the red star is the physical point. $2+1$ simulations lie on the vertical symmetry axis. The physical point is slightly off the $2+1$ axis because $m_d > m_u$.

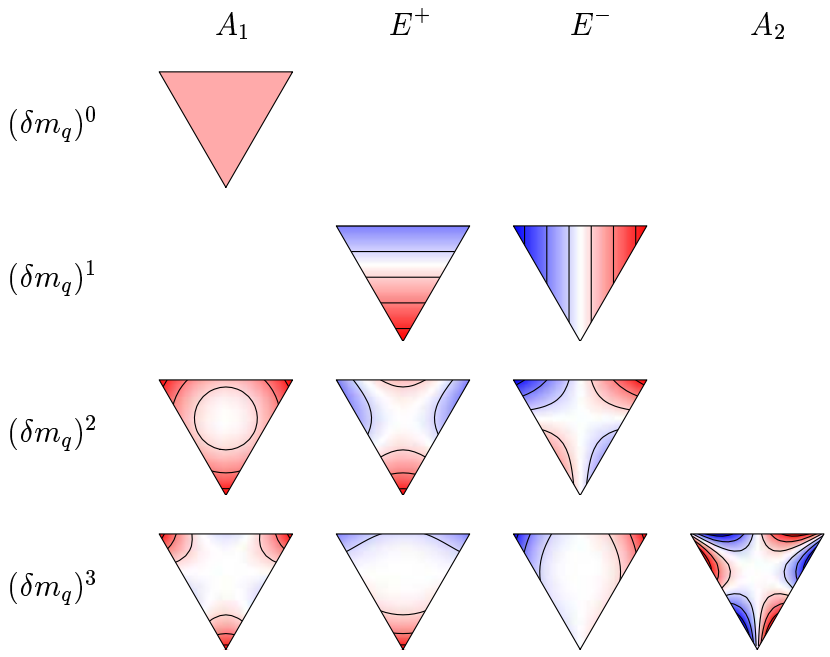


Figure 6: Contour plots of the polynomials relevant for the constant $\overline{m}$ Taylor expansion, see Table 3. A red(dish) colour denotes a positive number while a blue(ish) colour indicates a negative number. If $m_u = m_d$ (the $2+1$ case), only the polynomials in the A_1 and E^+ columns contribute. Each triangle in this figure uses the coordinate system explained in Fig. 5.

δm_s^R by adding the two possible E^+ octet polynomials. Note that if we keep $\overline{m}$ constant, we only need to consider the improvement terms b_2 and b_4. The b_1 and b_3 terms could be absorbed into the Z factors. Simplifications of this sort are very common if $\overline{m}$ is kept fixed.

We get expressions for the u and d quark mass improvement by flavour-permuting eq. (17)

$$\begin{aligned}
\delta m_u^R &= Z_m^{NS}\left[\delta m_u + a\left\{b_3\overline{m}\delta m_u + b_4(3\delta m_u^2 - (\delta m_s - \delta m_d)^2)\right\}\right] \\
\delta m_d^R &= Z_m^{NS}\left[\delta m_d + a\left\{b_3\overline{m}\delta m_d + b_4(3\delta m_d^2 - (\delta m_s - \delta m_u)^2)\right\}\right] \\
\delta m_u^R - \delta m_d^R &= Z_m^{NS}\left[\delta m_u - \delta m_d\right. \\
&\qquad \left. + a\left\{b_3\overline{m}(\delta m_u - \delta m_d) + 6b_4\delta m_s(\delta m_d - \delta m_u)\right\}\right] .
\end{aligned} \tag{18}$$

The improvement terms for $\delta m_u - \delta m_d$ are proportional to the two E^-, $SU(3)$-octet, quadratic polynomials. (We have to use the identity, eq. (11), to bring the result to the desired form – which will often be the case in what follows.)

Table 3 is based purely on flavour arguments, we would hope that all the results are true whether we use bare or renormalised quantities, and also independently of whether we work with a naive bare mass, or a bare mass with $O(a)$ improvement terms. Let us check if this is true. The first thing we need to know is whether the zero-sum identity eq. (11) survives renormalisation and improvement. Using the previous equations we find

$$\begin{aligned}
\delta m_u^R + \delta m_d^R + \delta m_s^R &= Z_m^{NS}\left[(\delta m_u + \delta m_d + \delta m_s)\right. \\
&\qquad + a\left\{b_3\overline{m}(\delta m_u + \delta m_d + \delta m_s)\right. \\
&\qquad\quad \left.\left. + b_4(\delta m_u + \delta m_d + \delta m_s)^2\right\}\right] \\
&= 0 ,
\end{aligned} \tag{19}$$

showing that eq. (11) is not violated by improvement or renormalisation.

The next point we want to check is if the symmetry of a polynomial depends on whether we expand in terms of improved or unimproved masses. As an example, let us look at the quadratic polynomial

$$\delta m_s^R(\delta m_d^R - \delta m_u^R) , \tag{20}$$

which has permutation symmetry E^-, and $SU(3)$ content octet and 27-plet. Expanding to first order in the lattice spacing a we find

$$\begin{aligned}
\delta m_s^R(\delta m_d^R - \delta m_u^R) &= (Z_m^{NS})^2\left[\delta m_s(\delta m_d - \delta m_u)\right. \\
&\qquad + a\left\{2b_3\overline{m}\delta m_s(\delta m_d - \delta m_u)\right. \\
&\qquad\quad \left.\left. + \ 2b_4(\delta m_u - \delta m_d)(\delta m_u^2 + \delta m_d^2 + \delta m_s^2)\right\}\right] .
\end{aligned} \tag{21}$$

The mass improvement terms have generated two extra cubic polynomials, but they are both polynomials with the same symmetry as the initial polynomial.

The same holds for the other quadratic terms. This shows that Table 3 applies both to improved and unimproved masses.

Thus our conclusion is that the flavour expansion results are true whether we use bare or renormalised quantities, and also independently of whether we work with a naive bare mass, or a bare mass with $O(a)$ improvement terms.

Finally we compare these results with those obtained in [12], to see whether we can match the 4 improvement terms found in eq. (17) to the 4 terms introduced there, namely

$$\begin{aligned} m_q^R &= Z_m^{NS}\left[m_q + (r_m - 1)\overline{m}\right. \\ &\qquad \left. + a\left\{b_m m_q^2 + 3\overline{b}_m m_q \overline{m} + (r_m d_m - b_m)\overline{m^2} + 3(r_m \overline{d}_m - \overline{b}_m)\overline{m}^2\right\}\right] , \end{aligned} \tag{22}$$

where $\overline{m^2} = \frac{1}{3}(m_u^2 + m_d^2 + m_s^2)$. At first this looks different from eq. (17), but this is just due to a different choice of basis polynomials. The quadratic polynomials in eq. (22) are simple linear combinations of those in eq. (17).

From eq. (17) we have

$$\begin{aligned} m_s^R &= \delta m_s^R + \overline{m}^R \\ &= Z_m^{NS}\left[m_s + (r_m - 1)\overline{m} + a\left\{b_3 \overline{m}\delta m_s + b_4(3\delta m_s^2 - (\delta m_u - \delta m_d)^2)\right.\right. \\ &\qquad \left.\left. + r_m b_1 \overline{m}^2 + r_m b_2(\delta m_s^2 + \delta m_u^2 + \delta m_d^2)\right\}\right] , \end{aligned} \tag{23}$$

so we now equate the terms to those in eq. (22). We must first re-write

$$3\delta m_s^2 - (\delta m_u - \delta m_d)^2 = 6\left[m_s^2 - 2\overline{m}m_s - \overline{m^2} + 2\overline{m}^2\right] , \tag{24}$$

so

$$\begin{aligned} m_s^R &= Z_m^{NS}\left[m_s + (r_m - 1)\overline{m}\right. \\ &\qquad + a\left\{b_3 \overline{m}(m_s - \overline{m}) + 6b_4(m_s^2 - 2\overline{m}m_s - \overline{m^2} + 2\overline{m}^2)\right. \\ &\qquad \left.\left. + r_m b_1 \overline{m}^2 + 3r_m b_2(\overline{m^2} - \overline{m}^2)\right\}\right] , \end{aligned} \tag{25}$$

which gives the results

$$\begin{array}{rclcrcl} b_m &=& 6b_4 & & b_1 &=& 3\overline{d}_m + d_m \\ \overline{b}_m &=& \frac{1}{3}b_3 - 4b_4 & , \quad \text{or} \quad & b_2 &=& \frac{1}{3}d_m \\ d_m &=& 3b_2 & & b_3 &=& 3\overline{b}_m + 2b_m \\ \overline{d}_m &=& \frac{1}{3}b_1 - b_2 & & b_4 &=& \frac{1}{6}b_m \end{array} . \tag{26}$$

2.5 SU(3) and S_3 classification of hadron mass matrices

In eq. (12) we split the quark mass matrix into a singlet part and two octet parts. We want to make a similar decomposition of the hadron mass matrices. We start with the decuplet mass matrix because it is simpler than the octet mass matrix.

2.5.1 The decuplet mass matrix

The decuplet mass matrix is a 10×10 diagonal matrix. From $SU(3)$ group algebra we know

$$10 \otimes \overline{10} = 1 \oplus 8 \oplus 27 \oplus 64\,. \tag{27}$$

The singlet matrix is the identity matrix, the octet representation contains 2 diagonal matrices (λ_3 and λ_8), the 27-plet has 3 diagonal matrices, and the 64-plet includes 4 diagonal matrices, see Fig. 7. This gives us a basis of 10 diagonal

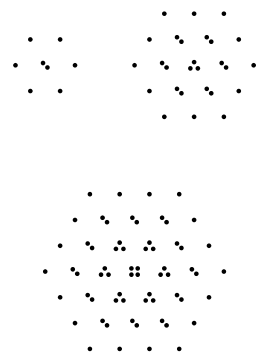


Figure 7: An illustration of the octet, 27-plet and 64-plet representations of $SU(3)$. The number of spots in the central location gives the number of flavour-conserving operators in each multiplet. In the octet, the 2 operators form an E doublet of the permutation group. In the 27-plet the 3 operators are an A_1 singlet and an E doublet. In the 64-plet the centre operators are an A_1 singlet, an E doublet and an A_2 singlet.

matrices, into which we can decompose the decuplet mass matrix.

We can use the Casimir operator to project out the diagonal matrices in a particular $SU(3)$ representation (see Appendix B.3 for a fuller discussion). As an example of a matrix with pure octet symmetry, we can take the operator $2I_3$. (We have multiplied I_3 by 2 simply to avoid having fractions in the matrix.) Since we know the isospins of all the decuplet baryons, we can write down

$$\begin{array}{c} \Delta^- \;\; \Delta^0 \;\; \Delta^+ \;\; \Delta^{++} \; \Sigma^{*-} \;\; \Sigma^{*0} \;\; \Sigma^{*+} \;\; \Xi^{*-} \;\; \Xi^{*0} \;\; \Omega^- \\ \begin{pmatrix} -3 & 0 & 0 & 0 & 0 & 0 & 0 & 0 & 0 & 0 \\ 0 & -1 & 0 & 0 & 0 & 0 & 0 & 0 & 0 & 0 \\ 0 & 0 & 1 & 0 & 0 & 0 & 0 & 0 & 0 & 0 \\ 0 & 0 & 0 & 3 & 0 & 0 & 0 & 0 & 0 & 0 \\ 0 & 0 & 0 & 0 & -2 & 0 & 0 & 0 & 0 & 0 \\ 0 & 0 & 0 & 0 & 0 & 0 & 0 & 0 & 0 & 0 \\ 0 & 0 & 0 & 0 & 0 & 0 & 2 & 0 & 0 & 0 \\ 0 & 0 & 0 & 0 & 0 & 0 & 0 & -1 & 0 & 0 \\ 0 & 0 & 0 & 0 & 0 & 0 & 0 & 0 & 1 & 0 \\ 0 & 0 & 0 & 0 & 0 & 0 & 0 & 0 & 0 & 0 \end{pmatrix} \end{array} \equiv \begin{array}{ccccccc} & & -3 & & -1 & & 1 & & 3 \\ & & & -2 & & 0 & & 2 & \\ & & & & -1 & & 1 & & \\ & & & & & 0 & & & \end{array} \tag{28}$$

where we have used a more compact notation to record the diagonal elements on the right-hand side. The entry in the Δ^- column of the matrix is -3, so on the right-hand side we put a -3 in the position of the Δ^- in the usual decuplet diagram, and so on. By considering the reflection and rotation symmetries of the right-hand side of eq. (28) we can see that this matrix corresponds to the basis element E^- of the doublet representation of S_3.

In Fig. 8 we show all 10 diagonal matrices, in this compact notation. These

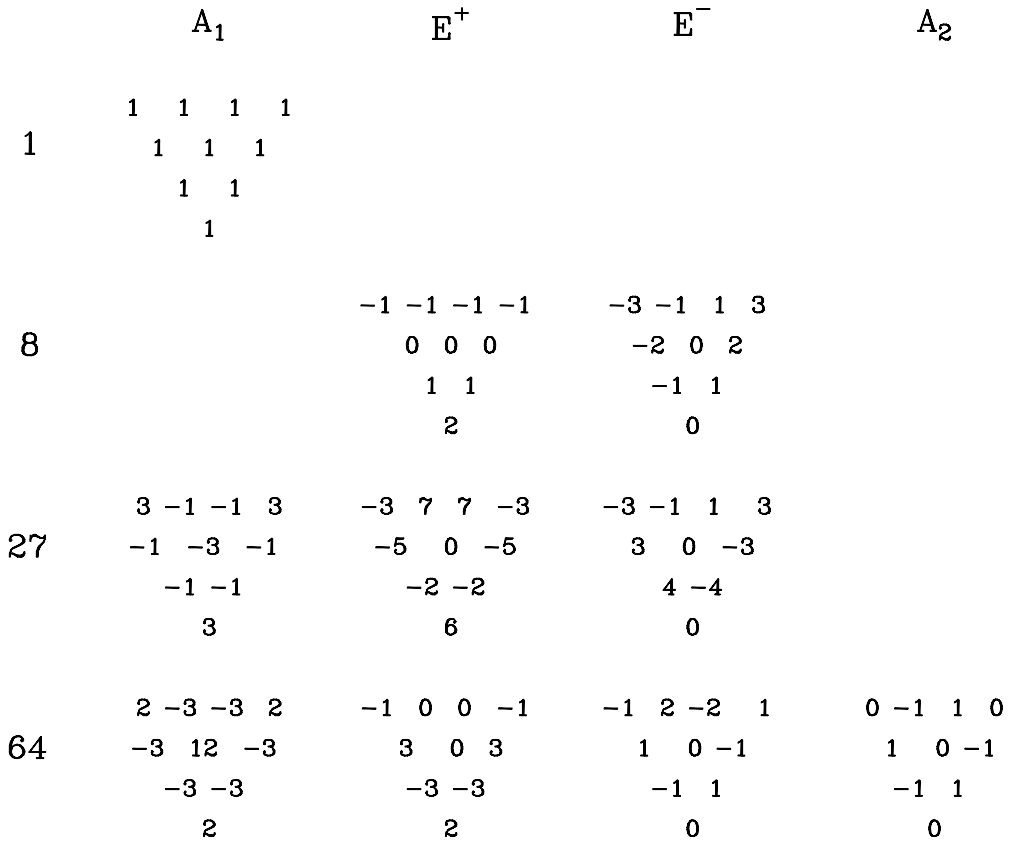


Figure 8: The matrices for projecting out decuplet mass contributions of known symmetry – see eq. (28) for an explanation of the notation.

matrices are orthogonal, in the sense

$$\mathrm{Tr}[\tau_a \tau_b] = 0 \quad \text{if} \quad a \neq b\,, \tag{29}$$

(where τ_a is any of the matrices of Fig. 8) so they can be used to project out mass combinations which have simple quark mass dependencies, see Fig. 8, and Table 4.

Let us now give some examples of mass formulae. First we look at the singlet of the decuplet mass matrix. Because we are keeping $\overline{m}$ = constant only the

Δ^-	Δ^0	Δ^+	Δ^{++}	Σ^{*-}	Σ^{*0}	Σ^{*+}	Ξ^{*-}	Ξ^{*0}	Ω^-	S_3	$SU(3)$
1	1	1	1	1	1	1	1	1	1	A_1	1
−1	−1	−1	−1	0	0	0	1	1	2	E^+	8
−3	−1	1	3	−2	0	2	−1	1	0	E^-	8
3	−1	−1	3	−1	−3	−1	−1	−1	3	A_1	27
−3	7	7	−3	−5	0	−5	−2	−2	6	E^+	27
−3	−1	1	3	3	0	−3	4	−4	0	E^-	27
2	−3	−3	2	−3	12	−3	−3	−3	2	A_1	64
−1	0	0	−1	3	0	3	−3	−3	2	E^+	64
−1	2	−2	1	1	0	−1	−1	1	0	E^-	64
0	−1	1	0	1	0	−1	−1	1	0	A_2	64

Table 4: Decuplet mass matrix contributions, classified by permutation and $SU(3)$ symmetry, see Fig. 8.

terms with ticks in Table 3 contribute. This gives from Table 4,

$$\begin{aligned} & M_{\Delta^-} + M_{\Delta^0} + M_{\Delta^+} + M_{\Delta^{++}} \\ & + M_{\Sigma^{*-}} + M_{\Sigma^{*0}} + M_{\Sigma^{*+}} + M_{\Xi^{*-}} + M_{\Xi^{*0}} + M_{\Omega^-} \\ & \quad = \ \ 10 M_0 \ + B_1 \ (\delta m_u^2 + \delta m_d^2 + \delta m_s^2) + C_1 \ \delta m_u \delta m_d \delta m_s \, . \end{aligned} \tag{30}$$

This equation being a singlet has the same form as for r_0/a, eq. (16).

As a further example for the 27-plet component of the decuplet mass matrix, we see from Table 4 that there are three mass combinations which transform as 27-plets, giving three related mass relations

$$\begin{aligned} & 3M_{\Delta^-} - M_{\Delta^0} - M_{\Delta^+} + 3M_{\Delta^{++}} \\ & - M_{\Sigma^{*-}} - 3M_{\Sigma^{*0}} - M_{\Sigma^{*+}} - M_{\Xi^{*-}} - M_{\Xi^{*0}} + 3M_{\Omega^-} \\ & \quad = b_{27} \left[\delta m_u^2 + \delta m_d^2 + \delta m_s^2 \right] + 9 c_{27} \delta m_u \delta m_d \delta m_s \end{aligned} \tag{31}$$

$$\begin{aligned} & -3M_{\Delta^-} + 7M_{\Delta^0} + 7M_{\Delta^+} - 3M_{\Delta^{++}} \\ & - 5M_{\Sigma^{*-}} - 5M_{\Sigma^{*+}} - 2M_{\Xi^{*-}} - 2M_{\Xi^{*0}} + 6M_{\Omega^-} \\ & \quad = b_{27} \left[3\delta m_s^2 - (\delta m_u - \delta m_d)^2 \right] + 3 c_{27} \delta m_s \left(\delta m_u^2 + \delta m_d^2 + \delta m_s^2 \right) \end{aligned} \tag{32}$$

$$\begin{aligned} & -3M_{\Delta^-} - M_{\Delta^0} + M_{\Delta^+} + 3M_{\Delta^{++}} \\ & + 3M_{\Sigma^{*-}} - 3M_{\Sigma^{*+}} + 4M_{\Xi^{*-}} - 4M_{\Xi^{*0}} \\ & \quad = 2 b_{27} (\delta m_d - \delta m_u) \delta m_s + c_{27} (\delta m_u - \delta m_d) \left(\delta m_u^2 + \delta m_d^2 + \delta m_s^2 \right) \, . \end{aligned} \tag{33}$$

The coefficients in eqs. (31)–(33) are connected, they all involve just one quadratic parameter, b_{27}, and one cubic parameter, c_{27}. We now want to explain the different numerical coefficients in front of these parameters. These can be checked by considering some simple symmetry limits. First consider the isospin limit, equal masses for the u and d quarks, $\delta m_u \to \delta m_l$, $\delta m_d \to \delta m_l$, $\delta m_s \to -2\delta m_l$ (from

eq. (11)). In this limit, eq. (33) reduces to $0 = 0$, while eqs. (31), (32) both become

$$4M_\Delta - 5M_{\Sigma^*} - 2M_{\Xi^*} + 3M_\Omega = 6b_{27}\delta m_l^2 - 18c_{27}\delta m_l^3 \,. \tag{34}$$

To include eq. (33) in our checks, we can take the U-spin limit, $m_s \to m_d$, i.e. $\delta m_s \to \delta m_d$, $\delta m_u \to -2\delta m_d$. In this limit all decuplet baryons with the same electric charge would have equal mass, because they would be in the same U-spin multiplet, so $M_{\Omega^-} \to M_{\Delta^-}, M_{\Xi^{*-}} \to M_{\Delta^-}, M_{\Sigma^{*-}} \to M_{\Delta^-}$ and similarly for the other charges. Now, all three equations become identical,

$$4M_{\Delta^-} - 5M_{\Delta^0} - 2M_{\Delta^+} + 3M_{\Delta^{++}} = 6b_{27}\delta m_d^2 - 18c_{27}\delta m_d^3 \,, \tag{35}$$

which again confirms that the numerical coefficients in eqs. (31)–(33) are correct.

Finally note that we can find all the coefficients in these equations from a 2+1 simulation, and use them to (fully) predict the results of a $1+1+1$ simulation.

2.5.2 The octet mass matrix

We can analyse the possible terms in the octet mass matrix in the same way as we did for the decuplet. We first consider the baryon octet. Using the same technique as for the decuplet mass matrix we find the results given in Table 5. However there is a complication in the octet case which we do not have in the

n	p	Σ^-	Σ^0	Λ	Σ^+	Ξ^-	Ξ^0	S_3	$SU(3)$
1	1	1	1	1	1	1	1	A_1	1
−1	−1	0	0	0	0	1	1	E^+	8_a
−1	1	−2	0	0	2	−1	1	E^-	8_a
1	1	−2	−2	2	−2	1	1	E^+	8_b
−1	1	0	mix		0	1	−1	E^-	8_b
1	1	1	−3	−3	1	1	1	A_1	27
1	1	−2	3	−3	−2	1	1	E^+	27
−1	1	0	mix		0	1	−1	E^-	27
1	−1	−1	0	0	1	1	−1	A_2	$10,\overline{10}$
0	0	0	mix		0	0	0	A_2	$10,\overline{10}$

Table 5: Mass matrix contributions for octet baryons, classified by permutation and $SU(3)$ symmetry. Note that the first two octet quantities (the 8_a) are proportional to the hypercharge Y and to isospin I_3, respectively.

decuplet, caused by the fact that we have two particles (the Λ and Σ^0) with the same Y and I_3 quantum numbers. If $m_u \neq m_d$ these states mix. There are interesting connections between the elements of the Λ/Σ^0 mixing matrix and the splittings of the other baryons, but since in this article we are concerned with 2+1 simulations, where this mixing does not arise, we will not discuss this further

here. We can however pick out several useful mass relations which are unaffected by Λ/Σ^0 mixing

$$\begin{aligned} & M_n + M_p + M_\Lambda + M_{\Sigma^-} + M_{\Sigma^0} + M_{\Sigma^+} + M_{\Xi^-} + M_{\Xi^0} \\ & \quad = \quad 8M_0 + b_1(\delta m_u^2 + \delta m_d^2 + \delta m_s^2) + c_1 \delta m_u \delta m_d \delta m_s \\ & M_n + M_p - 3M_\Lambda + M_{\Sigma^-} - 3M_{\Sigma^0} + M_{\Sigma^+} + M_{\Xi^-} + M_{\Xi^0} \\ & \quad = \quad b_{27}(\delta m_u^2 + \delta m_d^2 + \delta m_s^2)\,. \end{aligned} \tag{36}$$

At order δm_q^3 we meet some quantities in the baryon octet masses (the 10 and $\overline{10}$ combinations) which can not be deduced from $2+1$ flavour measurements – though valence $1+1+1$ on a $2+1$ background would be a possible method of estimating these quantities.

One early prediction concerning hyperon masses was the Coleman-Glashow relation [13]

$$M_n - M_p - M_{\Sigma^-} + M_{\Sigma^+} + M_{\Xi^-} - M_{\Xi^0} \approx 0\,. \tag{37}$$

Deviations from this relation are barely detectable, using a recent precision measurement of the Ξ^0 mass [14] gives the value [15], $M_n - M_p - M_{\Sigma^-} + M_{\Sigma^+} + M_{\Xi^-} - M_{\Xi^0} = -0.29 \pm 0.26\,\mathrm{MeV}$. The original Coleman-Glashow argument showed why the leading electromagnetic contribution to this quantity vanishes (in modern terms, the leading electromagnetic mass contributions are unchanged by the operation $d \leftrightarrow s$ because the s and d quarks have the same charge, but the quantity in eq. (37) is odd under this operation). To understand the smallness of the Coleman-Glashow quantity we also need to explain why the contribution from flavour $SU(3)$ breaking due to quark mass differences is small. The mass combination appears in Table 5 as one of the A_2 quantities. We can understand the success of the Coleman-Glashow relation by noting that the only polynomial in Table 3 with A_2 symmetry is $O(\delta m_q^3)$, so that the predicted violation of the Coleman-Glashow relation is

$$\begin{aligned} & M_n - M_p - M_{\Sigma^-} + M_{\Sigma^+} + M_{\Xi^-} - M_{\Xi^0} \\ & \quad = \quad c_{10}(\delta m_s - \delta m_u)(\delta m_s - \delta m_d)(\delta m_u - \delta m_d)\,. \end{aligned} \tag{38}$$

The polynomial is zero if any pair of quarks have the same mass, so we would need to measure the masses of baryons in a $1+1+1$ setting to determine c_{10} and predict the violation of the Coleman-Glashow relation.

Turning now to the mesons, both the pseudoscalar and vector meson octet have a similar mass matrix, so they do not have to be considered separately. In Table 6 we give the mass matrix contributions for the octet mesons, classified by permutation and $SU(3)$ symmetry.

Some contributions allowed for baryons, Table 5, are absent for mesons because they would violate charge conjugation, giving (for example) different masses to the K^+ and K^-. In particular, there are two octets, 8_a and 8_b, in the baryon

K^0	K^+	π^-	π^0	η_8	π^+	K^-	$\overline{K}^0$		
K^{*0}	K^{*+}	ρ^-	ρ^0	ϕ_8	ρ^+	K^{*-}	$\overline{K}^{*0}$	S_3	$SU(3)$
1	1	1	1	1	1	1	1	A_1	1
1	1	−2	−2	2	−2	1	1	E^+	8_b
−1	1	0	mix		0	1	−1	E^-	8_b
1	1	1	−3	−3	1	1	1	A_1	27
1	1	−2	3	−3	−2	1	1	E^+	27
−1	1	0	mix		0	1	−1	E^-	27

Table 6: Mass matrix contributions for octet mesons, classified by permutation and $SU(3)$ symmetry.

table, Table 5, but only the 8_b octet is permitted in Table 6. When we write down the mass formulae, this will mean that the baryon mass formula will have two independent terms linear in the quark mass, but the meson mass formula will only have a single linear term.

3 Theory for $2+1$ flavours

If we take any mass relation from the previous $1+1+1$ section, and put $m_u = m_d = m_l$ we will get a valid mass relation for the $2+1$ case. In the $2+1$ case only one variable is needed to parametrise the symmetry breaking, since from eq. (11),

$$\delta m_s = -2\delta m_l \,, \tag{39}$$

where

$$\delta m_l = m_l - \overline{m} \,. \tag{40}$$

In the $2+1$ case we can simplify the mass matrix Tables 4, 5, 6. The E^- and A_2 matrices are not needed, their coefficients are always proportional to $m_u - m_d$, which we are now setting to zero. In the higher representations (27-plet and 64-plet) only one linear combination of the A_1 and E^+ matrices appears in the $2+1$ case (it is the linear combination which does not split particles within an isospin multiplet). Therefore, in this section we just need the simplified matrix Tables 7, 8 and 9.

In the $2+1$ limit the decuplet baryons have 4 different masses (for the Δ, Σ^*, Ξ^*, and Ω). Similarly, for the octet baryons there are also 4 distinct masses, $(N, \Lambda, \Sigma, \Xi)$; and for octet mesons, 3 masses. In the meson octet the K and $\overline{K}$ must have the same mass, but there is no reason why the N and Ξ (which

Δ^-	Δ^0	Δ^+	Δ^{++}	Σ^{*-}	Σ^{*0}	Σ^{*+}	Ξ^{*-}	Ξ^{*0}	Ω^-	$SU(3)$
1	1	1	1	1	1	1	1	1	1	1
−1	−1	−1	−1	0	0	0	1	1	2	8
3	3	3	3	−5	−5	−5	−3	−3	9	27
−1	−1	−1	-1	4	4	4	−6	−6	4	64

Table 7: Decuplet mass matrix contributions for the $2+1$ case, classified by $SU(3)$ symmetry. Compare with Table 4.

n	p	Σ^-	Σ^0	Λ	Σ^+	Ξ^-	Ξ^0	$SU(3)$
1	1	1	1	1	1	1	1	1
−1	−1	0	0	0	0	1	1	8_a
1	1	−2	−2	2	−2	1	1	8_b
3	3	−1	−1	−9	−1	3	3	27

Table 8: Mass matrix contributions for octet baryons for the $2+1$ case, classified by $SU(3)$ symmetry. Compare with Table 5.

occupy the corresponding places in the baryon octet, see Figs. 2 and 3), should have equal masses once flavour $SU(3)$ is broken.

Again we have the singlet quantities X_S which are stationary at the symmetry point as given in Table 2, but which now simplify to give Table 10. In the notation we have now assumed isospin invariance, so that for example $M_\Delta \equiv M_{\Delta^{++}} = M_{\Delta^+} = M_{\Delta^0} = M_{\Delta^-}$. (The corresponding mass values we use in this article are given in section 9.)

Furthermore this can obviously be generalised. Let us first define the quark mass combinations $m_\eta = (m_l + 2m_s)/3$ and $m_K = (m_l + m_s)/2$. Then $m_l + m_\eta = 2\overline{m}$ and $m_l + 2m_K = 3\overline{m}$ are constants on our trajectory and so $\delta m_l + \delta m_\eta = 0$ and also $\delta m_l + 2\delta m_K = 0$. For example, this means that any functions of the

K^0	K^+	π^-	π^0	η_8	π^+	K^-	$\overline{K}^0$	
K^{*0}	K^{*+}	ρ^-	ρ^0	ϕ_8	ρ^+	K^{*-}	$\overline{K}^{*0}$	$SU(3)$
1	1	1	1	1	1	1	1	1
1	1	−2	−2	2	−2	1	1	8_b
3	3	−1	−1	−9	−1	3	3	27

Table 9: Mass matrix contributions for octet mesons for the $2+1$ case, classified by $SU(3)$ symmetry. Compare with Table 6.

Pseudoscalar	$X_\pi^2 = \frac{1}{3}(2M_K^2 + M_\pi^2)$
mesons	$X_{\eta_8}^2 = \frac{1}{2}(M_\pi^2 + M_{\eta_8}^2)$
Vector	$X_\rho = \frac{1}{3}(2M_{K^*} + M_\rho)$
mesons	$X_{\phi_8} = \frac{1}{2}(M_\rho + M_{\phi_8})$
	$X_{\phi_s} = \frac{1}{3}(2M_\rho + M_{\phi_s})$
Octet	$X_N = \frac{1}{3}(M_N + M_\Sigma + M_\Xi)$
baryons	$X_\Lambda = \frac{1}{2}(M_\Sigma + M_\Lambda)$
Decuplet	$X_\Delta = \frac{1}{3}(2M_\Delta + M_\Omega)$
baryons	$X_{\Xi^*} = \frac{1}{3}(M_\Delta + M_{\Sigma^*} + M_{\Xi^*})$
	$X_{\Sigma^*} = M_{\Sigma^*}$

Table 10: Permutation invariant mass combinations, see Fig. 4. ϕ_s is a fictitious $s\overline{s}$ particle; η_8 a pure octet meson.

form

$$2f(m_K) + f(m_l) \quad \text{or} \quad g(m_s) + 2g(m_l) \quad \text{or} \quad h(m_\eta) + h(m_l)\,, \tag{41}$$

will also have zero derivative at the symmetric point. These equations generalise the meson sector of Table 10.

In Table 11 we present the $2+1$ baryon decuplet results corresponding to Table 4 or eqs. (30)–(33) and the baryon octet from Table 5 or eq. (36). Similarly the mesons are given in Table 12. Particular combinations chosen to remove the unknown M_{η_8}, M_{ϕ_8} masses are given in Table 13.

We can see how well this works in practice by looking, for example, at the physical masses of the decuplet baryons. If we consider the physical values of the four decuplet mass combinations in Table 11 and using mass values given later in Table 17, we get

$$\begin{aligned}
4M_\Delta + 3M_{\Sigma^*} + 2M_{\Xi^*} + M_\Omega &= 13.82 \text{ GeV} && \text{singlet} && \propto (\delta m_l)^0 \\
-2M_\Delta \quad\quad + M_{\Xi^*} + M_\Omega &= 0.742 \text{ GeV} && \text{octet} && \propto \delta m_l \\
4M_\Delta - 5M_{\Sigma^*} - 2M_{\Xi^*} + 3M_\Omega &= -0.044 \text{ GeV} && 27-\text{plet} && \propto \delta m_l^2 \\
-M_\Delta + 3M_{\Sigma^*} - 3M_{\Xi^*} + M_\Omega &= -0.006 \text{ GeV} && 64-\text{plet} && \propto \delta m_l^3\,,
\end{aligned} \tag{42}$$

with a strong hierarchy in values, corresponding to the leading term in the Taylor expansion. Each additional factor of δm_l reduces the value by about an order of magnitude, the 64-plet combination is more than 2000 times smaller than the singlet combination. This suggests that the Taylor expansion converges well all the way from the symmetric point to the physical point. (Though of course it is possible that the singlet and octet curvature terms are larger than those in the 27 and 64.) Unfortunately it may be very difficult to see a signal in the 64-plet channel.

$SU(3)$	Mass Combination	Expansion			
1	$2M_N + 3M_\Sigma + M_\Lambda + 2M_\Xi$	1,		δm_l^2,	δm_l^3
8	$M_\Xi - M_N$		δm_l,	δm_l^2,	δm_l^3
8	$-M_N + 3M_\Sigma - M_\Lambda - M_\Xi$		δm_l,	δm_l^2,	δm_l^3
27	$2M_N - M_\Sigma - 3M_\Lambda + 2M_\Xi$			δm_l^2,	δm_l^3
1	$4M_\Delta + 3M_{\Sigma^*} + 2M_{\Xi^*} + M_\Omega$	1,		δm_l^2,	δm_l^3
8	$-2M_\Delta + M_{\Xi^*} + M_\Omega$		δm_l,	δm_l^2,	δm_l^3
27	$4M_\Delta - 5M_{\Sigma^*} - 2M_{\Xi^*} + 3M_\Omega$			δm_l^2,	δm_l^3
64	$-M_\Delta + 3M_{\Sigma^*} - 3M_{\Xi^*} + M_\Omega$				δm_l^3

Table 11: Baryon mass combinations classified by $SU(3)$ representation, in the $2+1$ case.

$SU(3)$	Mass Combination	Expansion			
1	$3M_\pi^2 + 4M_K^2 + M_{\eta_8}^2$	1,		δm_l^2,	δm_l^3
8	$-3M_\pi^2 + 2M_K^2 + M_{\eta_8}^2$		δm_l,	δm_l^2,	$\delta m l^3$
27	$-M_\pi^2 + 4M_K^2 - 3M_{\eta_8}^2$			δm_l^2,	δm_l^3
1	$3M_\rho + 4M_{K^*} + M_{\phi_8}$	1,		δm_l^2,	δm_l^3
8	$-3M_\rho + 2M_{K^*} + M_{\phi_8}$		δm_l,	δm_l^2,	δm_l^3
27	$-M_\rho + 4M_{K^*} - 3M_{\phi_8}$			δm_l^2,	δm_l^3

Table 12: Meson mass combinations classified by $SU(3)$ representation, in the $2+1$ case. Octet-singlet mixing is not taken into account.

$SU(3)$	Mass Combination	Expansion			
1, 27	$2M_K^2 + M_\pi^2$	1,		δm_l^2,	δm_l^3
8, 27	$M_K^2 - M_\pi^2$		δm_l,	δm_l^2,	δm_l^3
1, 27	$2M_{K^*} + M_\rho$	1,		δm_l^2,	δm_l^3
8, 27	$M_{K^*} - M_\rho$		δm_l,	δm_l^2,	δm_l^3

Table 13: Meson mass combinations free from mixing problems, classified by $SU(3)$ representation. These combinations have been chosen to eliminate the η_8 and ϕ_8 states, so they now contain mixtures of different $SU(3)$ representations.

We can now 'invert' the results in Tables 11, 12 to give the expansion for each hadron mass[4] from the symmetry point $\overline{m} = m_0$. This inversion is made easier by orthogonality relations between the different $SU(3)$ representations. We can simply read off the answers from the Tables 7, 8 and 9. This leads to the constrained fit formulae

$$\begin{aligned} M_\pi^2 &= M_0^2 + 2\alpha\delta m_l + (\beta_0 + 2\beta_1)\delta m_l^2 \\ M_K^2 &= M_0^2 - \alpha\delta m_l + (\beta_0 + 5\beta_1 + 9\beta_2)\delta m_l^2 \\ M_{\eta_8}^2 &= M_0^2 - 2\alpha\delta m_l + (\beta_0 + 6\beta_1 + 12\beta_2 + \beta_3)\delta m_l^2 \,, \end{aligned} \tag{43}$$

$$\begin{aligned} M_\rho &= M_0 + 2\alpha\delta m_l + (\beta_0 + 2\beta_1)\delta m_l^2 \\ M_{K^*} &= M_0 - \alpha\delta m_l + (\beta_0 + 5\beta_1 + 9\beta_2)\delta m_l^2 \\ M_{\phi_8} &= M_0 - 2\alpha\delta m_l + (\beta_0 + 6\beta_1 + 12\beta_2 + \beta_3)\delta m_l^2 \,, \end{aligned} \tag{44}$$

$$\begin{aligned} M_N &= M_0 + 3A_1\delta m_l + (B_0 + 3B_1)\delta m_l^2 \\ M_\Lambda &= M_0 + 3A_2\delta m_l + (B_0 + 6B_1 - 3B_2 + 9B_4)\delta m_l^2 \\ M_\Sigma &= M_0 - 3A_2\delta m_l + (B_0 + 6B_1 + 3B_2 + 9B_3)\delta m_l^2 \\ M_\Xi &= M_0 - 3(A_1 - A_2)\delta m_l + (B_0 + 9B_1 - 3B_2 + 9B_3)\delta m_l^2 \,, \end{aligned} \tag{45}$$

$$\begin{aligned} M_\Delta &= M_0 + 3A\delta m_l + (B_0 + 3B_1)\delta m_l^2 \\ M_{\Sigma^*} &= M_0 + 0 + (B_0 + 6B_1 + 9B_2)\delta m_l^2 \\ M_{\Xi^*} &= M_0 - 3A\delta m_l + (B_0 + 9B_1 + 9B_2)\delta m_l^2 \\ M_\Omega &= M_0 - 6A\delta m_l + (B_0 + 12B_1)\delta m_l^2 \,. \end{aligned} \tag{46}$$

(The values of the constants are obviously different for each octet or decuplet.) We see that the linear terms are highly constrained. The decuplet baryons have only one slope parameter, A, while the octet baryons have two slope parameters, A_1, A_2. Mesons have fewer slope parameters than octet baryons because of constraints due to charge conjugation, leaving again just one slope parameter.

The quadratic terms are much less constrained; indeed only for the baryon decuplet is there any constraint. The coefficients of the δm_l^2 terms appear complicated; there seem to be too many for the meson and baryon octets, eqs. (43) – (45). In the next section, we generalise these formulae to the case of different valence quark masses to sea quark masses or 'partial quenching' when this choice of coefficients becomes relevant. Note that not all the coefficients can thus be determined: for η_8 and ϕ_8 the β_3-coefficient cannot be found from partially quenched results.

[4]Alternatively, of course, the methods of Appendix B.4 can be directly applied.

An $s\bar{s}$ meson state has charge 0, isospin 0, the same quantum numbers as a $(u\bar{u} + d\bar{d})$ meson. In the real world we should therefore expect that $I = 0$ (isoscalar) mesons will always be mixtures of $s\bar{s}$ and $l\bar{l}$, to a greater or lesser extent. The mixing has been investigated in detail in [16].

On the lattice we can remove the mixing by just dropping disconnected contributions, and only keeping the connected part of the meson propagator. (In fact this calculation is easier and cheaper than the full calculation.) Theoretically the resulting pure $s\bar{s}$ meson is best treated in the context of partial quenching. We can get its mass formula simply by making the substitution for the valence quark mass $\delta\mu_s \to -2\delta\mu_l$ in the mass formula for the partially quenched $I = 1$ mesons as described in section 4, eq. (57) to give

$$\begin{aligned} M_{\eta_s}^2 &= M_0^2 - 4\alpha\delta m_l + (\beta_0 + 8\beta_1)\delta m_l^2 \\ M_{\phi_s} &= M_0 - 4\alpha\delta m_l + (\beta_0 + 8\beta_1)\delta m_l^2 \,. \end{aligned} \tag{47}$$

(These are, as previously mentioned, the masses that can be (easily) found from lattice simulations rather than M_{η_8} and M_{ϕ_8}.) The pseudoscalar $s\bar{s}$ state, the η_s or 'strange pion', does not correspond to any real-world state, but the vector $s\bar{s}$ meson, the ϕ_s, is very close to the real-world ϕ. Phenomenologically, the observed fact that the ϕ almost always decays to $K\bar{K}$ (84 %) rather than $\rho\pi$ [17] is best explained by saying that the ϕ is almost purely $s\bar{s}$.

As eqs. (43)–(46) have been derived using only group theoretic arguments, they will be valid for results derived on any lattice volume (though the coefficients are still functions of the volume).

Finally there is the practical question of whether fits should be against the (light) quark mass or alternatively against the pseudoscalar pion mass. In Appendix C we argue that 'internally' at least the fits should be made against the quark mass. Of course this is only a useful observation when quadratic or higher terms are involved. To leading order eqs. (44)–(46) can be written as

$$\delta M \equiv M - M_0 = c_M \delta m_l \,, \tag{48}$$

(together with $\delta M^2 \equiv M^2 - M_0^2 = c_M \delta m_l$ in the case of pseudoscalar mesons, eq. (43)). The coefficients c_M can be found from these equations. Thus an expansion in δm_l is equivalent to an expansion in δM or δM^2.

4 Partial quenching

In partial quenching (PQ) measurements are made with the mass of the valence quarks different from the sea quarks. In this case the sea quark masses m_l, m_s remain constrained by $\overline{m}$ = constant, but the valence quark masses μ_l, μ_s are unconstrained. We define

$$\delta\mu_q = \mu_q - \overline{m} \,, \quad q = l, s \,. \tag{49}$$

When $\mu \to m$ (i.e. return to the 'unitary line') then the following results collapse to the previous results of eqs. (43) – (46). Here we sketch some results, see [18] for more details.

In Table 3 we have often used the identity $\delta m_u + \delta m_d + \delta m_s = 0$ to simplify the symmetric polynomials. Since we are not going to keep $\mu_u + \mu_d + \mu_s$ constant, we write out our basis polynomials in full, without the constraint $\sum \delta\mu_q = 0$, in Table 14. We can check that the polynomials in Table 14 reduce to multiples of those in Table 3 when the identity $\sum \delta\mu_q = 0$ is applied. For example, $2\delta\mu_s - \delta\mu_u - \delta\mu_d = 3\delta\mu_s - (\delta\mu_u + \delta\mu_d + \delta\mu_s)$, so when the zero-sum identity is applied, and $\mu_q \to m_q$ the polynomial $2\delta\mu_s - \delta\mu_u - \delta\mu_d$ in Table 14 reduces to the corresponding

Polynomial	S_3	$SU(3)$		
1	A_1	1		
$\delta\mu_u + \delta\mu_d + \delta\mu_s$	A_1	1		
$2\delta\mu_s - \delta\mu_u - \delta\mu_d$	E^+		8	
$\delta\mu_u - \delta\mu_d$	E^-		8	
$(\delta\mu_u + \delta\mu_d + \delta\mu_s)^2$	A_1	1		
$(\delta\mu_u + \delta\mu_d + \delta\mu_s)(2\delta\mu_s - \delta\mu_u - \delta\mu_d)$	E^+		8	
$(\delta\mu_u + \delta\mu_d + \delta\mu_s)(\delta\mu_u - \delta\mu_d)$	E^-		8	
$(\delta\mu_s - \delta\mu_u)^2 + (\delta\mu_s - \delta\mu_d)^2 + (\delta\mu_u - \delta\mu_d)^2$	A_1	1		27
$(\delta\mu_s - \delta\mu_u)^2 + (\delta\mu_s - \delta\mu_d)^2 - 2(\delta\mu_u - \delta\mu_d)^2$	E^+		8	27
$(\delta\mu_s - \delta\mu_u)^2 - (\delta\mu_s - \delta\mu_d)^2$	E^-		8	27
$\delta m_u^2 + \delta m_d^2 + \delta m_s^2$	A_1	1		27

Table 14: All the quark-mass polynomials needed for partially quenched masses, classified by symmetry properties. The table includes entries up to $O(\mu_q^2)$.

polynomial δm_s in Table 3.

4.1 PQ decuplet baryons

In the partially quenched case we know that the hadron mass formulae should have an $SU(3)$ symmetry for interchanging the sea quarks, and another $SU(3)$ symmetry for operations on the valence quarks. The sea quark symmetry will always be singlet, the valence quark terms for a hadron in the octet can be in any representation which occurs in $\overline{8} \otimes 8$ and the decuplet can be in any representation which occurs in $10 \otimes \overline{10}$.

Let us see what sort of mass relations symmetry allows us, taking the decuplet baryons as our example. Starting with linear terms in the quark masses, we can form two polynomials of the valence masses, a singlet combination $(2\delta\mu_l + \delta\mu_s)$ and an octet combination with E^+ symmetry, $(\delta\mu_s - \delta\mu_l)$. These are the polynomials on line 2 and line 3 of Table 14. (A first-order term in the sea quark masses

is ruled out because we are keeping $2m_l + m_s$ constant.) We can read off the coefficients each polynomial must have by looking for the A_1 singlet and E^+ octet entries in Fig. 8, or in Tables 4 or 7. Thus a singlet polynomial must have the same flavour coefficients for every baryon and the octet polynomial must have a coefficient proportional to the hypercharge.

So, at first sight we would expect

$$\begin{aligned} M_\Delta &= M_0 + \alpha_1(2\delta\mu_l + \delta\mu_s) - \alpha_2(\delta\mu_s - \delta\mu_l) \\ M_{\Sigma^*} &= M_0 + \alpha_1(2\delta\mu_l + \delta\mu_s) \\ M_{\Xi^*} &= M_0 + \alpha_1(2\delta\mu_l + \delta\mu_s) + \alpha_2(\delta\mu_s - \delta\mu_l) \\ M_\Omega &= M_0 + \alpha_1(2\delta\mu_l + \delta\mu_s) + 2\alpha_2(\delta\mu_s - \delta\mu_l)\,, \end{aligned} \tag{50}$$

with no connection between α_1 and α_2. However, it is clear that the Δ mass cannot know anything about the strange valence mass, and the Ω mass must similarly be independent of $\delta\mu_l$. These constraints are both satisfied if

$$\alpha_1 = \alpha_2 \equiv A\,, \tag{51}$$

giving us a leading-order formula

$$\begin{aligned} M_\Delta &= M_0 + 3A\delta\mu_l \\ M_{\Sigma^*} &= M_0 + A(2\delta\mu_l + \delta\mu_s) \\ M_{\Xi^*} &= M_0 + A(\delta\mu_l + 2\delta\mu_s) \\ M_\Omega &= M_0 + 3A\delta\mu_s\,. \end{aligned} \tag{52}$$

We can continue this procedure to the quadratic level. Again, the number of terms is reduced by keeping the sum of the sea quark masses fixed; and we again find the number of coefficients reduced by the constraint that the Δ mass is independent of $\delta\mu_s$, and the Ω mass independent of $\delta\mu_l$. The most general quadratic formula, consistent with the above constraint, and with $SU(3)$ symmetry, is

$$\begin{aligned} M_\Delta &= M_0 + 3A\delta\mu_l + B_0\delta m_l^2 + 3B_1\delta\mu_l^2 \\ M_{\Sigma^*} &= M_0 + A(2\delta\mu_l + \delta\mu_s) + B_0\delta m_l^2 + B_1(2\delta\mu_l^2 + \delta\mu_s^2) + B_2(\delta\mu_s - \delta\mu_l)^2 \\ M_{\Xi^*} &= M_0 + A(\delta\mu_l + 2\delta\mu_s) + B_0\delta m_l^2 + B_1(\delta\mu_l^2 + 2\delta\mu_s^2) + B_2(\delta\mu_s - \delta\mu_l)^2 \\ M_\Omega &= M_0 + 3A\delta\mu_s + B_0\delta m_l^2 + 3B_1\delta\mu_s^2\,. \end{aligned} \tag{53}$$

These formulae apply when the sum of the sea quark masses is held constant, $\frac{1}{3}(2m_l + m_s) = m_0$, but the valence quark masses are completely free, because at this level (terms up to second order) a restriction on valence masses would not lead to any reduction in the number of free parameters.

We can check the formulae (53) by forming the $SU(3)$ mass combinations of Table 11, and checking that in each case only polynomials of the appropriate symmetry appear in the answer.

There are some combinations of the partially quenched masses, eqs. (53), which have simpler dependences on the valence quark masses and only involve a small number of fit parameters. Examples include

$$\begin{aligned} -M_\Delta + M_{\Sigma^*} + M_{\Xi^*} - M_\Omega &= 2B_2(\delta\mu_s - \delta\mu_l)^2 \\ M_{\Xi^*} - M_{\Sigma^*} &= A(\delta\mu_s - \delta\mu_l) + B_1(\delta\mu_s^2 - \delta\mu_l^2) \\ M_\Omega - M_\Delta &= 3A(\delta\mu_s - \delta\mu_l) + 3B_1(\delta\mu_s^2 - \delta\mu_l^2)\,. \end{aligned} \quad (54)$$

Let us use these formulae to illustrate how partially quenched measurements might help us fit masses on the constant sea-quark mass line. If we only use unitary data, with $\frac{1}{3}(2m_l^R + m_s^R) = m_0^R$, we are limited to points on the line between the endpoints $(m_l^R, m_s^R) = (0, 3m_0^R)$ and $(m_l^R, m_s^R) = (\frac{3}{2}m_0^R, 0)$, which means that the quark mass splitting is limited to the range $-\frac{3}{2}m_0^R < (m_s^R - m_l^R) < 3m_0^R$. In the partially quenched case, we can increase μ_s without having to decrease μ_l, so we can make the splitting $\mu_s^R - \mu_l^R$ much larger than $m_s^R - m_l^R$, which gives a much better lever-arm to determine B_1 and B_2.

Because the decuplet baryon has a particularly high degree of symmetry we can give an alternative derivation of eq. (53), with less explicit reference to the flavour group. Consider a decuplet baryon made from quarks of type a, b and c. Since the decuplet is a fully symmetric representation, the mass of the baryon must be a symmetric function of $\delta\mu_a, \delta\mu_b$ and $\delta\mu_c$.

The mass can also depend on the sea quark masses $\delta m_u, \delta m_d, \delta m_s$, but this dependence must be in a flavour singlet way. If we keep the sum of the sea quark masses fixed, the first singlet polynomial allowed (see Table 3) is $\frac{1}{6}(\delta m_u^2 + \delta m_d^2 + \delta m_s^2)$, where we have chosen the prefactor $\frac{1}{6}$ to lead to a tidy expression in the limit when $m_u = m_d$. Since this mass polynomial is flavour singlet, it can only appear in the coefficient of the identity matrix – i.e. it must make the same contribution to every decuplet baryon. We therefore know that the mass formula for the abc decuplet baryon must have the form

$$\begin{aligned} M(abc) &= M_0 + B_0\tfrac{1}{6}(\delta m_u^2 + \delta m_d^2 + \delta m_s^2) + F_{sym}(\delta\mu_a, \delta\mu_b, \delta\mu_c) \\ &\to M_0 + B_0\delta m_l^2 + F_{sym}(\delta\mu_a, \delta\mu_b, \delta\mu_c)\,, \end{aligned} \quad (55)$$

in the $2+1$ limit.

Now let us consider what terms are possible in the completely symmetric function F_{sym}. There is only one symmetric linear term, $\delta\mu_a + \delta\mu_b + \delta\mu_c$. There are two symmetric quadratic terms we can write down, $\delta\mu_a^2 + \delta\mu_b^2 + \delta\mu_c^2$ and $\delta\mu_a\delta\mu_b + \delta\mu_a\delta\mu_c + \delta\mu_b\delta\mu_c$, or linear combinations of these two terms. We get simpler final expressions if we choose the basis $\delta\mu_a^2 + \delta\mu_b^2 + \delta\mu_c^2$ and $\delta\mu_a^2 + \delta\mu_b^2 + \delta\mu_c^2 - \delta\mu_a\delta\mu_b - \delta\mu_a\delta\mu_c - \delta\mu_b\delta\mu_c$, giving us the general mass formula

$$\begin{aligned} M(abc) &= M_0 + A(\delta\mu_a + \delta\mu_b + \delta\mu_c) + B_0\delta m_l^2 + B_1(\delta\mu_a^2 + \delta\mu_b^2 + \delta\mu_c^2) \\ &\quad + B_2(\delta\mu_a^2 + \delta\mu_b^2 + \delta\mu_c^2 - \delta\mu_a\delta\mu_b - \delta\mu_a\delta\mu_c - \delta\mu_b\delta\mu_c)\,. \end{aligned} \quad (56)$$

Calculating $M(lll), M(sll), M(ssl)$ and $M(sss)$ gives the partially quenched mass formulae in eq. (53). Remember that these formulae are only complete for the case $m_u + m_d + m_s$ held constant. If the average sea quark mass is allowed to vary, more terms become possible, including 'mixed' polynomials which contain both δm_q and $\delta\mu_q$. With fixed average sea quark mass, such mixed polynomials do not arise until the cubic order.

This argument gives us the same result as the full group-theory derivation, though in some sense it explains less. For instance, it does not immediately explain why the mass combinations of Table 11 give particularly tidy polynomials, or where the hierarchy in eq. (42) comes from.

4.2 PQ octet mesons

As in the previous section, we find the meson mass formula by constructing the most general matrix consistent with $SU(3)$ symmetry, and the constraint that the partially quenched pion mass must know nothing about μ_s. The resulting mass formulae for partially quenched mesons take the form:

$$\begin{aligned} M_\pi^2 &= M_0^2 + 2\alpha\delta\mu_l + \beta_0\delta m_l^2 + 2\beta_1\delta\mu_l^2 \\ M_K^2 &= M_0^2 + \alpha(\delta\mu_l + \delta\mu_s) + \beta_0\delta m_l^2 + \beta_1(\delta\mu_l^2 + \delta\mu_s^2) + \beta_2(\delta\mu_s - \delta\mu_l)^2 \\ M_{\eta_s}^2 &= M_0^2 + 2\alpha\delta\mu_s + \beta_0\delta m_l^2 + 2\beta_1\delta\mu_s^2 \,. \end{aligned} \tag{57}$$

Again the η_s is the meson made of a partially quenched $\overline{s}_{val}s_{val}$ quarks (i.e. the 'strange pion') which in the partially quenched framework can be observed and can yield useful information about the extrapolation constants. The PQ $M_{\eta_s}^2$ can thus be obtained from the PQ M_π^2 by simply changing $\mu_l \to \mu_s$ which changes the top row of eq. (57) into the bottom row.

Some useful combinations, which avoid the delicate η sector, are

$$\begin{aligned} M_K^2 - M_\pi^2 &= \alpha(\delta\mu_s - \delta\mu_l) + \beta_1(\delta\mu_s^2 - \delta\mu_l^2) + \beta_2(\delta\mu_s - \delta\mu_l)^2 \\ 2M_K^2 + M_\pi^2 &= 3M_0^2 + \alpha(4\delta\mu_l + 2\delta\mu_s) + 3\beta_0\delta m_l^2 \\ &\quad + \beta_1(4\delta\mu_l^2 + 2\delta\mu_s^2) + 2\beta_2(\delta\mu_s - \delta\mu_l)^2 \,. \end{aligned} \tag{58}$$

$M_K^2 - M_\pi^2$ is useful as a measure of the quark mass splitting, $2M_K^2 + M_\pi^2$ as a quantity which is nearly constant along our trajectory.

The same form, mutatis mutandis, applies to the other meson octets, e.g. the ρ, K^*, ϕ system. We thus have

$$\begin{aligned} M_\rho &= M_0 + 2\alpha\delta\mu_l + \beta_0\delta m_l^2 + 2\beta_1\delta\mu_l^2 \\ M_{K^*} &= M_0 + \alpha(\delta\mu_l + \delta\mu_s) + \beta_0\delta m_l^2 + \beta_1(\delta\mu_l^2 + \delta\mu_s^2) + \beta_2(\delta\mu_s - \delta\mu_l)^2 \\ M_{\phi_s} &= M_0 + 2\alpha\delta\mu_s + \beta_0\delta m_l^2 + 2\beta_1\delta\mu_s^2 \,, \end{aligned} \tag{59}$$

following the pattern of eq. (57).

We can give a similar elementary argument to derive the partially quenched mass formula for mesons with different quarks (e.g. the K, K^* and the charged π and ρ). Consider an $a\bar{b}$ meson. It must have the same mass as its antiparticle, the $b\bar{a}$ meson. So, by the same argument as in eq. (55) we will have a mass formula

$$M(a\bar{b}) = M(b\bar{a}) = M_0 + \beta_0 \tfrac{1}{6}(\delta m_u^2 + \delta m_d^2 + \delta m_s^2) + F_{sym}(\delta\mu_a, \delta\mu_b)\,. \qquad (60)$$

The only linear symmetric polynomial is $\delta\mu_a + \delta\mu_b$, while there are two independent quadratic possibilities, which can be chosen to be $\delta\mu_a^2 + \delta\mu_b^2$ and $(\delta\mu_a - \delta\mu_b)^2$. With this choice we get the meson mass formula

$$M(a\bar{b}) = M_0 + \alpha(\delta\mu_a + \delta\mu_b) + \beta_0 \tfrac{1}{6}(\delta m_u^2 + \delta m_d^2 + \delta m_s^2) + \beta_1(\delta\mu_a^2 + \delta\mu_b^2) + \beta_2(\delta\mu_a - \delta\mu_b)^2\,, \qquad (61)$$

which reduces to eqs. (57) and (59). (For pseudoscalar mesons we expect M^2 to have a smoother Taylor expansion than M itself, so we keep the form of eq. (61), but apply it to the squares of the pseudoscalar masses.) This formula will also apply to the $s\bar{s}$ meson with annihilation 'switched off', i.e. with disconnected diagrams dropped.

We cannot see a way to extend this argument to include the η_8 or ϕ_8 mesons. Using our full group argument we find the formulae eq. (43) and eq. (44), which involve an additional quadratic parameter, β_3. Physically it is very reasonable that the η_8 and ϕ_8 should have a term that cannot be linked by symmetry to the mass of a meson with two different valence quarks — the η_8 and ϕ_8 have contributions from $q\bar{q}$ annihilation, which is absent in the other mesons of the multiplet, so it would be surprising if symmetry could completely determine the masses of these 'central' mesons.

4.3 PQ octet baryons

The number of free coefficients in the meson case was reduced by the requirement that K and $\overline{K}$ have the same masses. However, there is no similar constraint linking N and Ξ, so more coefficients are allowed, both at the linear and quadratic levels. Arguing as before, we find

$$\begin{aligned}
M_N &= M_0 + 3A_1\delta\mu_l + B_0\delta m_l^2 + 3B_1\delta\mu_l^2 \\
M_\Lambda &= M_0 + A_1(2\delta\mu_l + \delta\mu_s) - A_2(\delta\mu_s - \delta\mu_l) + B_0\delta m_l^2 \\
&\quad + B_1(2\delta\mu_l^2 + \delta\mu_s^2) - B_2(\delta\mu_s^2 - \delta\mu_l^2) + B_4(\delta\mu_s - \delta\mu_l)^2 \\
M_\Sigma &= M_0 + A_1(2\delta\mu_l + \delta\mu_s) + A_2(\delta\mu_s - \delta\mu_l) + B_0\delta m_l^2 \\
&\quad + B_1(2\delta\mu_l^2 + \delta\mu_s^2) + B_2(\delta\mu_s^2 - \delta\mu_l^2) + B_3(\delta\mu_s - \delta\mu_l)^2 \\
M_\Xi &= M_0 + A_1(\delta\mu_l + 2\delta\mu_s) - A_2(\delta\mu_s - \delta\mu_l) + B_0\delta m_l^2 \\
&\quad + B_1(\delta\mu_l^2 + 2\delta\mu_s^2) - B_2(\delta\mu_s^2 - \delta\mu_l^2) + B_3(\delta\mu_s - \delta\mu_l)^2\,. \qquad (62)
\end{aligned}$$

As usual, the nucleon mass has been made independent of $\delta\mu_s$. Some useful combinations, which only depend on a few parameters, are

$$\begin{aligned} 2M_N - M_\Sigma - 3M_\Lambda + 2M_\Xi &= (B_3 - 3B_4)(\delta\mu_s - \delta\mu_l)^2 \qquad (63) \\ M_\Xi - M_\Sigma &= (A_1 - 2A_2)(\delta\mu_s - \delta\mu_l) + (B_1 - 2B_2)(\delta\mu_s^2 - \delta\mu_l^2)\,. \end{aligned}$$

As mentioned previously, we can check that when $\mu \to m$ (i.e. return to the 'unitary line') then these results return to the previous results of eqs. (43) – (46).

As with the decuplet baryons, and the partially quenched mesons, we can give an alternative derivation, with less use of explicit group theory. However, the argument for partially quenched octet baryons is slightly more complicated, because there are fewer symmetry constraints. We will first consider the baryons of the type aab, two valence quarks of flavour a, and one of flavour b. These form the outer hexagon of the octet diagram. As before, the sea quarks must contribute equally to all masses in the octet, the mass formula must take the form

$$M(aab) = M_0 + B_0\tfrac{1}{6}(\delta m_u^2 + \delta m_d^2 + \delta m_s^2) + F(\delta\mu_a, \delta\mu_b)\,, \qquad (64)$$

but now the dependence on the valence quark masses is not symmetric under $a \leftrightarrow b$, so the function F need not be symmetric. This means there are two independent linear terms (we choose $(2\delta\mu_a + \delta\mu_b)$ and $(\delta\mu_b - \delta\mu_a)$). There are three independent quadratic terms, we choose $(2\delta\mu_a^2 + \delta\mu_b^2)$ and $(\delta\mu_b^2 - \delta\mu_a^2)$ (to mirror the pattern of the linear terms) and $(\delta\mu_b - \delta\mu_a)^2$. Thus, the general formula for the aab baryons can be written

$$\begin{aligned} M(aab) &= M_0 + A_1(2\delta\mu_a + \delta\mu_b) + A_2(\delta\mu_b - \delta\mu_a) + B_0\tfrac{1}{6}(\delta m_u^2 + \delta m_d^2 + \delta m_s^2) \\ &\quad + B_1(2\delta\mu_a^2 + \delta\mu_b^2) + B_2(\delta\mu_b^2 - \delta\mu_a^2) + B_3(\delta\mu_b - \delta\mu_a)^2\,. \qquad (65) \end{aligned}$$

Taking the cases $M(lll), M(lls)$ and $M(ssl)$ gives the N, Σ and Ξ masses of eq. (62).

We have not found an equally simple argument for the mass of the Λ. The result of the group theoretical calculation, as set out in Appendix B, is

$$\begin{aligned} M_\Lambda &= M_0 + A_1(2\delta\mu_l + \delta\mu_s) - A_2(\delta\mu_s - \delta\mu_l) + B_0\tfrac{1}{6}(\delta m_u^2 + \delta m_d^2 + \delta m_s^2) \\ &\quad + B_1(2\delta\mu_l^2 + \delta\mu_s^2) - B_2(\delta\mu_s^2 - \delta\mu_l^2) + B_4(\delta\mu_s - \delta\mu_l)^2\,. \qquad (66) \end{aligned}$$

Most terms are related to terms in the Σ mass, the M_0, A_1, B_0 and B_1 terms are the same for Λ and Σ, while the A_2 and B_2 terms have opposite signs for the Λ and Σ. However, for the term $(\delta\mu_s - \delta\mu_l)^2$ there is no connection between the coefficient in the Λ mass and the coefficient of this term in the other masses, and we need to introduce a new parameter, that can only be determined by simulating the Λ. We can understand this from Table 8. There is a particular combination of singlet, 8_b and 27-plet matrices which gives 0 for all the baryons in the outer ring, and only acts on the central baryons. Clearly, the coefficient of this matrix only appears in the Λ mass, so at the quadratic level, we can no longer predict the Λ mass from the other masses in the octet. We have a similar situation with the mesons – there is a quadratic coefficient that we only see in the η_8 mass formula.

4.4 Generalising a constant $\overline{\mathrm{m}}$ formula

We have stressed the advantages of keeping the average sea-quark mass, $\overline{m}$, constant when approaching the physical point. This leads to simpler extrapolation formulae, and results closer to the physical values for flavour singlets and for partially quenched calculations. If we want to move away from the surface $\overline{m} = m_0$, for example to consider a completely different trajectory, such as $m_s =$ constant or $m_s^R =$ constant, then it would be useful to know how to generalise our constant $\overline{m}$ formulae to cover the full parameter space.

The procedure is simple; every constant parameter in our formulae becomes a function of $\overline{m}$, which we can then Taylor expand around $\overline{m} = m_0$. Taking as a first example our cubic formula eq. (16) for a flavour singlet quantity (such as r_0)

$$\begin{aligned}
\frac{r_0}{a} &= \alpha + \beta(\delta m_u^2 + \delta m_d^2 + \delta m_s^2) + \gamma\, \delta m_u \delta m_d \delta m_s \,, \\
&\to \alpha + \alpha'(\overline{m} - m_0) + \frac{1}{2!}\alpha''(\overline{m} - m_0)^2 + \frac{1}{3!}\alpha'''(\overline{m} - m_0)^3 \\
&\quad + \beta(\delta m_u^2 + \delta m_d^2 + \delta m_s^2) + \beta'(\overline{m} - m_0)(\delta m_u^2 + \delta m_d^2 + \delta m_s^2) \\
&\quad + \gamma\, \delta m_u \delta m_d \delta m_s \,,
\end{aligned} \tag{67}$$

yielding a cubic formula with 7 parameters. The extra polynomials appearing in this formula are the 'unticked' A_1 polynomials in Table 3.

We can take a slightly more complicated example, the partially quenched formula for the Σ baryon. In eq. (62) we give the quadratic formula, valid with $\overline{m}$ held constant. Thus to construct the quadratic formula without this constraint, we must Taylor expand the parameters M_0, A_1, A_2, giving

$$\begin{aligned}
M_\Sigma &= M_0 + M_0'(\overline{m} - m_0) + \frac{1}{2!}M_0''(\overline{m} - m_0)^2 + A_1(2\delta\mu_l + \delta\mu_s) \\
&\quad + A_2(\delta\mu_s - \delta\mu_l) + A_1'(\overline{m} - m_0)(2\delta\mu_l + \delta\mu_s) + A_2'(\overline{m} - m_0)(\delta\mu_s - \delta\mu_l) \\
&\quad + B_0\delta m_l^2 + B_1(2\delta\mu_l^2 + \delta\mu_s^2) + B_2(\delta\mu_s^2 - \delta\mu_l^2) + B_3(\delta\mu_s - \delta\mu_l)^2 \,.
\end{aligned} \tag{68}$$

Note that this formula contains 'mixed' polynomials such as $(\overline{m} - m_0)(\delta\mu_s - \delta\mu_l)$, involving both valence and sea quarks. If we restrict ourselves to the constant $\overline{m}$ surface such mixed polynomials only show up at the cubic level.

4.5 The usefulness of PQ

There are several possible advantages to considering PQ results.

1. The coefficients that appear in the expansions about the flavour symmetric line in the PQ case are the same as those that appear on the 'unitary' case. Hence this may be a computationally cheaper way of obtaining them.

2. PQ results can be helpful in choosing the next point to simulate, because the meson masses measured in the partially quenched approximation are very close to those found in a full calculation, giving us a preview of results on the next simulation point. We understand theoretically why this works well on our trajectory, with $\overline{m}$ held fixed. The reason is that the effect on the sea of making the u and d quarks lighter is largely cancelled by the effect of making the s quark heavier (the cancellation is perfect at the flavour symmetric point). Therefore partial quenching works best when only the non-singlet part of the quark mass matrix is varied (as is the case here). If the singlet part (the average sea-quark mass) is changed, there is no compensation, and the partially quenched results are less reliable.

3. We can use partial quenching to get a good estimate of results at the physical point, by taking configurations generated with quark masses some distance short of the physical point, and then at the measurement stage using valence quarks chosen to give the physical π and K masses. Important physical effects, such as the light pion cloud, would be incorporated in the results. The effects of partially quenching can be further reduced by repeating the calculation with several choices of sea-quark masses, and making an extrapolation towards the physical sea-quark mass values.

4. It is necessary in the determination of strange (or $s\overline{s}$) mesons without disconnected pieces.

We can also show that on this trajectory the errors of the partially quenched approximation are much smaller than on other trajectories. In leading order χPT (terms linear in the quark mass), the suggested procedure (valence quarks at the physical value, sea quarks anywhere on the physical constant $\overline{m}_{sea}$) is exact. See Table VIII of [21] for the leading order formulae for both octet and decuplet baryon masses. At this order partial quenching moves all the octet baryons by the same amount, and all decuplets also move together. The leading order partial quenching errors are

$$\begin{aligned} M_{oct}^{PQ} - M_{oct}^{*} &= 6\sigma_M(\overline{m} - \overline{m}^{*}) \\ M_{dec}^{PQ} - M_{dec}^{*} &= -6\overline{\sigma}_M(\overline{m} - \overline{m}^{*})\,, \end{aligned} \tag{69}$$

(using the notation of [21] for quark masses and the σ coefficients). The superscript * denotes quantities at the physical point. Since we have tuned $\overline{m}$ to be equal to the physical value, the partial quenching error vanishes on our trajectory, but not on other trajectories, which vary $\overline{m}$.

We can give a partial derivative argument, like that of section 1 or [1], which explains why this is so. Take the proton mass as an example, but any quantity will work the same way. The proton mass will depend on the valence quark masses and the sea quark masses, so we can write

$$M_p^{PQ}(\mu_u, \mu_d; m_u, m_d, m_s)\,. \tag{70}$$

M^{PQ} is the mass of a partially quenched hadron calculated on a sea background. The dependence on the three sea masses must be completely symmetrical, unlike the dependence on valence masses. At the symmetric point

$$\frac{\partial M_p^{PQ}}{\partial m_u} = \frac{\partial M_p^{PQ}}{\partial m_d} = \frac{\partial M_p^{PQ}}{\partial m_s}\,, \tag{71}$$

so if the sea quark masses are changed in a way which preserves $\overline{m}$, while the valence masses are held constant, M_p^{PQ} will not change (to leading order). We can see these benefits of the constant $\overline{m}$ procedure in the mass formulae of this section. If we make our valence quark masses equal to the quark masses at the physical point, the only difference between the partially quenched hadron mass and the physical hadron mass comes from the B_0 or β_0 term in eqs. (53), (57), (62) which gives a quadratic mass shift

$$M^* - M^{PQ} = B_0[(\delta m_l^*)^2 - \delta m_l^2]\,, \tag{72}$$

(where δm_l^* refers to δm_l at the physical sea point), which is one power higher in the quark mass than the usual result on other trajectories, eq. (69). This partial quenching shift is the same for all particles in a multiplet, so splittings are unaffected by partial quenching at this order - we would have to expand to cubic terms to see partial quenching errors in the splittings.

5 Applications to chiral perturbation theory

Almost all LO (i.e. leading order or zero loop) chiral perturbation theory (χPT) results follow simply from flavour blindness, without any input from chiral symmetry. The linear terms in m_q, which are usually called LO χPT results, were originally discovered by Gell-Mann and Okubo [7, 8], using the (non-chiral) $SU(3)$ argument we are using in this article.

The only case where we need to invoke chiral symmetry is for the pseudoscalar meson mass formula, where it is chiral symmetry which tells us that we have massless Goldstone bosons if 2 or more quark masses vanish.

Beyond leading order we cannot derive the χPT result in full solely from flavour blindness, but we can still make useful statements about the form that higher order contributions must take.

5.1 Decuplet baryon masses at $\mathbf{O(m_q^{3/2})}$

$O(m_q^{3/2})$ χPT is based on one-loop graphs, all with a pseudo-Goldstone boson. So we should expect that the individual terms in the χPT answer will be functions of M_π or of M_K or of $M_{\eta 8}$, with no mixed terms (such as $M_\pi^2 M_K^2$), which can only arise at the two-loop level.

As an example, let us examine the $2+1$ next to leading order (NLO) results for the decuplet baryon masses, [22]. Taking the formulae for individual masses, and grouping them into the multiplets of Table 11, we know that in each case we are only allowed chiral perturbation theory expressions in the corresponding multiplet:

$$\begin{aligned}
4M_\Delta + 3M_{\Sigma^*} + 2M_{\Xi^*} + M_\Omega &= 10M_0 + 20(\gamma_M - 3\overline{\sigma}_M)\overline{m} \\
&\quad -\frac{5\mathcal{H}^2}{72\pi f^2}\,\frac{5}{3}\left[3M_\pi^3 + 4M_K^3 + M_{\eta_8}^3\right] \\
&\quad -\frac{\mathcal{C}^2}{(4\pi f)^2}\,\frac{5}{3}\left[3\mathcal{F}_-(M_\pi) + 4\mathcal{F}_-(M_K) + \mathcal{F}_-(M_{\eta_8})\right] \qquad (73) \\
-2M_\Delta + M_{\Xi^*} + M_\Omega &= -10\gamma_M \delta m_l \\
&\quad -\frac{5\mathcal{H}^2}{72\pi f^2}\,\frac{1}{2}\left[-3M_\pi^3 + 2M_K^3 + M_{\eta_8}^3\right] \\
&\quad -\frac{\mathcal{C}^2}{(4\pi f)^2}\,\frac{1}{3}\left[-3\mathcal{F}_-(M_\pi) + 2\mathcal{F}_-(M_K) + \mathcal{F}_-(M_{\eta_8})\right] \qquad (74) \\
4M_\Delta - 5M_{\Sigma^*} - 2M_{\Xi^*} + 3M_\Omega &= \frac{5\mathcal{H}^2}{72\pi f^2}\,\frac{7}{9}\left[-M_\pi^3 + 4M_K^3 - 3M_{\eta_8}^3\right] \\
&\quad -\frac{\mathcal{C}^2}{(4\pi f)^2}\,\frac{7}{9}\left[-\mathcal{F}_-(M_\pi) + 4\mathcal{F}_-(M_K) - 3\mathcal{F}_-(M_{\eta_8})\right] \qquad (75) \\
-M_\Delta + 3M_{\Sigma^*} - 3M_{\Xi^*} + M_\Omega &= 0\,, \qquad (76)
\end{aligned}$$

using the notation of [22] (In particular $\mathcal{F}_-(M_i)$ is short-hand for the function $\mathcal{F}(M_i, -\Delta, \mu)$ defined there). The coefficients on the right-hand side of eq. (76) must follow the pattern of Table 12, but any function of the meson masses is allowed. We proved a weaker version of this result in [1], using the permutation group instead of full $SU(3)$.

The meson mass matrix, $8 \otimes 8$, contains no 64, there are no possible 1-loop terms to place on the right-hand side of eq. (76), so this mass combination must be zero in NLO χPT. We have already noted in Table 11 that this combination has a Taylor expansion beginning at $O(\delta m_l^3)$ and is very small experimentally, eq. (43).

5.2 Relationships between expansion coefficients

We now investigate the relation between the parameters of χPT and the Taylor coefficients in our approach, eqs. (43) – (46).

For example for the pseudoscalar octet, using the $2+1$ results in [23] and assuming their validity up to the point on the flavour symmetric line (the kaon mass is always smaller here than the physical kaon mass), we find

$$M_0^2 = \overline{\chi}\left[1 - \frac{16\overline{\chi}}{f_0^2}\left(3L_4 + L_5 - 6L_6 - 2L_8\right) + \frac{\overline{\chi}}{24\pi^2 f_0^2}\ln\frac{\overline{\chi}}{\Lambda_\chi^2}\right]$$

$$
\begin{aligned}
\alpha &= Q_0 \left[1 - \frac{16\overline{\chi}}{f_0^2}\left(3L_4 + 2L_5 - 6L_6 - 4L_8\right) + \frac{\overline{\chi}}{8\pi^2 f_0^2}\ln\frac{\overline{\chi}}{\Lambda_\chi^2}\right] \\
\beta_0 &= -\frac{Q_0^2}{6\pi^2 f_0^2} \\
\beta_1 &= \frac{Q_0^2}{f_0^2}\left[-32\left(L_5 - 2L_8\right) + \frac{1}{24\pi^2}\left(7 + 4\ln\frac{\overline{\chi}}{\Lambda_\chi^2}\right)\right] \\
\beta_2 &= \frac{Q_0^2}{f_0^2}\left[16\left(L_5 - 2L_8\right) - \frac{1}{24\pi^2}\left(3 + 2\ln\frac{\overline{\chi}}{\Lambda_\chi^2}\right)\right], \qquad (77)
\end{aligned}
$$

where $\chi_q = 2Q_0 m_q$ with $Q_0 = B_0^R Z_m^{NS}$ so that here we have $\overline{\chi} = 2Q_0(1+\alpha_Z)\overline{m}$ which is kept constant. The L_is are appropriate low energy constants or LECs.

We first note that when expanding the χPT about a point on the $SU(3)$ flavour symmetry line gives to leading order only one parameter, α as expected. (This means, in particular, that the flavour singlet combination, X_π^2, vanishes to leading order, as discussed previously.) Secondly, while we can fit to α and β_0, β_1 and β_2, it will be difficult to determine the individual LECs. The best we can probably hope for are these combinations.

5.3 Chiral non-analytic behaviour

We briefly discuss the question of how chiral logs, or other chiral singularities, fit with the Taylor expansion. The answer is that the chiral singularity should show up in the large-n behaviour of the coefficients of δm_q^n.

For example if we make a Taylor expansion about $\overline{\chi}$ of the singular term $\chi_l^2 \ln(\chi_l/\Lambda_\chi^2)$ which occurs in the chiral expansion of M_π^2, we would find

$$
\chi_l^2 \ln\chi_l = \left[\overline{\chi} + \delta\chi_l\right]^2 \ln\overline{\chi} + \overline{\chi}\delta\chi_l + \frac{3}{2}\delta\chi_l^2 + \overline{\chi}^2 \sum_{n=3}^{\infty} \frac{2(-1)^{n-1}}{n(n-1)(n-2)}\left(\frac{\delta\chi_l}{\overline{\chi}}\right)^n, \quad (78)
$$

where $\delta\chi_l = \chi_l - \overline{\chi}$. So at large n the coefficients of $\delta\chi_l^n$ are proportional to $\overline{\chi}^{2-n}/n^3$. If we look at the first singular term in the baryon mass formula, $\chi_l^{3/2}$, and expand, we would get a series $\sim \overline{\chi}^{3/2-n}\delta\chi_l^n/n^{5/2}$ at large n.

This is general, the power of n with which the terms drop off tells us the chiral singularity. If the singularity is $\chi_l^p \ln(\chi_l/\Lambda_\chi^2)$, with integer p, then the series drops like $1/n^{p+1}$. If the singularity is χ_l^q, with non-integer q, then the series drops like $1/n^{q+1}$. (If we have a singularity in $\ln(\chi_\eta/\Lambda_\chi^2)$ or $\ln(\chi_K/\Lambda_\chi^2)$, where $\chi_\eta = (\chi_l + 2\chi_s)/3$, $\chi_K = (\chi_l + \chi_s)/2$ we just change χ_l to χ_η or χ_K in the Taylor series.) Needless to say, this large-n behaviour would prove difficult to see in practice, because the coefficients are small these terms only become important close to the chiral limit.

6 The path to the physical point

In section 1 the proposed path to the physical point was introduced. We shall now discuss this a little further.

For the simulation it is easiest to keep the (bare) singlet quark mass fixed,

$$\overline{m} = \tfrac{1}{3}(2m_l + m_s) = m_0 = \text{constant}\,, \tag{79}$$

starting from some reference point $(m_l, m_s) = (m_0, m_0)$ on the flavour symmetric line. We can use the singlet combinations from Table 10 to locate the starting point of our path to the physical point by fixing a dimensionless ratio such as

$$\frac{X_\pi^2}{X_N^2} = \text{physical value} = \left.\frac{X_\pi^2}{X_N^2}\right|^* . \tag{80}$$

Note also that at the flavour symmetric point $X_\pi = M_\pi|_0$ so this determines our starting pion mass (from the experimental values given later in Table 16) to be $\sim 410\,\text{MeV}$.

However the equivalence of eqs. (79), (80) is only strictly true at lowest order. While at this order it does not matter whether we kept the quark mass singlet constant, eq. (79), or a particle mass singlet constant, eq. (80), higher order terms mean that it now does. If we make different choices of the quantity we keep constant at the experimentally measured physical value, for example

$$\frac{X_\pi^2}{X_N^2}\,, \quad \frac{X_\pi^2}{X_\Delta^2}\,, \quad \frac{X_\pi^2}{X_\rho^2}\,, \quad \ldots\,, \tag{81}$$

we get slightly different trajectories. The different trajectories begin at slightly different points along the flavour $SU(3)$ symmetric line. Initially they are all parallel with slope -2, but away from the symmetry line they can curve, but will all meet at the physical point. (Numerically we shall later see that this seems to be a small effect.)

An additional effect comes from the choice of Wilson lattice fermions. The physical domain is defined by

$$\begin{aligned} m_l^R &\geq 0 \\ m_s^R &\geq 0\,, \end{aligned} \tag{82}$$

which using eq. (5) translates to

$$m_l \geq -\frac{\frac{1}{3}\alpha_Z}{(1+\frac{2}{3}\alpha_Z)} m_s\,, \qquad m_s \geq -\frac{\frac{2}{3}\alpha_Z}{(1+\frac{1}{3}\alpha_Z)} m_l\,, \tag{83}$$

leading to a non-rectangular region and possibly negative bare quark mass. (These features disappear of course for chiral fermions when $\alpha_Z = 0$.)

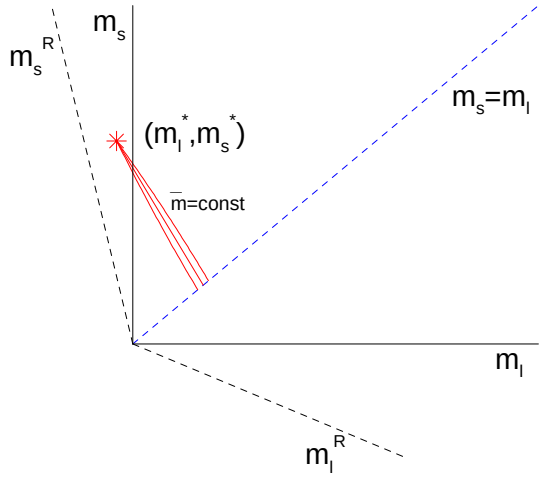


Figure 9: Sketch of some possible paths (red lines) in the m_l–m_s plane to the physical point (m_l^*, m_s^*). Due to eq. (83) the m_l^R and m_s^R axes are not orthogonal when plotted in the bare quark mass plane.

These two features are sketched in Fig. 9, which shows possible paths in the m_l–m_s plane starting from the flavour symmetric line. In this figure the horizontal and vertical axes are the bare quark masses, m_l and m_s respectively. Because of renormalisation effects, eq. (83), lines of constant renormalised mass, m_l^R = constant or m_s^R = constant, will be at an angle. This is in contrast with Fig. 1, where renormalised masses were used as the axes.

7 The lattice – generalities

After the general discussion of $SU(3)$ flavour expansions described in sections 2–5 (which are lattice independent), we now turn to more specific lattice considerations.

7.1 Lattice simulations

We use a clover action for $2+1$ flavours with a single step of mild stout smearing as described in Appendix D. Further details are given in [24] together with a non-perturbative determination of the improvement coefficient for the clover term, using the Schrödinger functional method.

The bare quark masses are defined as

$$am_q = \frac{1}{2}\left(\frac{1}{\kappa_q} - \frac{1}{\kappa_{0;c}}\right) , \tag{84}$$

where vanishing of the quark mass along the $SU(3)$ flavour symmetric line determines $\kappa_{0;c}$. We then keep $\overline{m} = \text{constant} \equiv m_0$ which gives

$$\kappa_s = \frac{1}{\frac{3}{\kappa_0} - \frac{2}{\kappa_l}} \,. \tag{85}$$

So once we decide on a κ_l this then determines κ_s.

How accurately must we satisfy eq. (85)? In choosing suitable (κ_l, κ_s), the natural scale is to say that changes in $\overline{m}$ should be small when compared to $\overline{m}$ itself, i.e. $|\overline{m} - m_0| \ll m_0$ which gives

$$\left| \frac{1}{3} \left(\frac{2}{\kappa_l} + \frac{1}{\kappa_s} \right) - \frac{1}{\kappa_0} \right| \ll \frac{1}{\kappa_0} - \frac{1}{\kappa_{0;c}} \,, \tag{86}$$

which is satisfied if we give all our κs to 6 significant figures.

Furthermore note that we are not expanding about the chiral limit, but have expansions around a flavour symmetric point which does not require knowledge of $\kappa_{0;c}$. This follows as

$$\begin{aligned} \delta m_q &= m_q - \overline{m} \\ &= \frac{1}{2a} \left(\frac{1}{\kappa_q} - \frac{1}{\kappa_0} \right) . \end{aligned} \tag{87}$$

HMC (hybrid Monte Carlo) and RHMC (rational HMC) were used for the 2 and 1 fermion flavours respectively, [25], to generate the gauge configurations. We note the following in connection with the simulations and our path choice:

- The simulations should equilibrate quickly from one point to another along this path, because the effects of making the strange quark mass heavier tend to be cancelled by making the u and d quarks lighter.

- The simulation cost change should be moderate for this path. This may be motivated by the following crude cost argument. Modelling the cost, C, as

  $$C \propto \frac{1}{am_l^R} + \frac{k}{am_s^R} \,, \tag{88}$$

  where k is the relative cost of the two algorithms, gives on the line $a\overline{m} = \text{constant}$

  $$C(\xi) \propto \frac{1}{(1+\alpha_Z) + \xi} + \frac{k}{(1+\alpha_Z) - 2\xi} \,, \tag{89}$$

  with

  $$\xi = \delta m_l / \overline{m} \,, \tag{90}$$

  (alternatively we could consider M_π^2 / X_π^2). The cost $C(\xi)/C(0)$ from the symmetric point $\xi = 0$, is plotted in Fig. 10. There is little change in a reasonably large range of ξ starting from $\xi = 0$.

Both these points are indeed found in practice (at least approximately).

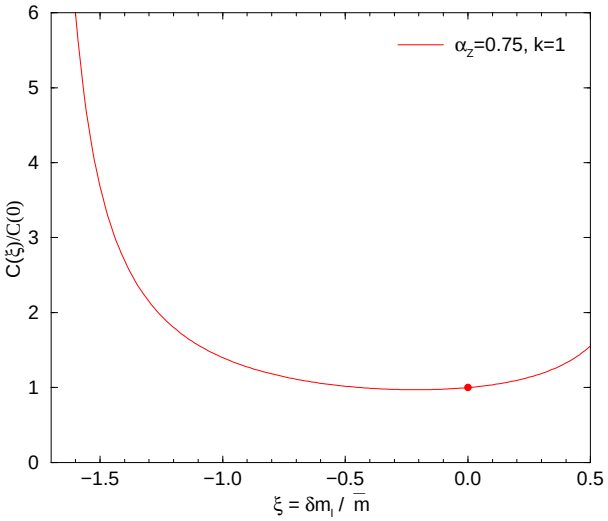


Figure 10: Simulation cost $C(\xi)/C(0)$ against ξ where $\xi = \delta m_l/\overline{m}$ (with, for example $\alpha_Z = 0.75$, cf. eq. (104), and $k = 1$). The symmetric point is denoted by a (red) filled circle. Very roughly we need to reach a region where $\xi \lesssim -1.5$.

7.2 O(a) improvement of the coupling constant

$O(a)$ improvement leads to a change in the coupling constant via [26],

$$g_0^2 \to \tilde{g}_0^2 = g_0^2\,(1 + b_g a\overline{m})\,, \tag{91}$$

where b_g is some function of g_0^2. Not much is known about the value of b_g. For Wilson glue and $\alpha = 0$ (i.e. no-stout smeared links) Wilson-Dirac fermions the lowest order perturbative result is $b_g = 0.01200 n_f g_0^2 + O(g_0^4)$, [26], which is small but increasing with n_f (here $n_f = 3$). A crude estimate was made in [27] and indicated a possible 1–2% effect (but with considerable uncertainty).

In general from eq. (91) when we vary a quark mass then g_0 must be changed to keep $\tilde{g}_0$ constant. However for our choice of path ($\overline{m}$ = constant) the relation between g_0 and $\tilde{g}_0$ is fixed, so only a small overall shift of results might be necessary – nothing else changes as we traverse our path. Therefore in the following we shall not consider the effect of b_g any further.

7.3 Hadron 'sources' and 'sinks'

The operators (or interpolators) used to determine the hadron masses are uniformly taken to be Jacobi smeared ([28] and [29] (Appendix C)) and to be non-relativistic, NR, ([30], [31] and [32] (Appendix C)). Specifically, we consider the following hadron sources and sinks:

- Pseudoscalar meson octet

$$\mathcal{M}_\pi(x) \;=\; \overline{d}(x)\gamma_5 u(x)$$

$$\begin{aligned}\mathcal{M}_K(x) &= \overline{s}(x)\gamma_5 u(x)\\ \mathcal{M}_{\eta_s}(x) &= \overline{s}(x)\gamma_5 s(x)\end{aligned} \tag{92}$$

- Vector meson octet

$$\begin{aligned}\mathcal{M}_{\rho\, i}(x) &= \overline{d}(x)\gamma_i u(x)\\ \mathcal{M}_{K^*\, i}(x) &= \overline{s}(x)\gamma_i u(x)\\ \mathcal{M}_{\phi_s\, i}(x) &= \overline{s}(x)\gamma_i s(x)\end{aligned} \tag{93}$$

- Baryon octet

$$\begin{aligned}\mathcal{B}_{N\,\alpha}(x) &= \epsilon^{abc} u^a_\alpha(x)\left[u^b(x)^{T_D} C\gamma_5 d^c(x)\right]\\ \mathcal{B}_{\Lambda\,\alpha}(x) &= \epsilon^{abc}\left(2s^a_\alpha(x)\left[u^b(x)^{T_D} C\gamma_5 d^c(x)\right]\right.\\ &\qquad \left. + d^a_\alpha(x)\left[u^b(x)^{T_D} C\gamma_5 s^c(x)\right] - u^a_\alpha(x)\left[d^b(x)^{T_D} C\gamma_5 s^c(x)\right]\right)\\ \mathcal{B}_{\Sigma\,\alpha}(x) &= \epsilon^{abc} u^a_\alpha(x)\left[u^b(x)^{T_D} C\gamma_5 s^c(x)\right]\\ \mathcal{B}_{\Xi\,\alpha}(x) &= \epsilon^{abc} s^a_\alpha(x)\left[s^b(x)^{T_D} C\gamma_5 u^c(x)\right]\end{aligned} \tag{94}$$

- Baryon decuplet

$$\begin{aligned}\mathcal{B}_{\Delta\,\alpha}(x) &= \epsilon^{abc}\left(2u^a_\alpha(x)\left[u^b(x)^{T_D} C\gamma_- d^c(x)\right] + d^a_\alpha(x)\left[u^b(x)^{T_D} C\gamma_- u^c(x)\right]\right)\\ \mathcal{B}_{\Sigma^*\,\alpha}(x) &= \epsilon^{abc}\left(2u^a_\alpha(x)\left[u^b(x)^{T_D} C\gamma_- s^c(x)\right] + s^a_\alpha(x)\left[u^b(x)^{T_D} C\gamma_- u^c(x)\right]\right)\\ \mathcal{B}_{\Xi^*\,\alpha}(x) &= \epsilon^{abc}\left(2s^a_\alpha(x)\left[s^b(x)^{T_D} C\gamma_- u^c(x)\right] + u^a_\alpha(x)\left[s^b(x)^{T_D} C\gamma_- s^c(x)\right]\right)\\ \mathcal{B}_{\Omega\,\alpha}(x) &= \epsilon^{abc} s^a_\alpha(x)\left[s^b(x)^{T_D} C\gamma_- s^c(x)\right]\end{aligned} \tag{95}$$

where $C = \gamma_2\gamma_4$ and $\gamma_- = \frac{1}{2}(\gamma_2 + i\gamma_1)$ and the superscript ^{T_D} is a transpose in Dirac space. The u and d quarks are considered as distinct, but of degenerate mass.

The correlation functions (on a lattice of temporal extension T) we use are given by

$$\begin{aligned}C_{\pi_O}(t) &= \frac{1}{V_s}\left\langle \sum_{\vec{y}} \mathcal{M}_{\pi_O}(\vec{y},t) \sum_{\vec{x}} \mathcal{M}^\dagger_{\pi_O}(\vec{x},0)\right\rangle\\ &\propto A\left(e^{-M_{\pi_O} t} + e^{-M_{\pi_O}(T-t)}\right), \qquad \pi_O = \pi, K, \eta_s\\ C_{\rho_O}(t) &= \frac{1}{3V_s}\sum_i \left\langle \sum_{\vec{y}} \mathcal{M}_{\rho_O\, i}(\vec{y},t) \sum_{\vec{x}} \mathcal{M}^\dagger_{\rho_O\, i}(\vec{x},0)\right\rangle\\ &\propto A\left(e^{-M_{\rho_O} t} + e^{-M_{\rho_O}(T-t)}\right), \qquad \rho_O = \rho, K^*, \phi_s\\ C_{N_O}(t) &= \frac{1}{V_s}\,\mathrm{Tr}_D\Gamma_{unpol}\left\langle \sum_{\vec{y}} \mathcal{B}_{N_O}(\vec{y},t) \sum_{\vec{x}} \overline{\mathcal{B}}_{N_O}(\vec{x},0)\right\rangle\end{aligned}$$

$$
\begin{aligned}
&\propto \quad Ae^{-M_{N_O}t} + Be^{-M'_{N_O}(T-t)}\,, \qquad N_O = N, \Sigma, \Xi \\
C_{N_\Lambda}(t) &= \frac{1}{V_s}\,\mathrm{Tr}_D\Gamma_{pol}\left\langle \sum_{\vec{y}} \mathcal{B}_{N_\Lambda}(\vec{y},t) \sum_{\vec{x}} \overline{\mathcal{B}}_{N_\Lambda}(\vec{x},0)\right\rangle \\
&\propto \quad Ae^{-M_{N_\Lambda}t} + Be^{-M'_{N_\Lambda}(T-t)}\,, \\
C_{\Delta_O}(t) &= \frac{1}{V_s}\,\mathrm{Tr}_D\Gamma_{pol}\left\langle \sum_{\vec{y}} \mathcal{B}_{\Delta_O}(\vec{y},t) \sum_{\vec{x}} \overline{\mathcal{B}}_{\Delta_O}(\vec{x},0)\right\rangle \\
&\propto \quad Ae^{-M_{\Delta_O}t} + Be^{-M'_{\Delta_O}(T-t)}\,, \qquad \Delta_O = \Delta, \Sigma^*, \Xi^*, \Omega
\end{aligned} \tag{96}
$$

with $\Gamma_{unpol} = \frac{1}{2}(1+\gamma_4)$ and $\Gamma_{pol} = \Gamma_{unpol}(1+i\gamma_3\gamma_5)$. M' is the lowest excited state with opposite parity to M.

8 The lattice – results

All the results given in this article will be at $\beta \equiv 10/g_0^2 = 5.50$, $\alpha = 0.1$, together with $c_{sw} = 2.65$, see Appendix D. (This β value was located by an initial series of short degenerate quark mass runs, to give a rough idea of the associated scale.) The hadron masses will be given below in a series of Tables 19–30. The runs on $24^3 \times 48$ lattices have $O(2000)$ trajectories, while the runs on $32^3 \times 64$ lattices have $O(1500)$–$O(2000)$ trajectories. Errors are determined using the bootstrap method. Experimental values of the hadron masses are given in section 9.

8.1 Locating κ_0 and the $\mathbf{m_s^R}$–$\mathbf{m_l^R}$ plane

From the discussion in section 6 for our path choice, we must first determine the starting value on the flavour symmetric line. A series of runs along the $SU(3)$ flavour line determines this point, κ_0, by checking when X_π^2/X_S^2, $S = N$, Δ, ρ are equal to their physical values, see eqs. (80), (81). (This would also include $S = r$ if we have previously determined the physical value of r_0.) On the flavour symmetric line obviously all the particles in the multiplet are mass degenerate, so for example taking $S = N$ means that

$$
\frac{(aM_\pi)^2}{(aM_N)^2} = \left.\frac{X_\pi^2}{X_N^2}\right|^*\,, \tag{97}
$$

where, to emphasise that the left-hand side are the lattice measurements, we temporarily include the lattice spacing. (Again, the star denotes the experimental value.)

Once we have located a promising κ_0 (or better a small range of κ_0s) then we keep $\overline{m}$ = constant and pick appropriate (κ_l, κ_s) values, using eq. (85). Again, setting X_π^2/X_N^2 = physical value, eq. (80) can be re-written as

$$
\frac{2M_K^2 - M_\pi^2}{X_N^2} = c_N - 2\frac{M_\pi^2}{X_N^2}\,, \qquad c_N = 3\left.\frac{X_\pi^2}{X_N^2}\right|^*\,, \tag{98}
$$

considering for the present only lowest order in the flavour expansion. In Fig. 11 we plot $(2M_K^2 - M_\pi^2)/X_N^2$ versus M_π^2/X_N^2. This is equivalent to plotting m_s^R

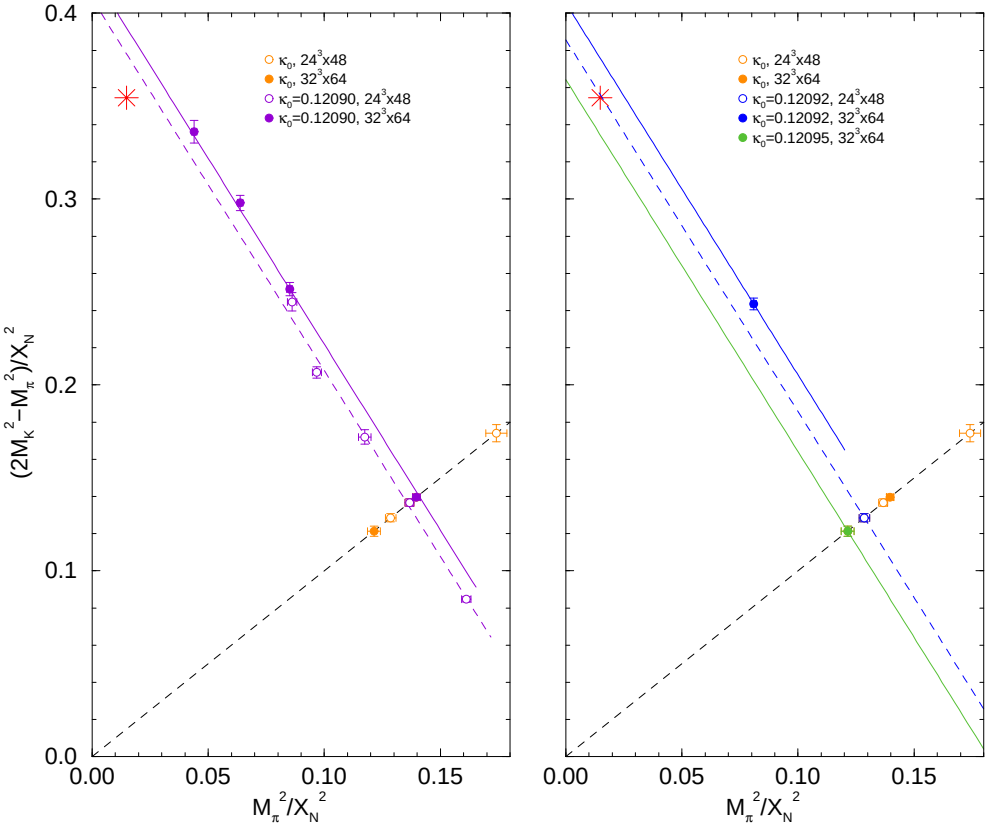


Figure 11: $(2M_K^2 - M_\pi^2)/X_N^2$ versus M_π^2/X_N^2 for $\kappa_0 = 0.12090$ (left panel) and 0.12092, 0.12095 (right panel). The dashed black line, $y = x$ represents the $SU(3)$ flavour symmetric line. Filled points are on $32^3 \times 64$ lattices while open points are on a $24^3 \times 48$ sized lattice. Shown are points on the flavour symmetric line (coloured orange) followed by results with $\overline{m}$ = constant (coloured violet, left panel; blue and green, right panel). The fits are from eq. (98) with c_N a free parameter. The physical value is denoted by a (red) star.

against m_l^R because from LO χPT, $M_\pi^2 \propto m_l^R$ and $2M_K^2 - M_\pi^2 \propto m_s^R$.

Note that simulations with a 'light' strange quark mass and heavy 'light' quark mass are possible – here the right most points in Fig. 11. In this inverted strange world we would expect the weak interaction decays $p \to \Sigma$ or Λ.

Also shown in Fig. 11 are fits using eq. (98) leaving c_N as a free parameter starting from the flavour symmetric points

$$\kappa_0 = 0.12090\,, \quad \kappa_0 = 0.12092\,, \quad \kappa_0 = 0.12095\,, \tag{99}$$

(the latter two points are reference points). It is seen from the figure that this range covers the possible paths to the physical point. There are two observations

to be made. Firstly we note that there does not seem to be much non-linearity in the data, i.e. the leading order in the expansion about the flavour symmetric line already seems sufficient. So if $c_N = 3(X_\pi^2/X_N^2)|^*$ then the lines would go exactly through the physical point. Also this means from the discussion in section 6 that using other singlet scale choices should lead to a similar result. Secondly, as noted before at the end of section 3, as the expansions have been derived using only group theoretic arguments, they will be valid for results derived on any lattice volume (though the coefficients of the expansion are still functions of the volume). So here, to test this, we have made separate fits for the two volumes — $24^3 \times 48$ and $32^3 \times 64$. Indeed this shows that finite size effects are present but small.

Thus our present conclusion is that κ in the range 0.12090 – 0.12095 is within a few percent of the reference κ_0. Most of the results reported here will be at $\kappa_0 = 0.12090$.

8.2 Determination of $\kappa_{0;c}$, α_Z

Although not strictly necessary, we briefly indicate here the determination of $\kappa_{0;c}$ and α_Z to illustrate some of the discussion in section 6. Using lowest order χPT (i.e. the fact that the pion mass vanishes if the masses of the light quarks vanish) and

$$(aM_\pi)^2 \propto am_l^R \propto am_l + \alpha_Z a\overline{m}\,, \tag{100}$$

where the constant of proportionality from eq. (77) is $2a\alpha = 2aQ_0 = 2aB_0^R Z_m^{NS}$, we first determine $\kappa_{0;c}$ (the critical hopping parameter on the flavour symmetric line) as defined in eq. (84). In Fig. 12 we show the plot of $(aM_\pi)^2$ versus $1/\kappa_l$ together with linear fits. For the flavour symmetric case, from the blue points we find

$$\frac{1}{\kappa_{0;c}} = 8.25768(23)\,, \qquad \text{or} \quad \kappa_{0;c} = 0.121099(4)\,, \tag{101}$$

which is in good agreement with the Schrödinger functional determination, see Appendix D. Note that for $\kappa_l < \kappa_{0;c}$ the bare am_q is negative, but the renormalised m_q^R is always positive, eq. (83) and Fig. 9. This occurs for the last point on the $32^3 \times 64$ line in Fig. 12.

α_Z can then be estimated using the $\overline{m}$ = constant line as here $(aM_\pi)^2$ vanishes at κ_c giving

$$\alpha_Z = -\frac{am_q|_{\kappa=\kappa_c}}{a\overline{m}} = \frac{\left(\frac{1}{\kappa_{0;c}} - \frac{1}{\kappa_c}\right)}{\left(\frac{1}{\kappa_0} - \frac{1}{\kappa_{0;c}}\right)}\,. \tag{102}$$

Using the $32^3 \times 64$ data only (green points) gives

$$\frac{1}{\kappa_c} = 8.24727(17)\,, \qquad \text{or} \quad \kappa_c = 0.121252(3)\,. \tag{103}$$

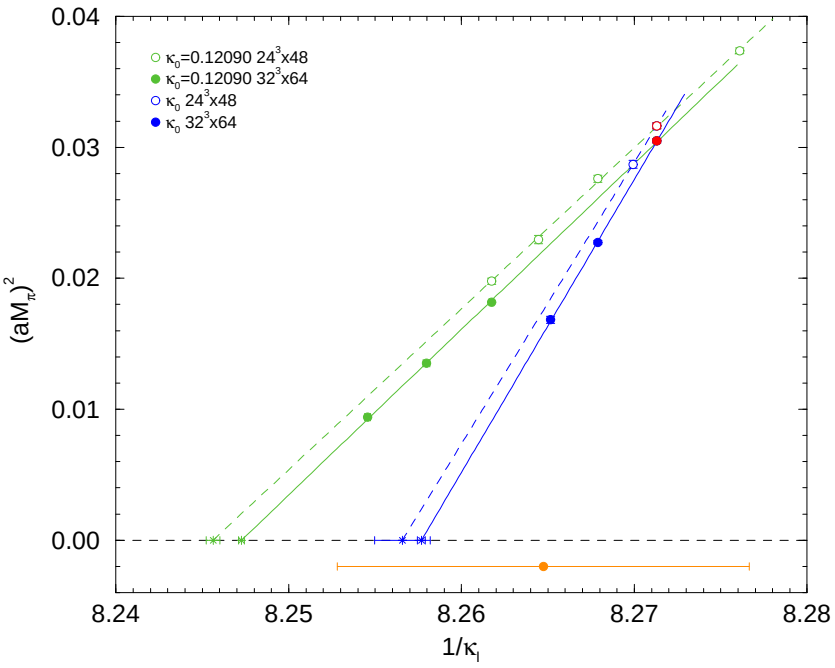


Figure 12: $(aM_\pi)^2$ versus $1/\kappa_l$ for both the flavour symmetric case (blue points) and keeping $\overline{m}$ constant (green points). $24^3 \times 48$ volumes are opaque circles and $32^3 \times 64$ volumes are filled circles. The $\kappa_0 = 0.12090$ points are highlighted in red. The chirally extrapolated values from the linear fits are denoted by stars. The horizontal (orange) filled circle is the Schrödinger functional estimate.

Hence this gives here

$$\alpha_Z \sim 0.76\,. \tag{104}$$

Note that the determination is quite sensitive to small changes in $\kappa_{0;c}$ and κ_c. We conclude that for clover fermions at our lattice spacing α_Z is indeed non-zero.

8.3 Singlet quantities and the scale

We take Fig. 11 as a sign that singlet quantities are very flat and the fluctuations are due to low statistics. We now investigate this further. In Fig. 13 we show aX_S for $S = \Delta,\ N,\ \rho$ and π against M_π^2/X_π^2 for $\kappa_0 = 0.12090$ (left panel) and comparison results for 0.12092, 0.12095 (right panel) together with constant fits. This indicates that other singlet quantities are also rather flat (we interpret variations in X_Δ to be due to statistical fluctuations). Again fits are made for each lattice volume separately.

We showed in section 2.2 that singlet quantities must have zero derivative at the symmetric point. A second derivative would be allowed, but we see from the left-hand panel of Fig. 13 that it must be very small.

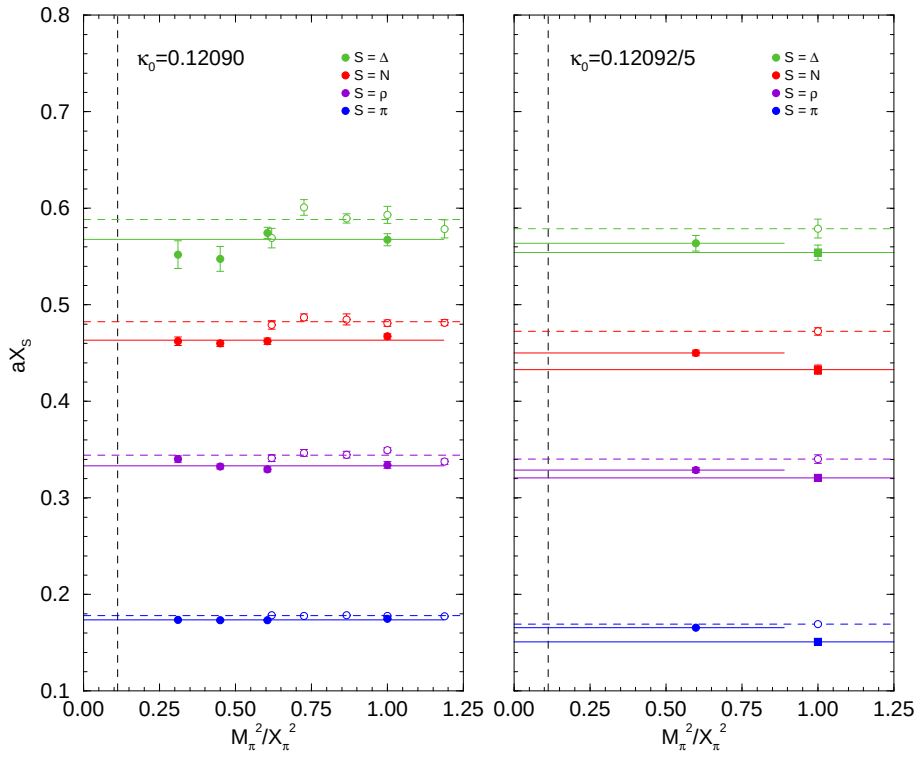


Figure 13: aX_S for $S = \Delta$, N, ρ and π versus M_π^2/X_π^2 for $\kappa_0 = 0.12090$ (left panel, circles) and 0.12092, 0.12095 (right panel, circles and squares respectively) together with constant fits. Filled points and lines are for $32^3 \times 64$ lattices, while opaque points and dashed lines are for $24^3 \times 48$ lattices. (In the right panel the lower filled points and lines are for $\kappa_0 = 0.12095$.) The physical point corresponds to the dashed line at $M_\pi^2/X_\pi^2 = M_\pi^2/X_\pi^2|^*$, while the symmetric point corresponds to $M_\pi^2/X_\pi^2 = 1$ in the figure.

8.3.1 Finite size effects

In Fig. 13 there are again indications of relatively small finite size effects. We now briefly investigate this a little more. While we do not attempt to formally derive a formula here, we do have the obvious constraint that the finite size X_S must also be flat at the symmetry point (symmetry arguments apply in any volume). The various possibilities are given in eq. (41). The first f-term counts the contributions of the kaons and charged pions; the second g-term is irrelevant because the strange pion is fictitious. The third h-term accounts for the η and π^0. So it is likely that the first term is dominant because there are more particles exchanged (the functional forms are all likely to be similar). So if we only want a rough estimate (for the x-axis of the plot) then we shall just choose the first term.

Thus from eq. (41) and as we shall consider only the lowest order term from eq. (48), we expect the finite size functional form to be

$$X_S(L) = X_S\left(1 + c_S \tfrac{1}{3}[f_L(M_\pi) + 2f_L(M_K)]\right) . \tag{105}$$

Lowest order χPT, [33, 34] indicates that a suitable form for $f_L(M)$ is

$$\begin{aligned} f_L(M) &= (aM)^2 \frac{e^{-ML}}{(ML)^{\frac{3}{2}}} , \qquad \text{meson} , \\ f_L(M) &= (aM)^2 \frac{e^{-ML}}{(X_N L)} , \qquad \text{baryon} . \end{aligned} \tag{106}$$

In Fig. 14 we plot $(f_L(M_\pi) + 2f_L(M_K))/3$ against aX_S for $S = \Delta$, N, ρ and π on

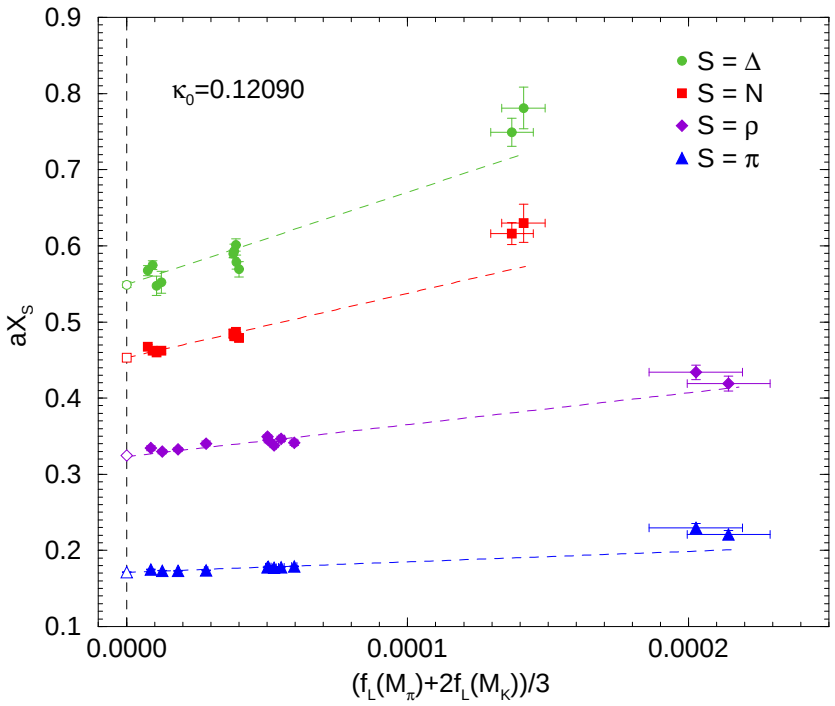


Figure 14: aX_S versus $(f_L(M_\pi)+2f_L(M_K))/3$ for $\kappa_0 = 0.12090$, with $S = \Delta$ (circles), N (squares), ρ (diamonds) and π (upper triangles). The left-most clusters of points are from the $32^3 \times 64$ lattices ($L = 32a$), then follow $24^3 \times 48$ and finally $16^3 \times 32$ lattices. The dashed lines are linear fits.

$32^3 \times 64$, $24^3 \times 48$ and $16^3 \times 32$ lattices for $\kappa_0 = 0.12090$. The fits are linear. A reasonable agreement is seen. (The noisiest signal is for $S = \Delta$.) We see that the extrapolated (i.e. $L \to \infty$) results are very close to the largest lattice results (i.e. $32^3 \times 64$), so we conclude that using the largest lattice size available should only

introduce small errors. We shall also go a little further and assume that finite size effects for masses are similar to those of X_S for each mass of the appropriate multiplet. Thus we shall later consider ratios M/X_S for all the available lattice data; finite size results then tend to cancel in the ratio.

8.3.2 Scale estimation

One advantage of our method is that X_S remains constant and can be used to determine the scale. We do not have to first extrapolate to the physical limit in distinction to other methods.

The result of section 8.3.1 is that the largest volumes available seem to have small finite size effects, so we now simply take the largest volume available. In Fig. 15 we plot aX_S/X_S^*, for $S = N$, Δ, ρ, π using the largest volume fitted results

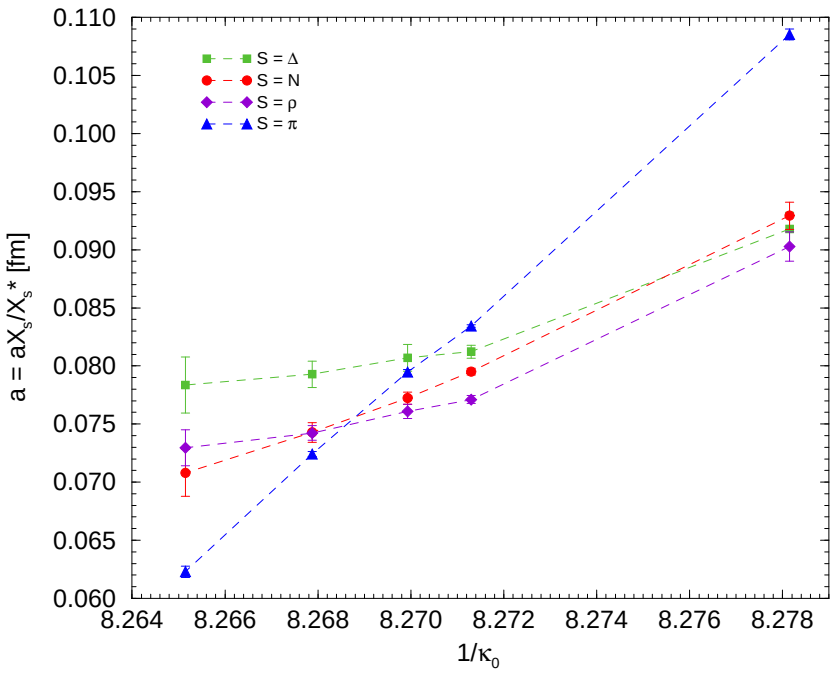


Figure 15: aX_S/X_S^* against $1/\kappa_0$ for $S = \Delta$ (green squares), N (red circles), ρ (violet diamonds), π (blue upper triangles) with $\kappa_0 = 0.12080$, 0.12090, 0.12092, 0.12095 and 0.12099.

from Fig. 13 (together with smaller data sets for $\kappa_0 = 0.12080$ and $\kappa_0 = 0.12099$). The experimental values of X_S^* are given in section 9.1. This ratio gives estimates for the lattice spacing a for the various scales[5]. We would expect most variation

[5]For example for $\kappa_0 = 0.12090$ we find that $a = 0.0834(1)$ fm, $0.0812(6)$ fm, $0.0795(3)$ fm and $0.0771(3)$ fm using X_π, X_Δ, X_N, X_ρ to set the scale respectively.

of the ratio with X_π and convergence to a common scale where the lines cross, assuming

- the simulation statistics are sufficient
- all $O(a^2)$ corrections are negligible
- there is little (or no) curvature present in X_S.

This appears to be the case, with the possible exception of the decuplet scale. However this is the channel with the worst signal, and may be showing some curvature (we cannot at present say whether there might be large $O(a^2)$ effects), so presently we just consider the approximate crossing of the other lines giving $a \sim 0.075$ – $0.078\,\mathrm{fm}$.

As discussed in section 8.3.1 we expect a (partial) cancellation of finite size effects (and also statistical fluctuations) within the same multiplet so we shall adopt the philosophy when considering the hadron spectrum of first finding the ratio of the mass to the singlet quantity from the same multiplet. For example, we can take as our base singlet quantity as the baryon octet X_N (not only are these stable particles under QCD interactions and so might physically be considered a good choice, but X_N also has smaller numerical errors than X_Δ on the lattice). To translate from one scale to another we then need the ratio aX_S/aX_N. In Fig. 16 we plot X_S/X_N for various X_S (with $S = \Delta,\ \rho,\ \pi$). Also shown are constant fits to the two volumes — $24^3 \times 48$ and $32^3 \times 64$. The change in the ratios between the two volumes is seen to be small. Note also that all ratios are close to their physical values. We use the results of the largest volume, which are given in Table 15. In the last column of this table we have used the experimental

Ratio	$\kappa_0 = 0.12090$	$\times(X_N/X_S)\vert^*$
aX_π/aX_N	0.3751(13)	1.049(4)
aX_ρ/aX_N	0.7200(38)	0.971(5)
aX_Δ/aX_N	1.219(9)	1.017(8)

Table 15: Lattice ratios of singlet quantities aX_S/aX_N, $S = \pi,\ \rho,\ \Delta$ from $32^3 \times 64$ lattices. In the last column we have multiplied by the experimental inverse ratio, taken from Table 16. If we had perfect scaling then this ratio should be 1.0.

values of X_S (as given in Table 16) to form the ratio $aX_S/aX_N \times (X_N/X_S)|^*$. This should be one. As can be seen from Fig. 16, this is the case and Table 15 confirms that the ratios are 1 within a few percent. All this shows that $\kappa_0 = 0.12090$ has $\overline{m}$ very close to the correct physical value.

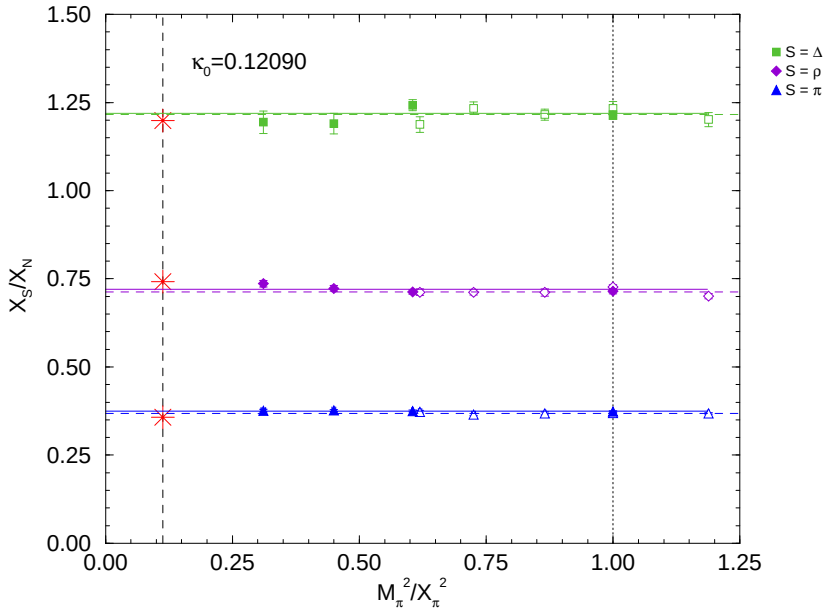


Figure 16: aX_S/aX_N versus M_π^2/X_π^2 for $S = \Delta$ (squares), ρ (diamonds) and π (upper triangles), top to bottom, for $\kappa_0 = 0.12090$. The dashed vertical line represents the physical value, while the dotted line gives the $SU(3)$ flavour symmetric point. Filled points are on $32^3 \times 64$ lattices while open points are on $24^3 \times 48$ sized lattices. Horizontal lines and dashed horizontal lines represent constant fits to either the $32^3 \times 64$ or $24^3 \times 48$ results respectively. For illustration, we also show the physical values – denoted by stars.

9 Spectrum results for $2 + 1$ flavours

We shall now discuss our lattice results.

9.1 Experimental values

As we will compare our lattice results with the experimental results, we first give the experimental masses from the Particle Data Group tables [17].

To minimise u–d quark mass differences (and also electromagnetic effects) for the experimental data, we average the particle masses over isospin I_3 (i.e. horizontally in Figs. 2, 3). This gives the experimental values in Table 17 (we postpone giving them here in order to display them with the lattice values in Table 17). Using these experimental numbers, the experimental values for the hadron singlet quantities used here are then given in Table 16.

Singlet	GeV
$X^*_\pi = \sqrt{(M^2_\pi + 2M^2_K)/3}\|^*$	0.4109
$X^*_\rho = (M_\rho + 2M_{K^*})/3\|^*$	0.8530
$X^*_N = (M_N + M_\Sigma + M_\Xi)/3\|^*$	1.1501
$X^*_\Delta = (2M_\Delta + M_\Omega)/3\|^*$	1.3788

Table 16: Experimental values for the X_S singlet quantities, X^*_S, $S = \pi$, ρ, N and Δ.

9.2 Mass hierarchy

We now consider the lattice results for the mass spectrum. First we check whether there is a strong hierarchy due to the $SU(3)$ flavour symmetry as found in eq. (42), namely

$$\begin{aligned}
4M_\Delta + 3M_{\Sigma^*} + 2M_{\Xi^*} + M_\Omega &\propto (\delta m_l)^0 \quad \text{singlet} \\
-2M_\Delta \quad + M_{\Xi^*} + M_\Omega &\propto \delta m_l \quad \text{octet} \\
4M_\Delta - 5M_{\Sigma^*} - 2M_{\Xi^*} + 3M_\Omega &\propto \delta m_l^2 \quad 27-\text{plet} \\
-M_\Delta + 3M_{\Sigma^*} - 3M_{\Xi^*} + M_\Omega &\propto \delta m_l^3 \quad 64-\text{plet}\,. \qquad (107)
\end{aligned}$$

In Fig. 17 we plot these mass combinations (over X_Δ) against $a\delta m_l$ for $\kappa_0 = 0.12090$. Also shown are the experimental values using the values from Table 17. Note the change of scale between the axes. There is reasonable agreement with these numbers. Well reproduced, as expected, is the order of magnitude drop in the hadron mass contributions with each additional power of δm_l. (See [35] for a similar investigation of octet baryons.) It is also seen that while $(-2M_\Delta + M_{\Xi^*} + M_\Omega)/X_\Delta$ has a linear gradient in δm_l, in the other fits any gradient is negligible as expected. To check for possible finite size effects we also plot a run at the same (κ_l, κ_s) but using a $24^3 \times 48$ lattice rather than $32^3 \times 64$. There is little difference and so it appears that considering ratios of quantities within the same multiplet leads to (effective) cancellation of finite size effects.

9.3 'Fan' plots

We now show a series of plots of the hadron masses from a small quark mass just above the flavour symmetric line down to the physical point. As the masses (of a particular octet or decuplet) are all degenerate at a point on the flavour symmetric line, then we would expect a 'fanning' out of masses from this point. We consider second order fits in the quark mass, but show plots using the pseudoscalar mass on the x-axis, i.e. from eq. (43). Thus we are using the quark mass as an 'internal parameter'. As discussed previously at the end of section 2 and in more detail in Appendix C this is the natural choice.

In Fig. 18 we begin with the pseudoscalar octet and show $M^2_{\pi_O}/X^2_\pi$ ($\pi_O = \pi$,

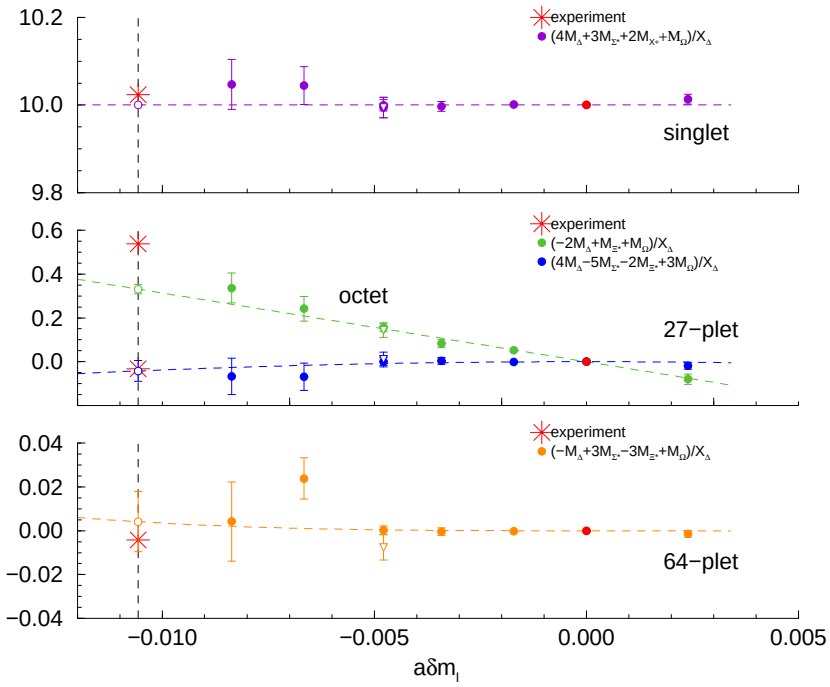


Figure 17: $(4M_\Delta + 3M_{\Sigma^*} + 2M_{\Xi^*} + M_\Omega)/X_\Delta$, $(-2M_\Delta + M_{\Xi^*} + M_\Omega)/X_\Delta$, $(4M_\Delta - 5M_{\Sigma^*} - 2M_{\Xi^*} + 3M_\Omega)/X_\Delta$ and $(-M_\Delta + 3M_{\Sigma^*} - 3M_{\Xi^*} + M_\Omega)/X_\Delta$ (filled circles) against δm_l together with a constant, linear, quadratic and cubic term in δm_l respectively, as given in eq. (107). Extrapolated values are shown as opaque circles. Experimental values are denoted by stars. The opaque triangle corresponds to a run at the same (κ_l, κ_s), but on a $24^3 \times 48$ lattice rather than a $32^3 \times 64$ lattice. The vertical line is at the value of δm_l – δm_l^* obtained from a quadratic fit to the pseudoscalar octet, eqs. (43), (47) as described in section 3 and Fig. 18.

K, η_s) against M_π^2/X_π^2 together with the combined fit of eqs. (43), (47). A typical 'fan' structure is seen with masses radiating from the common point on the symmetric line. Note that the right-most point has a small strange quark mass and a large 'light' quark mass, so that the order of the meson masses is inverted.

There is however little real content in this plot – the $\pi_O = \pi$ line is obviously trivial, for the $\pi_O = K$ line the chiral limit and gradient are known as we have

$$\frac{M_K^2}{X_\pi^2} = \frac{3}{2} - \frac{1}{2}\frac{M_\pi^2}{X_\pi^2}\,. \tag{108}$$

(This can also be seen to $O(\delta m_l^3)$ by using eq. (43) to form M_π^2/X_π^2 and M_K^2/X_π^2 to $O(\delta m_l^2)$.) An inspection of Fig. 18 shows that the numerical results indeed follow very well this line, with a gradient of $-1/2$ and having in the chiral limit a value of $3/2$.

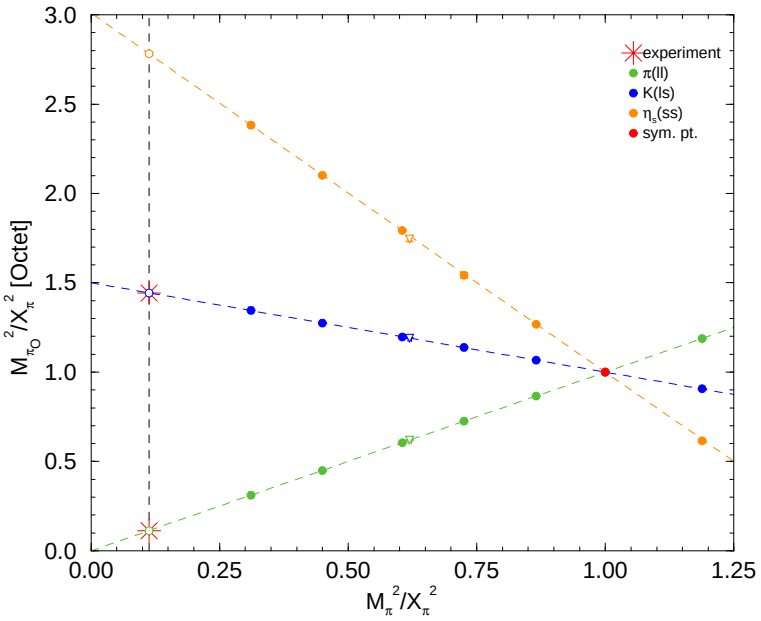


Figure 18: $M^2_{\pi_O}/X^2_\pi$ ($\pi_O = \pi$, K, η_s) against M^2_π/X^2_π together with the combined fit of eq. (43) for both the $32^3 \times 64$ and $24^3 \times 48$ lattices. The flavour symmetric point ('sym. pt.') when $\kappa_0 = 0.12090$ is denoted as a red point. Experimental values are denoted by stars. The opaque triangle corresponds to a run at the same mass but on a $24^3 \times 48$ lattice rather than $32^3 \times 64$.

However the graph does tell us that for the fictitious η_s particle, there is very little curvature which, as this is a constrained fit, must hold for all the pseudoscalar octet particles, including the fictitious one. We also note that ratios within the same multiplet do indeed tend to give cancellation of finite size effects.

In Fig. 19 we plot the vector octet multiplet M_{ρ_O}/X_ρ against M^2_π/X^2_π for $\rho_O = \rho$, K^*, ϕ_s. Again finite volume effects tend to cancel in the ratio (normalising with the singlet quantity from the same octet) and so both volumes have again been used in the fit. The combined fit uses eqs. (44), (43) again with the bare quark mass being an 'internal' parameter. Some moderate curvature is now seen in the extrapolations. Note that as $M_{\phi_s} \approx M_\phi$, the physical ϕ must indeed be almost a perfect $s\overline{s}$ state, i.e. we almost have 'ideal' mixing.

Continuing in Fig. 20 we plot the baryon octet M_{N_O}/X_N for $N_O = N$, Λ, Σ, Ξ against M^2_π/X^2_π and similarly in Fig. 21 we plot the corresponding baryon decuplet M_{Δ_O}/X_Δ for $\Delta_O = \Delta$, Σ^*, Ξ^*, Ω against M^2_π/X^2_π. Although we have included quadratic terms in the fit, there is really very little curvature in the results. In both these pictures the correct ordering of masses is achieved (also the reverse order behind the symmetric point when we have heavy l quark masses and light s quark masses). In particular in Fig. 20 we see that the Λ–Σ splitting is correct. This is a dynamical effect because Λ and Σ both have the same quark

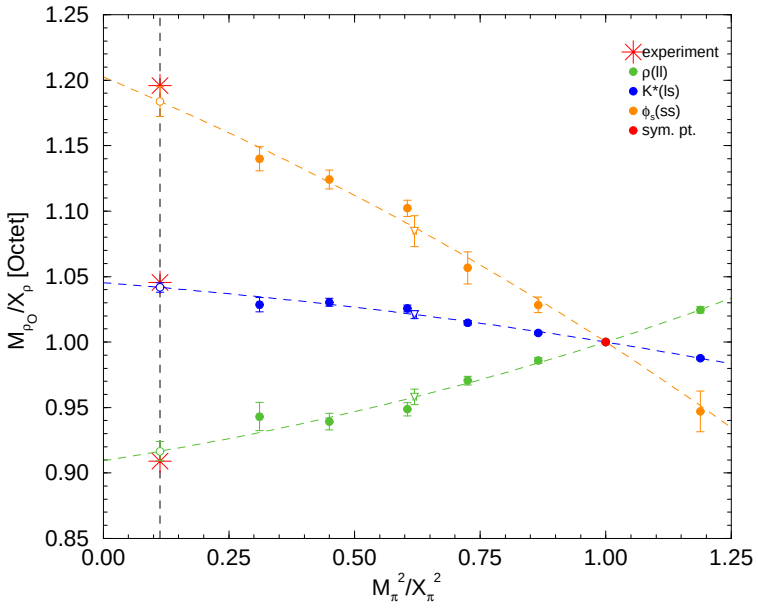


Figure 19: M_{ρ_O}/X_ρ ($\rho_O = \rho$, K^*, ϕ_s) against M_π^2/X_π^2 together with the combined fit of eqs. (44), (43) (the dashed lines). Same notation as in Fig. 18.

content. Also in Fig. 21 M_{Σ^*} is indeed constant as expected.

These results show that the Gell-Mann–Okubo relations work all the way from the symmetry point to the physical point.

The masses (using the scale determined by the appropriate X_S) are given in Table 17. The results are rather close to their experimental values. (M_{η_s} is taken from [36] which uses a quadratic mass formula and ideal mixing which is in agreement with the prediction of LO χPT).) However at present we are effectively using a different scale, X_S, for each multiplet. If we wish to convert these numbers to a base scale, say X_N, then they can be converted using

$$M_{S_O} = \frac{aM_{S_O}}{aX_N} \times X_N|^* = \left(\frac{aM_{S_O}}{aX_S} \times X_S|^*\right) \times \left(\frac{aX_S}{aX_N} \times \left.\frac{X_N}{X_S}\right|^*\right) , \qquad (109)$$

where the second factor is given in the last column of Table 15[6]. These numbers are all ~ 1 (within a few percent). However it is to be noted that this causes the largest discrepancy to the experimental value. So the largest source of error

[6]If using X_N there is an additional factor from the setting of $M_\pi^2/X_\pi^2|^*$ on the x-axis,

$$\left.\frac{M_\pi^2}{X_\pi^2}\right|^* \sim 0.1128 \to \left.\frac{M_\pi^2}{X_N}\right|^* \times \left(\frac{aX_N}{aX_\pi}\right)^2 \sim 0.1023\,.$$

The change in the hadron mass due to this is very small (very much smaller than the error bar), so we will ignore this here.

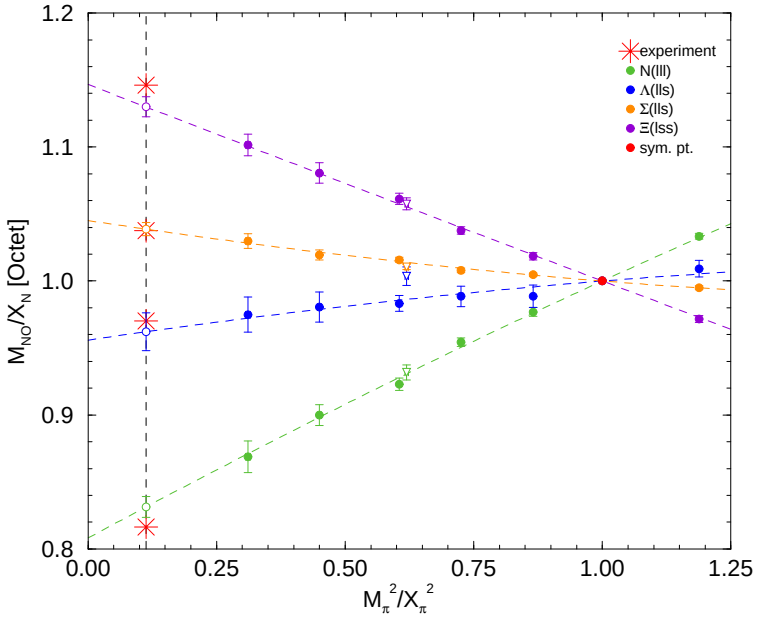


Figure 20: M_{N_O}/X_N ($N_O = N$, Λ, Σ, Ξ) against M_π^2/X_π^2 together with the combined fit of eqs. (45), (43) (the dashed lines). Same notation as in Fig. 18.

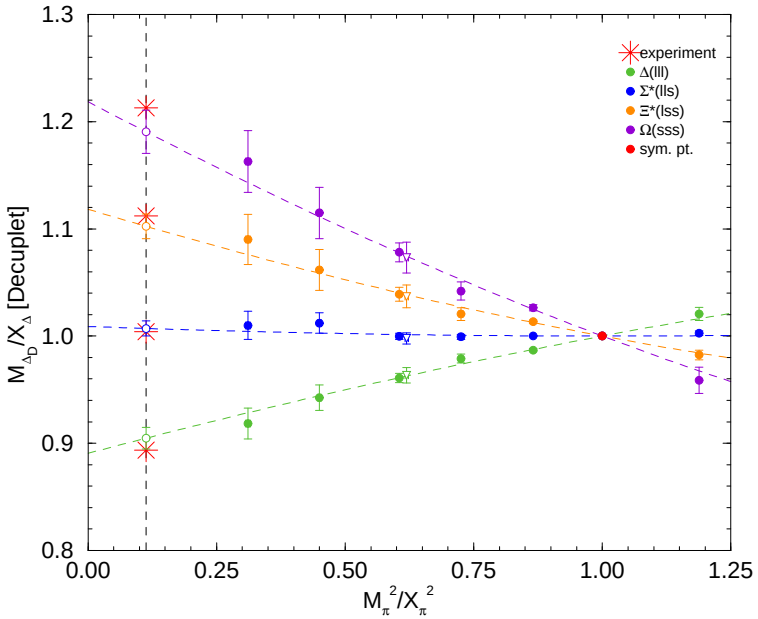


Figure 21: M_{Δ_O}/X_Δ ($\Delta_O = \Delta$, Σ^*, Ξ^*, Ω) against M_π^2/X_π^2 together with the combined fit of eqs. (46), (43). Same notation as in Fig. 18.

particle		expt[GeV]	aM/aX_S	result[GeV]
$M_\pi = (M_{\pi^+} + M_{\pi^0} + M_{\pi^-})/3$	ll	0.1380	0.3359*	0.145(1)
$M_K = M_{K^+} = M_{K^-}$	ls	0.4937	1.2015*	0.518(1)
M_{η_s}	ss	~ 0.685	1.668(3)	0.720(3)
$M_\rho = M_{\rho^+} = M_{\rho^-}$	ll	0.7755	0.9166(73)	0.759(7)
$M_{K^*} = M_{K^{*+}} = M_{K^{*-}}$	ls	0.8917	1.042(4)	0.863(6)
$M_{\phi_s} \sim M_\phi$	ss	1.0195	1.184(12)	0.980(11)
$M_N = (M_p + M_n)/2$	lll	0.9389	0.8313(77)	0.956(9)
M_Λ	lls	1.1157	0.9621(142)	1.107(16)
$M_\Sigma = (M_{\Sigma^+} + M_{\Sigma^0} + M_{\Sigma^-})/3$	lls	1.1932	1.039(5)	1.195(6)
$M_\Xi = (M_{\Xi^0} + M_{\Xi^-})/2$	lss	1.3183	1.130(7)	1.300(9)
M_Δ	lll	1.232	0.9047(100)	1.269(17)
$M_{\Sigma^*} = (M_{\Sigma^{*+}} + M_{\Sigma^{*0}} + M_{\Sigma^{*-}})/3$	lls	1.3846	1.007(7)	1.413(14)
$M_{\Xi^*} = (M_{\Xi^{*0}} + M_{\Xi^{*-}})/2$	lss	1.5334	1.102(11)	1.546(20)
$M_\Omega = M_{\Omega^-}$	sss	1.6725	1.191(20)	1.670(31)

Table 17: The hadron masses. The third column, 'expt', gives the isospin averaged masses. (The η_s mass is taken from [36].) The fourth column, aM/aX_S, gives the numerical results from Figs. 18 – 21. (The aM/aX_π values for M_π, M_K are exact.) The last column, 'result', has used eq. (109) to convert the scale to the base scale X_N.

appears to come from the uncertainty in the consistency of different flavour singlet quantities used to determine the common scale.

9.4 Partially quenched results

We illustrate partial quenching using baryon splittings as an example. The splittings depend mainly on $\mu_s - \mu_l$ and only weakly (at second order) on other quark combinations. In the PQ data shown here, we have points with a large splitting between μ_s and μ_l reaching up to points where $\mu_s - \mu_l$ is equal to its physical value. We can therefore make partially quenched splitting plots reaching down to the physical point.

We have generated partially quenched results on an ensemble with $\kappa_0 = 0.12090$ and lattice volume $24^3 \times 48$. The first baryon octet splitting 'flag' diagram, Fig. 22, shows just the PQ data. The second, Fig. 23, shows the PQ data in grey, compared with the unitary $24^3 \times 48$ data in colour. While only to be taken as an illustration, it shows that the PQ data has the potential to be a good predictor of real data.

Of course partially quenched data is not a complete substitute for simulations at the physical point, even for splittings. If we take the Σ-N splitting as an example, we find from eq. (62),

$$M_N - M_\Sigma \;=\; (A_1 + A_2)(\delta\mu_l - \delta\mu_s)$$

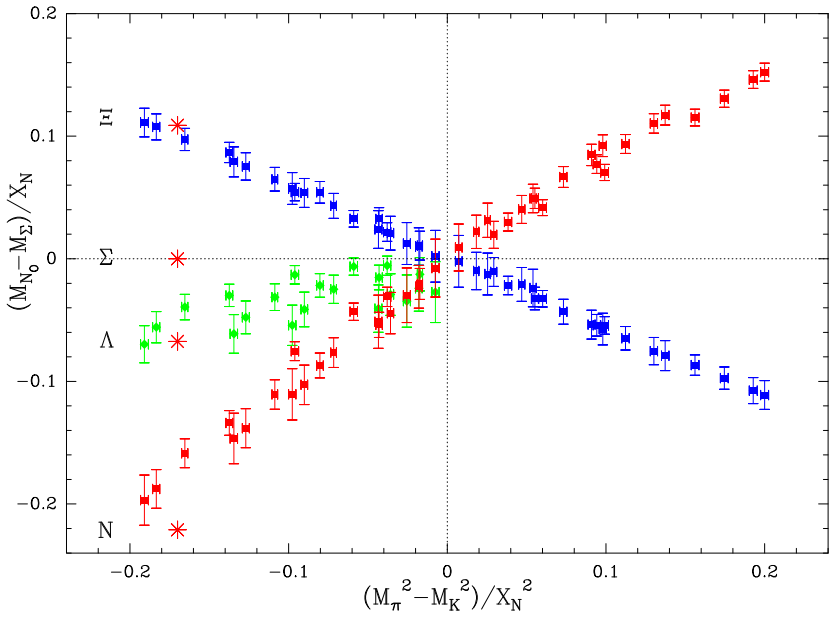


Figure 22: Partially quenched data, $(M_{N_O} - M_\Sigma)/X_N$ versus $(M_\pi^2 - M_K^2)/X_N^2$. The experimental points are denoted by red stars.

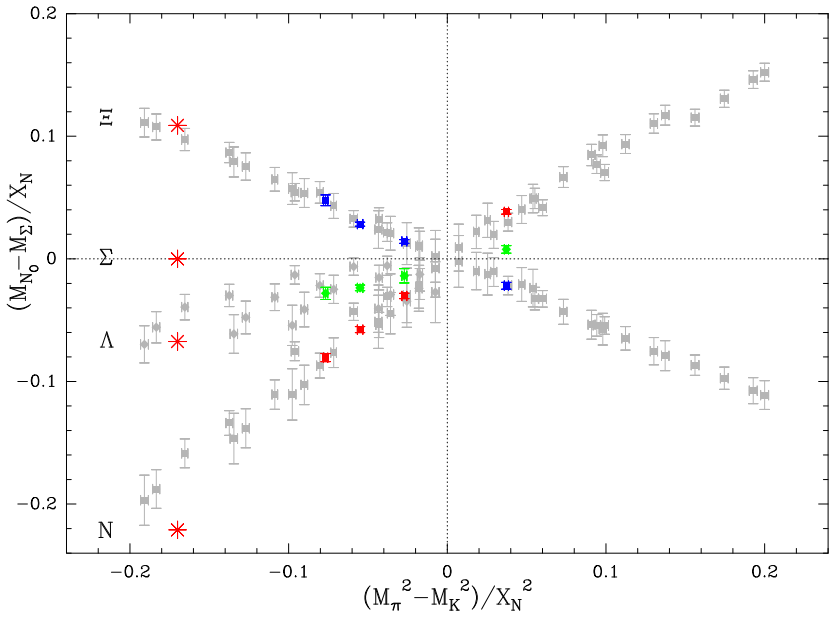


Figure 23: A comparison between partially quenched and full data from $24^3 \times 48$ lattices, $(M_{N_O} - M_\Sigma)/X_N$ versus $(M_\pi^2 - M_K^2)/X_N^2$. Same notation as in Fig. 22.

$$
\begin{aligned}
& +(B_1+B_2)(\delta\mu_l^2-\delta\mu_s^2)-B_3(\delta\mu_l-\delta\mu_s)^2 \\
= \; & (A_1+A_2)(\delta\mu_l-\delta\mu_s) \\
& +(B_1+B_2)(\delta\mu_l-\delta\mu_s)(\delta\mu_l+\delta\mu_s)-B_3(\delta\mu_l-\delta\mu_s)^2\,. \qquad (110)
\end{aligned}
$$

If we plot this baryon splitting against the quark mass splitting $(\delta\mu_l - \delta\mu_s)$ the A_1, A_2 and B_3 terms give a simple parabola (as does the B_4 term if we consider a splitting involving the Λ). However the B_1 and B_2 terms do not depend purely on the splitting $(\delta\mu_l-\delta\mu_s)$, they also depend on the quark-mass sum $(\delta\mu_l+\delta\mu_s)$. Thus the B_1 and B_2 terms lead to a broadening of data bands in Fig. 22 (two data points with the same value of $(\delta\mu_l-\delta\mu_s)$ may have differing values of $(\delta\mu_l+\delta\mu_s)$), and can lead to the partially quenched data missing the physical point slightly. Although we reach splittings $(\delta\mu_l - \delta\mu_s)$ equal to and even a little larger than the physical quark mass splitting, we do this with our light valence quark still noticeably heavier than the real u and d quarks, so $(\delta\mu_l + \delta\mu_s) > (\delta m_l^* + \delta m_s^*)$ at our end-point. The above argument still applies (with minor modifications) if we use the partially quenched meson mass difference $M_\pi^2 - M_K^2$ as a substitute for $(\delta\mu_l - \delta\mu_s)$ on the figure's x-axis.

10 Conclusions

We have outlined a programme to systematically approach the physical point in simulations of QCD with three flavours starting from a point on the $SU(3)$ flavour symmetric line by keeping the singlet quark mass constant. As we move from the symmetric point $(m_u, m_d, m_s) = (m_0, m_0, m_0)$ towards the physical point along our $\overline{m}$ = constant path, the s quark becomes heavier while the u and d quarks become lighter. These two effects tend to cancel in any flavour singlet quantity. The cancellation is perfect at the symmetric point, and we have found that it remains good down to the lightest points we have simulated.

Since gluonic properties are also flavour singlet, this means that all properties of our configurations, from simple ones such as the plaquette, to more complicated ones such as the potential and r_0, vary slowly along the trajectory. Compared with other paths, the properties of our configurations are already very close to those at the physical point. This has many advantages, from technical ones such as the rapid equilibration when we move to a new mass point, to physically useful results, such as the closeness between partially quenched and full physical results. In addition it also enables the lattice spacing to be determined without an extrapolation to the physical point, and indeed allows the consistency of various definitions to be discussed.

The flavour symmetry expansion is developed here, by classifying up to $O(\delta m_q^3)$ how quark-mass polynomials behave under the S_3 permutation group and the $SU(3)$ flavour group, leading to Table 3, given for $1 + 1 + 1$ quark flavours. We also show that for non-chiral (e.g. clover) fermions, where we have different

renormalisation for the singlet and non-singlet pieces and also have $O(a)$ improvement, that all the additional terms that appear are just these mass polynomials. In section 2.5 we classify the hadron mass matrices, and show that certain combinations, for example the Coleman-Glashow relation, have only small violations (in terms of the quark mass).

Turning now to $2+1$ quark flavours, we have found that the flavour symmetry expansion (again when holding the average quark mass, $\overline{m}$, constant) leads to highly constrained extrapolations (i.e. fits) for non-singlet quantities, such as hadronic masses here, and reduce the number of free parameters drastically. (There is a short discussion of this point at the end of section 2.3 and in section 4.4.) It is also to be noted that a $2+1$ simulation is sufficient to determine most of the expansion coefficients for the $1+1+1$ case (one exception being the particle at the centre of the octet multiplet).

In section 5 we discussed the relationship of the flavour symmetry expansion to the chiral perturbation expansion. Lattice simulations are at somewhat large pion masses which juxtaposes well with the flavour symmetry expansion presented here, while chiral perturbation theory is an expansion about a zero pion mass which lattice simulations strive to reach. In section 5 we give, as an example, the relationship between these expansions for the pseudoscalar octet. We also briefly discuss how a chiral singularity would show up in the flavour symmetric expansion and show that at large n the coefficient would drop like a higher power in $1/n$. (In practice this would be difficult to determine.)

We have also extended these results in section 4 to the partially quenched case (when the masses of the valence quarks do not have to be the same as the sea quark masses, but we still have the constraint for the sea quarks that $\overline{m}$ remains constant). In general we have shown (at least to quadratic quark mass order) that the number of expansion coefficients does not increase. Thus a (cheaper) simulation with partially quenched hadron masses may potentially be of help in determining these coefficients. We also show that on the trajectory $\overline{m}=$ constant the partially quenched error vanishes.

In sections 6–9 numerical results are presented. We first locate in section 9.1 a suitable point on the flavour symmetric line, which we take as our initial point for the trajectory $\overline{m}=$ constant. This path can be compared with the trajectory from other collaborations. In Fig. 24 we show the left panel of Fig. 11 again together with results from the PACS-CS Collaboration, [19] and the HS Collaboration, [20]. The strategy of the HS Collaboration was to keep the strange quark mass constant (by considering $(2M_K^2-M_\pi^2)/M_\Omega^2$ versus M_π^2/M_Ω^2, the 'JLAB' plot). We see that their points are indeed approximately constant on our plot.

We then show numerically that flavour singlet quantities, aX_S ($S=\Delta$, N, ρ and π) remain constant on the path $\overline{m}=$ constant. As the linear term is not present, this is a sensitive test of the presence of higher order terms in the flavour symmetry expansion and indicates that they appear to be small. This also allows an estimation of the scale, a, and a discussion of its consistency. As

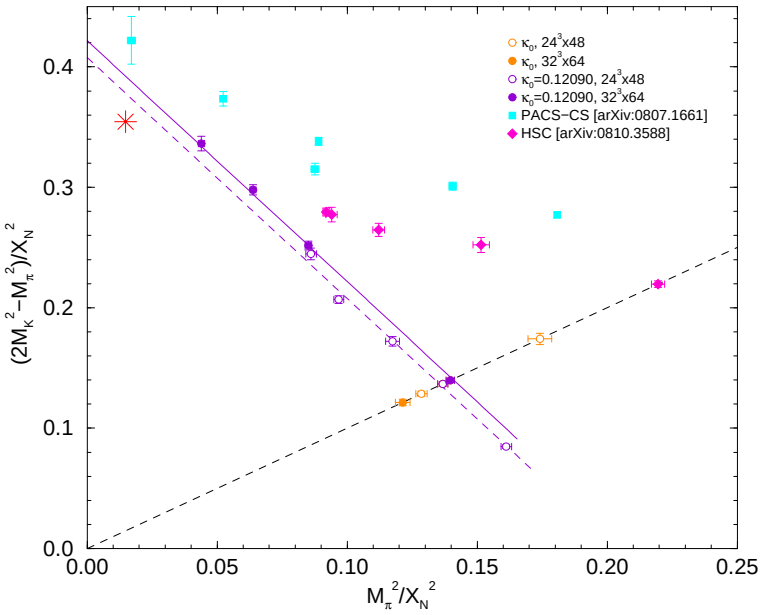


Figure 24: $(2M_K^2 - M_\pi^2)/X_N^2$ versus M_π^2/X_π^2 for $\kappa_0 = 0.12090$. The dashed black line, $y = x$ represents the $SU(3)$ flavour symmetric line. Filled violet circles are on $32^3 \times 64$ lattices while open violet circles are on a $24^3 \times 48$ sized lattice. Shown are also points on the flavour symmetric line (open and filled orange circles). The fits are from eq. (98). Results from the PACS-CS Collaboration, [19] and the HS Collaboration, [20] are given by cyan coloured squares and magenta coloured diamonds respectively. The physical value is denoted by a (red) star.

can be seen from Fig. 24 our trajectory does not reach the physical point exactly. This is reflected in the fact that different definitions of the scale in Table 15 (last column) give results varying by a few percent.

Results for the hadron mass spectrum are then shown. Numerically we first see a mass hierarchy, which confirms our theoretical expectation from the flavour symmetric expansion. A series of 'fan' plots for the various multiplets are then given, with fits which use the flavour symmetric expansion and show that indeed all fits for the pseudoscalar, vector and baryon octets and baryon decuplet are highly linear. The higher order terms are very small – one early hint of this is the fact that the Gell-Mann–Okubo relations work so well for hadron masses. We also note that simulations with a 'light' strange quark mass and heavy 'light' quark mass are possible – here the right most points in Figs. 18 – 21. In this inverted strange world we would expect the weak interaction decays $p \to \Sigma$ or Λ.

In Fig. 25 we plot the results from Table 17 and compare them with the experimental results (also given in this table) for the octet and decuplet hadron multiplets. This means that our physical input necessary to determine the hadron mass spectrum is κ_0 (i.e. ideally the value corresponding to $\overline{m}^R = \overline{m}^{R\,*}$), together

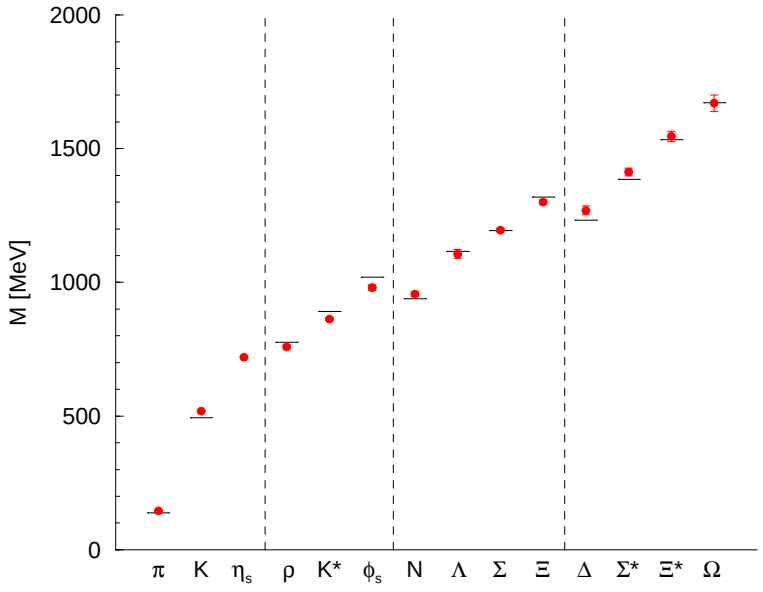


Figure 25: The masses of the octet and decuplet multiplets as given in Table 17 using X_N to determine the scale, together with the experimental values (short horizontal lines).

with $m_\pi^2/X_\pi^2|^*$ and $X_N|^*$.

Exploratory partially quenched results for the baryon octet spectrum are shown, using the heavier $24^3 \times 48$ data. It is illustrated that they contain useful information and allow for the possibility that partially quenched results can help in the determination of coefficients in the flavour symmetry expansion. (We plan to discuss this further in [18].)

We are also applying this method to the computation of matrix elements, [37], some initial numerical results are given in [38, 39, 40].

Acknowledgements

The numerical calculations have been performed on the IBM BlueGeneL at EPCC (Edinburgh, UK), the BlueGeneL and P at NIC (Jülich, Germany), the SGI ICE 8200 at HLRN (Berlin-Hannover, Germany) and the JSCC (Moscow, Russia). We thank all institutions. The BlueGene codes were optimised using Bagel, [41]. This work has been supported in part by the EU grants 227431 (Hadron Physics2), 238353 (ITN STRONGnet) and by the DFG under contract SFB/TR 55 (Hadron Physics from Lattice QCD). JMZ is supported by STFC grant ST/F009658/1.

Appendix

A The permutation group S_3

If we have three quarks u, d and s with different masses, physics should be unchanged if we simply permute the names we give to the quarks. The permutation group is not the complete symmetry group – for example we could also perform $U(1)$ phase rotations on any particular quark flavour – but it is already enough to tell us something useful. The permutation group of 3 objects, S_3, is the same as the symmetry group of an equilateral triangle, C_{3v}. There are 6 group operations

1. The identity

$$u \to u\,,\ d \to d\,,\ s \to s\,, \tag{111}$$

2. Two cyclic permutations

$$u \to d\,,\ d \to s\,,\ s \to u \qquad \text{and} \qquad u \to s\,,\ s \to d\,,\ d \to u\,, \tag{112}$$

   which correspond to rotations of the triangle through $\pm 120^{\rm o}$, and for a diagram in the I_3–Y plane rotations through $\pm 120^{\rm o}$.

3. Three pair interchanges

$$u \leftrightarrow d\,,\ s \to s; \qquad u \leftrightarrow s\,,\ d \to d; \qquad d \leftrightarrow s\,,\ u \to u\,, \tag{113}$$

   which correspond to the 3 reflection symmetries of the triangle, and reflections of a diagram in the I_3–Y plane.

If an equation is to respect flavour blindness, both sides of the equation should transform the same way under all 6 operations. The representations of the group allow us to arrange for this to hold.

The permutation group S_3 is a subgroup of $SU(3)$ and has 3 irreducible representations [6]: two different singlets, A_1 and A_2; and a doublet E. The group properties of these are briefly summarised in Table 1 and discussed at greater length below.

A.1 Singlet representation A_1

The representation A_1, the trivial representation, includes objects which are invariant under all 6 group operations. Examples include gluonic quantities, such as glueball masses, r_0, $V(r)$, as well as certain averages over hadron multiplets.

(We shall collectively denote these objects by X.) Examples of quark mass polynomials with A_1 symmetry (complete up to $O(m_q^3)$) are

$$\begin{array}{lll} 1 & & \\ \overline{m} & & \\ \overline{m}^2\,, & \delta m_u^2+\delta m_d^2+\delta m_s^2 & \\ \overline{m}^3\,, & \overline{m}(\delta m_u^2+\delta m_d^2+\delta m_s^2)\,, & \delta m_u\delta m_d\delta m_s\,, \end{array} \tag{114}$$

and linear combinations of these. These are the 7 polynomials of symmetry A_1 listed in Table 3, the only change is that in the table we have made the replacement $\overline{m} \to (\overline{m} - m_0)$, appropriate for a Taylor expansion about the point (m_0, m_0, m_0). Any other completely symmetric polynomial is a linear combination of these, for example

$$m_u^3 + m_d^3 + m_s^3 = 3\overline{m}^3 + 3\overline{m}(\delta m_u^2 + \delta m_d^2 + \delta m_s^2) + 3\delta m_u\delta m_d\delta m_s\,. \tag{115}$$

A.2 Singlet representation $\mathbf{A_2}$

This consists of objects which are invariant under cyclic quark permutations (triangle rotations), but which change sign under pair exchanges (reflections). A_2 quantities automatically vanish if any two quark masses are the same. The lowest A_2 quantity for quark masses is $O(m_q^3)$,

$$\begin{aligned} & m_u m_s^2 - m_d m_s^2 + m_d^2 m_s - m_u^2 m_s + m_u^2 m_d - m_d^2 m_u \\ &= \quad (\delta m_s - \delta m_u)(\delta m_s - \delta m_d)(\delta m_u - \delta m_d)\,. \end{aligned} \tag{116}$$

Baryon mass combinations with A_2 symmetry are

$$M_n - M_p - M_{\Sigma^-} + M_{\Sigma^+} + M_{\Xi^-} - M_{\Xi^0}\,, \tag{117}$$

and the corresponding decuplet quantity, with the p and n replaced by Δ^+ and Δ^0, namely $M_{\Delta^+} - M_{\Delta^0} + M_{\Sigma^{*-}} - M_{\Sigma^{*+}} + M_{\Xi^{*0}} - M_{\Xi^{*-}}$. Because particle and anti-particle have the same mass, the mesonic analogue of eq. (117) vanishes.

Group theory tells us that in a $1+1+1$ flavour world, the splitting, eq. (117) would be proportional to eq. (116) and terms of even higher order in m_q (neglecting electromagnetic effects).

A.3 Doublet representation E

By considering A_2 we have found a mass splitting formula for the $1+1+1$ case, but by looking at the doublet E we are able to find some more formulae valid for the $2+1$ case which is of more interest for this work.

The E representation has two states, which mix under the cyclic permutations. We can choose to make one state of the doublet even under the reflection $u \leftrightarrow d$,

and the other state odd. (We could just as well choose any interchange to classify our states, but it makes best sense to choose $u \leftrightarrow d$, because the hadronic universe is almost invariant under that operation.) We have called the even member of the doublet E^+, the odd member E^-. (There does not appear to be a standard notation.)

An example of an E doublet would be the states

$$\frac{1}{\sqrt{6}}\left(2|s\rangle - |u\rangle - |d\rangle\right) \qquad \text{and} \qquad \frac{1}{\sqrt{2}}\left(|u\rangle - |d\rangle\right) . \tag{118}$$

It is easily checked that under any group operation they just mix with each other, for example under the cyclic operation $u \to d$, $d \to s$, $s \to u$:

$$\begin{aligned} \frac{1}{\sqrt{6}}\left(2|s\rangle - |u\rangle - |d\rangle\right) &\to \frac{1}{\sqrt{6}}\left(2|u\rangle - |d\rangle - |s\rangle\right) \\ &= \frac{\sqrt{3}}{2}\,\frac{1}{\sqrt{2}}\left(|u\rangle - |d\rangle\right) - \frac{1}{2}\,\frac{1}{\sqrt{6}}\left(2|s\rangle - |u\rangle - |d\rangle\right) \end{aligned} \tag{119}$$

and so on. In other words, the matrix for a cyclic permutation has the form

$$R = \begin{pmatrix} \cos\theta & \mp\sin\theta \\ \pm\sin\theta & \cos\theta \end{pmatrix} \tag{120}$$

with $\theta = 120^{\rm o}$.

Quark mass terms with E doublet symmetry are

$$\begin{aligned} &\left\{\tfrac{1}{\sqrt{6}}(2m_s - m_u - m_d) \quad , \quad \tfrac{1}{\sqrt{2}}(m_u - m_d)\right\} \\ &\left\{\tfrac{1}{\sqrt{6}}(2m_s^2 - m_u^2 - m_d^2) \quad , \quad \tfrac{1}{\sqrt{2}}(m_u^2 - m_d^2)\right\} \\ &\left\{\tfrac{1}{\sqrt{6}}(m_u m_s + m_d m_s - 2m_u m_d) \quad , \quad \tfrac{1}{\sqrt{2}}(m_u m_s - m_d m_s)\right\} \\ &\left\{\tfrac{1}{\sqrt{6}}(2m_s^3 - m_u^3 - m_d^3) \quad , \quad \tfrac{1}{\sqrt{2}}(m_u^3 - m_d^3)\right\} \\ &\left\{\tfrac{1}{2}(m_u m_s^2 + m_d m_s^2 - m_u^2 m_d - m_u m_d^2) \quad , \right. \\ &\qquad \left. \tfrac{1}{\sqrt{12}}(m_u m_s^2 + m_d m_s^2 + 2m_u^2 m_s - 2m_d^2 m_s + m_u^2 m_d + m_u m_d^2)\right\} \\ &\left\{\tfrac{1}{\sqrt{12}}(m_u m_s^2 + m_d m_s^2 - 2m_u^2 m_s - 2m_d^2 m_s + m_u^2 m_d + m_u m_d^2) \right. \\ &\qquad \left. , \quad \tfrac{1}{2}(-m_u m_s^2 + m_d m_s^2 + m_u^2 m_d - m_u m_d^2)\right\} \end{aligned} \tag{121}$$

The normalisations and phases have been chosen so that each pair transforms in the same way as eq. (118) under all group operations, i.e. the matrices which represent the group operations are the same for every pair.

B Some group theory

If the three quarks have equal masses, the QCD Lagrangian is invariant under a global $U(1)$ transformation of the quark fields

$$\psi \to e^{i\theta}\psi\,, \qquad \overline{\psi} \to \overline{\psi} e^{-i\theta}\,, \tag{122}$$

(corresponding to baryon number conservation) and a global $SU(3)$ flavour transformation

$$\psi \to U\psi\,, \qquad \overline{\psi} \to \overline{\psi}U^\dagger\,, \tag{123}$$

with U a unitary matrix with determinant 1.

If the quarks are all given different masses we still have the freedom to change the phase of each flavour separately, without changing the action, so we have conserved currents for each of the three flavours, and three independent $U(1)$ symmetries.

When the quarks have different masses, flavour $SU(3)$ is no longer a symmetry of the action, a global $SU(3)$ rotation no longer leaves the action unchanged, but we can still use $SU(3)$ to understand the action.

An analogy of our argument comes from ordinary mechanics or quantum mechanics. If we have a quantum mechanical problem which is not rotationally symmetric we lose the conservation of angular momentum. But we do still have the property that if we rotate the Hamiltonian, H, to give a new problem, with the Hamiltonian $H' \neq H$, then the eigenfunctions of the new Hamiltonian H' can be obtained by rotating the eigenfunctions of the original problem. In the case of broken flavour symmetry, imposing this (nearly trivial) condition will constrain the way in which hadron masses can depend on quark masses.

Consider the transformation of the quark mass matrix

$$\mathcal{M} \to U\mathcal{M}U^\dagger \equiv \mathcal{M}'\,, \tag{124}$$

(the flavour analogue of a global gauge rotation in colour). The quarks may have different masses, $\mathcal{M}' \neq \mathcal{M}$, although they are physically equivalent in the sense that the two matrices have the same eigenvalues, but the eigenvectors are rotated

$$\psi' = U\psi, \qquad \overline{\psi}' = \overline{\psi}U^\dagger\,. \tag{125}$$

Let us now use these definitions to investigate the group properties of mass polynomials.

B.1 Flavour permutations, S_3, as a subgroup of SU(3)

We want to concentrate initially on a set of $SU(3)$ matrices which map a diagonal mass matrix to another diagonal matrix when used in eq. (124). These are

- the identity matrix,

$$I = \begin{pmatrix} 1 & 0 & 0 \\ 0 & 1 & 0 \\ 0 & 0 & 1 \end{pmatrix} \tag{126}$$

- the cyclic permutations of the quark flavours,

$$\begin{aligned}
\begin{pmatrix} 0 & 0 & 1 \\ 1 & 0 & 0 \\ 0 & 1 & 0 \end{pmatrix} &= \exp\left\{ i \frac{2\pi}{3\sqrt{3}} \begin{pmatrix} 0 & i & -i \\ -i & 0 & i \\ i & -i & 0 \end{pmatrix} \right\} \\
\begin{pmatrix} 0 & 1 & 0 \\ 0 & 0 & 1 \\ 1 & 0 & 0 \end{pmatrix} &= \exp\left\{ -i \frac{2\pi}{3\sqrt{3}} \begin{pmatrix} 0 & i & -i \\ -i & 0 & i \\ i & -i & 0 \end{pmatrix} \right\}
\end{aligned} \tag{127}$$

- pair interchanges,

$$\begin{aligned}
\begin{pmatrix} 0 & -1 & 0 \\ -1 & 0 & 0 \\ 0 & 0 & -1 \end{pmatrix} &= \exp\left\{ i \frac{\pi}{2} \begin{pmatrix} 1 & 1 & 0 \\ 1 & 1 & 0 \\ 0 & 0 & -2 \end{pmatrix} \right\} \\
\begin{pmatrix} 0 & 0 & -1 \\ 0 & -1 & 0 \\ -1 & 0 & 0 \end{pmatrix} &= \exp\left\{ i \frac{\pi}{2} \begin{pmatrix} 1 & 0 & 1 \\ 0 & -2 & 0 \\ 1 & 0 & 1 \end{pmatrix} \right\} \\
\begin{pmatrix} -1 & 0 & 0 \\ 0 & 0 & -1 \\ 0 & -1 & 0 \end{pmatrix} &= \exp\left\{ i \frac{\pi}{2} \begin{pmatrix} -2 & 0 & 0 \\ 0 & 1 & 1 \\ 0 & 1 & 1 \end{pmatrix} \right\}
\end{aligned} \tag{128}$$

Note that when we interchange a quark pair, we also have to change the sign of the quarks, to keep the determinant equal to 1, as required for a matrix in $SU(3)$. These six matrices are all unitary with determinant 1, so they are all members of $SU(3)$. We have also shown that all the matrices can be written in the canonical $SU(3)$ form $\exp\{i \sum \alpha_j \lambda_j\}$. These matrices form a closed set under multiplication, with a multiplication table matching that of the group S_3, showing that the symmetries of the equilateral triangle are a subgroup of $SU(3)$.

B.2 Group classification of quark mass polynomials

This subsection explains how the final column of Table 3 was calculated.

We can establish many useful results from the S_3 subgroup, but it has its limitations, it does not connect particles in different permutation sets, see Fig. 4. By considering S_3 alone we cannot write down a formula for the mass difference between the Σ^0 and Σ^-, we cannot even show that the two particles have the same mass in the $2+1$ case. To go further we need to consider the full $SU(3)$ group, even though this will involve operations which make the mass matrix non-diagonal.

We can write any $SU(3)$ rotation as a matrix of the form

$$U = \exp\left\{ i \sum_{j=1}^{8} \alpha_j \lambda_j \right\} , \tag{129}$$

where the λ_j are the 8 Gell-Mann matrices (and α_j are real parameters). Here we only need to consider infinitesimal transformations

$$\mathcal{M} \to U\mathcal{M}U^\dagger = \mathcal{M} + i\sum_{j=1}^{8} \alpha_j \left(\lambda_j \mathcal{M} - \mathcal{M}\lambda_j\right) = \mathcal{M} + i\sum_{j=1}^{8} \alpha_j \left[\lambda_j, \mathcal{M}\right] . \quad (130)$$

We write

$$\begin{aligned} \mathcal{O}_j\psi &= \lambda_j\psi \\ \mathcal{O}_j\overline{\psi} &= -\overline{\psi}\lambda_j \\ \mathcal{O}_j\mathcal{M} &= \left[\lambda_j, \mathcal{M}\right] , \end{aligned} \quad (131)$$

to represent the action of the eight generators of $SU(3)$ on spinors and on matrices. The eight operators $\mathcal{O}_j$ are analogous to the three operators J_j in angular momentum.

In $SU(2)$ we use the eigenvalues of the operator

$$J^2 = \sum_{j=1}^{3} J_j^2 , \quad (132)$$

to identify the irreducible representations of angular momentum. Similarly in $SU(3)$ we can use the eigenvalues of the quadratic Casimir operator [9, 10]

$$\mathcal{C} = \frac{1}{4}\sum_{j=1}^{8} \mathcal{O}_j^2 , \quad (133)$$

to identify irreducible representations of $SU(3)$. (The factor $\frac{1}{4}$ is a conventional normalisation.) Acting on a matrix

$$\mathcal{C}\mathcal{M} = \frac{1}{4}\sum_{j=1}^{8} \left[\lambda_j, \left[\lambda_j, \mathcal{M}\right]\right] = \frac{1}{4}\sum_{j=1}^{8} \left(\lambda_j^2\mathcal{M} - 2\lambda_j\mathcal{M}\lambda_j + \mathcal{M}\lambda_j^2\right) . \quad (134)$$

We can now begin classifying polynomial functions of $\mathcal{M}$.

At first order, where we have linear functions of mass and $\mathcal{M}$ can be decomposed as

$$\mathcal{M} = I\,\tfrac{1}{3}\mathrm{Tr}[\mathcal{M}] + \sum_{j=1}^{8} \lambda_j\,\tfrac{1}{2}\mathrm{Tr}[\lambda_j\mathcal{M}] , \quad (135)$$

it is simple. We have

$$\mathrm{Tr}[\mathcal{M}] = \mathcal{M}_{11} + \mathcal{M}_{22} + \mathcal{M}_{33} , \quad (136)$$

which does not change under $SU(3)$ transformations, so it is singlet.

The other elements of $\mathcal{M}$ can be assigned quantum numbers. For example $\mathcal{M}_{21}$ takes a u quark and changes it to a d, so it has $I_3 = -1$ and hypercharge $Y = 0$. The 6 off-diagonal elements of $\mathcal{M}$ form the outer ring of the octet, see for example Fig. 2. The two central elements of the octet are the combinations

$$\begin{aligned} 2\mathcal{M}_{33} - \mathcal{M}_{11} - \mathcal{M}_{22} &\propto \mathrm{Tr}[\lambda_8 \mathcal{M}] \\ \mathcal{M}_{11} - \mathcal{M}_{22} &\propto \mathrm{Tr}[\lambda_3 \mathcal{M}]\,. \end{aligned} \tag{137}$$

These both have $I_3 = Y = 0$. We can check that both are eigenstates of the Casimir operator, with eigenvalue 3, showing that both are pure octet quantities. If we make the substitutions

$$\mathcal{M}_{11} \to m_u\,, \quad \mathcal{M}_{22} \to m_d\,, \quad \mathcal{M}_{33} \to m_s\,, \tag{138}$$

we see that the quantities eqs. (136)–(137) are proportional to the three linear polynomials in Table 3, with the $SU(3)$ assignments given from their behaviour when operated on by the Casimir operator.

It gets more interesting at second order. $(\mathrm{Tr}[\mathcal{M}])^2$ and $\mathrm{Tr}[\mathcal{M}^2]$ are both flavour-singlet functions of the mass matrix. It is more convenient to work with the linear combinations

$$(\mathrm{Tr}[\mathcal{M}])^2\,, \qquad 3\mathrm{Tr}[\mathcal{M}^2] - (\mathrm{Tr}[\mathcal{M}])^2\,, \tag{139}$$

where we have chosen the coefficients so that the second combination will be zero at the $SU(3)$ symmetric point. At second order we should be able to construct functions of the mass matrix that are in the 1, 8 and 27 representations. One way of constructing a quantity that is purely 27-plet is by using the Casimir operator. If we take an arbitrary quadratic function of $\mathcal{M}$ it will usually be a mixture of all three representations. If we multiply by

$$(\mathcal{C} - 3)\mathcal{C}\,, \tag{140}$$

$\mathcal{C}$ will cancel the singlet part, $(\mathcal{C}-3)$ will eliminate the octet part (see Table 18), so

Representation	1	8	10	$\overline{10}$	27	64
Casimir eigenvalue	0	3	6	6	8	15

Table 18: The eigenvalues of the quadratic Casimir operator, $\mathcal{C}$, eq. (133), for the $SU(3)$ representations needed in this article.

the operator eq. (140) leaves a pure 27-plet function of $\mathcal{M}$. Using the eigenvalues in Table 18 we can construct similar operators to project out objects in the other representations of $SU(3)$. Of course it would be tedious to do this by hand: we

have programmed the group operations in Mathematica so that the group theory can be done more easily and rapidly.

Another useful technique is to use the raising and lowering operators $I_\pm$, $U_\pm$, $V_\pm$ [42] to move around within a multiplet. Once we have one state in a multiplet, these operators allow us to construct all the other states. Because infinitesimal $SU(3)$ operations do not preserve diagonality, a typical eigenstate of the Casimir operator will involve all nine elements of the quark mass matrix $\mathcal{M}$, not just the three diagonal elements. For example, if we explicitly write out the $SU(3)$ singlet quantity $3\mathrm{Tr}[\mathcal{M}^2] - (\mathrm{Tr}[\mathcal{M}])^2$ in eq. (139) it is

$$\begin{aligned} P_1 &= 2\mathcal{M}_{11}\mathcal{M}_{11} + 2\mathcal{M}_{22}\mathcal{M}_{22} + 2\mathcal{M}_{33}\mathcal{M}_{33} \\ &\quad +6\mathcal{M}_{12}\mathcal{M}_{21} + 6\mathcal{M}_{13}\mathcal{M}_{31} + 6\mathcal{M}_{23}\mathcal{M}_{32} \\ &\quad -2\mathcal{M}_{11}\mathcal{M}_{22} - 2\mathcal{M}_{11}\mathcal{M}_{33} - 2\mathcal{M}_{22}\mathcal{M}_{33}\,. \end{aligned} \tag{141}$$

We can use the techniques discussed in this section to write down a pure $SU(3)$ 27-plet quantity, with the same S_3 properties as eq. (141); the result is

$$\begin{aligned} P_{27}^{A_1} &= \mathcal{M}_{11}\mathcal{M}_{11} + \mathcal{M}_{22}\mathcal{M}_{22} + \mathcal{M}_{33}\mathcal{M}_{33} \\ &\quad -\mathcal{M}_{12}\mathcal{M}_{21} - \mathcal{M}_{13}\mathcal{M}_{31} - \mathcal{M}_{23}\mathcal{M}_{32} \\ &\quad -\mathcal{M}_{11}\mathcal{M}_{22} - \mathcal{M}_{11}\mathcal{M}_{33} - \mathcal{M}_{22}\mathcal{M}_{33}\,. \end{aligned} \tag{142}$$

Expressed this way, the 27-plet and singlet are clearly different functions of the full 9-element mass matrix. However, if we just consider a diagonal mass matrix, $\mathcal{M}_{ij} = 0$ if $i \neq j$, $\mathcal{M}_{11} = m_u$, $\mathcal{M}_{22} = m_d$, $\mathcal{M}_{33} = m_s$ then the quantities become indistinguishable:

$$\begin{aligned} P_1 &\to 2(m_u^2 + m_d^2 + m_s^2 - m_u m_d - m_u m_s - m_d m_s) \\ &= 3(\delta m_u^2 + \delta m_d^2 + \delta m_s^2) \\ P_{27}^{A_1} &\to m_u^2 + m_d^2 + m_s^2 - m_u m_d - m_u m_s - m_d m_s \\ &= \frac{3}{2}(\delta m_u^2 + \delta m_d^2 + \delta m_s^2)\,. \end{aligned} \tag{143}$$

Both collapse to the same quark mass polynomial, $\delta m_u^2 + \delta m_d^2 + \delta m_s^2$, so this polynomial is allowed to appear in equations for singlet and 27-plet physical quantities, but not in equations for any other $SU(3)$ representation. This polynomial is recorded in Table 3 with the symmetry representations A_1 and 1 or 27.

We can continue and use the methods of this subsection to classify all polynomials up to cubic order, the results are recorded in Table 3.

B.3 Matrix representations of SU(3)

To construct hadron mass matrices for octet and decuplet hadrons we need to analyse 8×8 and 10×10 matrices by their S_3 and $SU(3)$ properties.

To get started we need to construct 8×8 and 10×10 representations of the $SU(3)$ generators. We can do this by considering the known behaviour of the hadron multiplets under the $SU(2)$ subgroups, isospin I, U-spin and V-spin, and the hypercharge, Y, [42]:

$$\begin{array}{lll} \lambda_1 = 2I_1 & \lambda_2 = 2I_2 & \lambda_3 = 2I_3 \\ \lambda_4 = 2V_1 & \lambda_5 = 2V_2 & \\ \lambda_6 = 2U_1 & \lambda_7 = 2U_2 & \lambda_8 = \sqrt{3}\, Y \,. \end{array} \tag{144}$$

These 8×8 or 10×10 λ matrices have the same commutation relations as the usual 3×3 matrices

$$[\lambda_i, \lambda_j] = 2i f_{ijk} \lambda_k \,. \tag{145}$$

Once we have the eight λ matrices for our hadron multiplet we can use eq. (134) to classify any other matrices. For the hadron mass matrices, we need all the flavour-conserving matrices. For the decuplet mass matrix these are all diagonal matrices; but for the octet mass matrix they can include some off-diagonal elements, because the Σ^0 and Λ have the same flavour quantum numbers. Our results for the decuplet and octet matrices are given in Tables 4 and 5.

We have other methods of constructing the matrix representations of $SU(3)$. In addition to the Casimir projection method sketched here, we can start with one matrix which belongs to a known $SU(3)$ representation, and then build all the other matrices in that representation by repeatedly acting with raising and lowering operators. For example, in the decuplet case we know that the 10×10 matrix

$$\begin{pmatrix} 0 & 0 & 0 & 0 & 0 & 0 & 0 & 0 & 0 & 1 \\ 0 & 0 & 0 & 0 & 0 & 0 & 0 & 0 & 0 & 0 \\ 0 & 0 & 0 & 0 & 0 & 0 & 0 & 0 & 0 & 0 \\ 0 & 0 & 0 & 0 & 0 & 0 & 0 & 0 & 0 & 0 \\ 0 & 0 & 0 & 0 & 0 & 0 & 0 & 0 & 0 & 0 \\ 0 & 0 & 0 & 0 & 0 & 0 & 0 & 0 & 0 & 0 \\ 0 & 0 & 0 & 0 & 0 & 0 & 0 & 0 & 0 & 0 \\ 0 & 0 & 0 & 0 & 0 & 0 & 0 & 0 & 0 & 0 \\ 0 & 0 & 0 & 0 & 0 & 0 & 0 & 0 & 0 & 0 \\ 1 & 0 & 0 & 0 & 0 & 0 & 0 & 0 & 0 & 0 \end{pmatrix} , \tag{146}$$

must be a pure 64-plet, because it interchanges the Δ^- and the Ω^-, which changes strangeness by ± 3. From Fig. 7 we see that the 64-plet is the only representation in $10 \otimes \overline{10}$ that can change strangeness by 3 units. Starting from the matrix in eq. (146) we can construct a set of 64 matrices which transform amongst themselves under all group operations eq. (131).

Once we have classified all the 10×10 and 8×8 matrices according to their $SU(3)$ and S_3 behaviour, we can read off the rows of Tables 4 and 5. For example, knowing that the following 8×8 matrix is an octet with symmetry E^- gives the

fifth row of Table 5,

$$\begin{pmatrix} -1 & 0 & 0 & 0 & 0 & 0 & 0 & 0 \\ 0 & 1 & 0 & 0 & 0 & 0 & 0 & 0 \\ 0 & 0 & 0 & 0 & 0 & 0 & 0 & 0 \\ 0 & 0 & 0 & 0 & \frac{2}{\sqrt{3}} & 0 & 0 & 0 \\ 0 & 0 & 0 & \frac{2}{\sqrt{3}} & 0 & 0 & 0 & 0 \\ 0 & 0 & 0 & 0 & 0 & 0 & 0 & 0 \\ 0 & 0 & 0 & 0 & 0 & 0 & 1 & 0 \\ 0 & 0 & 0 & 0 & 0 & 0 & 0 & -1 \end{pmatrix} . \tag{147}$$

B.4 Hadron mass matrices

We describe the hadron masses via a hadron mass matrix $\mathcal{H}$, a 10×10 matrix for the decuplet baryons, an 8×8 matrix for octet baryons or mesons.

If the different quark flavours have different masses, a global $SU(3)$ rotation of the quark mass matrix, eq. (124), leads to a change in the quark mass matrix, $\mathcal{M} \to \mathcal{M}'$, but does not change the eigenvalues of the matrix, or the essential physics of the situation.

What will be the effect of a flavour rotation of the quark Lagrangian on a hadronic mass matrix $\mathcal{H}$?

If we are considering a Taylor expansion for hadronic masses, all the elements of $\mathcal{H}$ will be polynomials of the elements in the quark mass matrix, $\mathcal{M}_{ij}$. Flavour blindness requires that we still get equivalent physics when we change $\mathcal{M}_{ij} \to \mathcal{M}'_{ij}$, i.e. that the eigenvalues of $\mathcal{H}$ are unchanged, and the eigenvectors of $\mathcal{H}$ rotate according to eq. (125). Writing this as an equation,

$$\mathcal{H}' \equiv \mathcal{H}(\mathcal{M}'_{ij}) = U\mathcal{H}(\mathcal{M}_{ij})U^\dagger \,. \tag{148}$$

Using the unitarity of U we can rewrite this as an invariance condition,

$$U^\dagger \mathcal{H}(\mathcal{M}'_{ij})U = \mathcal{H}(\mathcal{M}_{ij}) \,. \tag{149}$$

The effect of changing $\mathcal{M}$ to $\mathcal{M}'$ can be exactly cancelled by the effect of an $SU(3)$ rotation on $\mathcal{H}$.

To construct an invariant matrix satisfying eq. (149) we have to pair up matrices of known symmetry, constructed as described in Appendix B.3, with $\mathcal{M}$ polynomials of known symmetry, constructed using the methods of Appendix B.2. This gives us a hadron mass matrix of the form

$$\begin{aligned} \mathcal{H} \;=\; & \sum(\text{singlet mass polynomial}) \times (\text{singlet matrix}) \\ & + \sum(\text{octet mass polynomial}) \times (\text{octet matrix}) \\ & + \sum(\text{27-plet mass polynomial}) \times (\text{27-plet matrix}) \\ & + \cdots \end{aligned} \tag{150}$$

To give an $SU(2)$ analogy, we can make a rotationally invariant system (i.e. a system with total spin zero), by coupling together two particles with the same J, but not by coupling together two particles with different J. Similarly, to give a hadron mass matrix under the $SU(3)$ operation, eq. (149), we must give every matrix a coefficient of the same symmetry, as shown schematically in eq. (150).

Once we have (with the help of Mathematica), constructed the most general matrix satisfying eq. (149), we make the substitutions $\mathcal{M}_{11} \to m_u$, $\mathcal{M}_{22} \to m_d$, $\mathcal{M}_{33} \to m_s$, and $\mathcal{M}_{ij} \to 0$ if $i \neq j$ to get mass formulae for all the hadrons.

We now consider an example. In Table 6 we list the 6 matrices which can occur in the octet meson mass matrix in the $1+1+1$ flavour case. In the $2+1$ flavour case ($m_u = m_d$) the two E^- matrices drop out, because their coefficients must be odd under the exchange $u \leftrightarrow d$, leaving just 4 matrices which can contribute. We calculate the most general form of the meson mass matrix, by demanding that it is invariant under $SU(3)$ rotations, eq. (149), and find that in the $2+1$ case with $\overline{m} =$ constant we get

$$\mathcal{H} = (M_0^2 + b_1 \delta m_l^2) \begin{pmatrix} 1 & 0 & 0 & 0 & 0 & 0 & 0 & 0 \\ 0 & 1 & 0 & 0 & 0 & 0 & 0 & 0 \\ 0 & 0 & 1 & 0 & 0 & 0 & 0 & 0 \\ 0 & 0 & 0 & 1 & 0 & 0 & 0 & 0 \\ 0 & 0 & 0 & 0 & 1 & 0 & 0 & 0 \\ 0 & 0 & 0 & 0 & 0 & 1 & 0 & 0 \\ 0 & 0 & 0 & 0 & 0 & 0 & 1 & 0 \\ 0 & 0 & 0 & 0 & 0 & 0 & 0 & 1 \end{pmatrix}$$

$$+(a_8 \delta m_l + b_8 \delta m_l^2) \begin{pmatrix} 1 & 0 & 0 & 0 & 0 & 0 & 0 & 0 \\ 0 & 1 & 0 & 0 & 0 & 0 & 0 & 0 \\ 0 & 0 & -2 & 0 & 0 & 0 & 0 & 0 \\ 0 & 0 & 0 & -2 & 0 & 0 & 0 & 0 \\ 0 & 0 & 0 & 0 & 2 & 0 & 0 & 0 \\ 0 & 0 & 0 & 0 & 0 & -2 & 0 & 0 \\ 0 & 0 & 0 & 0 & 0 & 0 & 1 & 0 \\ 0 & 0 & 0 & 0 & 0 & 0 & 0 & 1 \end{pmatrix}$$

$$+5 b_{27} \delta m_l^2 \begin{pmatrix} 1 & 0 & 0 & 0 & 0 & 0 & 0 & 0 \\ 0 & 1 & 0 & 0 & 0 & 0 & 0 & 0 \\ 0 & 0 & 1 & 0 & 0 & 0 & 0 & 0 \\ 0 & 0 & 0 & -3 & 0 & 0 & 0 & 0 \\ 0 & 0 & 0 & 0 & -3 & 0 & 0 & 0 \\ 0 & 0 & 0 & 0 & 0 & 1 & 0 & 0 \\ 0 & 0 & 0 & 0 & 0 & 0 & 1 & 0 \\ 0 & 0 & 0 & 0 & 0 & 0 & 0 & 1 \end{pmatrix}$$

$$+4b_{27}\delta m_l^2 \begin{pmatrix} 1 & 0 & 0 & 0 & 0 & 0 & 0 & 0 \\ 0 & 1 & 0 & 0 & 0 & 0 & 0 & 0 \\ 0 & 0 & -2 & 0 & 0 & 0 & 0 & 0 \\ 0 & 0 & 0 & 3 & 0 & 0 & 0 & 0 \\ 0 & 0 & 0 & 0 & -3 & 0 & 0 & 0 \\ 0 & 0 & 0 & 0 & 0 & -2 & 0 & 0 \\ 0 & 0 & 0 & 0 & 0 & 0 & 1 & 0 \\ 0 & 0 & 0 & 0 & 0 & 0 & 0 & 1 \end{pmatrix} \tag{151}$$

keeping terms up to quadratic order. From this we read off

$$\begin{aligned} M_\pi^2 &= M_0^2 - 2a_8\delta m_l + (b_1 - 2b_8 - 3b_{27})\delta m_l^2 \\ M_K^2 &= M_0^2 + a_8\delta m_l + (b_1 + b_8 + 9b_{27})\delta m_l^2 \\ M_{\eta_8}^2 &= M_0^2 + 2a_8\delta m_l + (b_1 + 2b_8 - 27b_{27})\delta m_l^2 \,. \end{aligned} \tag{152}$$

We can check that these equations are consistent with Table 12:

$$\begin{aligned} 3M_\pi^2 + 4M_K^2 + M_{\eta_8}^2 &= 8(M_0^2 + b_1\delta m_l^2) \\ -3M_\pi^2 + 2M_K^2 + M_{\eta_8}^2 &= 10(a_8\delta m_l + b_8\delta m_l^2) \\ -M_\pi^2 + 4M_K^2 - 3M_{\eta_8}^2 &= 120b_{27}\delta m_l^2 \,. \end{aligned} \tag{153}$$

An alternative method, as discussed in section 3, would be to start from the simultaneous equations in eq. (153) and solve the system to derive eq. (152). Note that in eq. (43) we have also re-written the results in a form to agree with the notation of the partially quenched results, so $a_8 = -\alpha$ and

$$\begin{aligned} b_1 &= \beta_0 + 4\beta_1 + 6\beta_2 + \tfrac{1}{8}\beta_3 \\ b_8 &= \beta_1 + 3\beta_2 + \tfrac{1}{10}\beta_3 \\ b_{27} &= -\tfrac{1}{40}\beta_3 \,. \end{aligned} \tag{154}$$

C Coordinate choice for partially quenched formulae

It is often convenient to plot quantities against the pseudoscalar meson mass squared, because then we know better the location of the physical point and the chiral limit. If we do want to use pseudoscalar mesons, the best choice is to replace the light sea quark by the full (non partially quenched) pion, the light valence quark by the partially quenched pion, and to replace the valence strange quark mass by the partially quenched $\overline{s}_{val}s_{val}$ meson (the 'strange pion'), which we call the η_s. This is a particle that doesn't exist in the real world, but which we can measure in the partially quenched channel. Determining the valence s quark mass from the kaon has disadvantages, as we shall shortly see.

We introduce the mesonic variables

$$\begin{aligned} x \equiv M^2_{\pi full} - M^2_\pi|_0 &= 2\alpha\delta m_l + \beta_0\delta m_l^2 + 2\beta_1\delta m_l^2 \\ y \equiv M^2_{\pi^{PQ}} - M^2_\pi|_0 &= 2\alpha\delta\mu_l + \beta_0\delta m_l^2 + 2\beta_1\delta\mu_l^2 \\ z \equiv M^2_{\eta_s} - M^2_\pi|_0 &= 2\alpha\delta\mu_s + \beta_0\delta m_l^2 + 2\beta_1\delta\mu_s^2\,, \end{aligned} \tag{155}$$

keeping terms up to second order in the quark masses. In terms of these variables the decuplet mass formulae eq. (53) become

$$\begin{aligned} M_\Delta &= M_0 + 3\tilde{A}y + \tilde{B}_0x^2 + 3\tilde{B}_1y^2 \\ M_{\Sigma^*} &= M_0 + \tilde{A}(2y+z) + \tilde{B}_0x^2 + \tilde{B}_1(2y^2+z^2) + \tilde{B}_2(z-y)^2 \\ M_{\Xi^*} &= M_0 + \tilde{A}(y+2z) + \tilde{B}_0x^2 + \tilde{B}_1(y^2+2z^2) + \tilde{B}_2(z-y)^2 \\ M_\Omega &= M_0 + 3\tilde{A}z + \tilde{B}_0x^2 + 3\tilde{B}_1z^2\,, \end{aligned} \tag{156}$$

with

$$\begin{aligned} \tilde{A} &\equiv \frac{A}{2\alpha} \\ \tilde{B}_0 &\equiv \frac{2\alpha B_0 - 3A\beta_0}{8\alpha^3} \\ \tilde{B}_1 &\equiv \frac{\alpha B_1 - A\beta_1}{4\alpha^3} \\ \tilde{B}_2 &\equiv \frac{B_2}{4\alpha^2}\,. \end{aligned} \tag{157}$$

The form of eq. (156) exactly repeats the form of eq. (53), but the new constants involve a combination of curvature terms from the pion mass equation and from the baryon mass equation.

Suppose we use the PQ kaon mass (instead of the strange pion) to represent the strange quark mass, i.e. we replace z defined in eq. (155) by

$$\begin{aligned} w &\equiv 2M^2_{K^{PQ}} - M^2_{\pi^{PQ}} - M^2_{\pi full} \\ &= 2\alpha\delta\mu_s + \beta_0\delta m_l^2 + 2\beta_1\delta\mu_s^2 + 2\beta_2(\delta\mu_s - \delta\mu_l)^2\,. \end{aligned} \tag{158}$$

At first order, w is just as good as z, but if we are interested in curvature, it is less suitable, because at second order it involves both the valence s and the valence l, unlike eq. (155). Using w instead of z, the decuplet mass formulae become

$$\begin{aligned} M_\Delta &= M_0 + 3\tilde{A}y + \tilde{B}_0x^2 + 3\tilde{B}_1y^2 \\ M_{\Sigma^*} &= M_0 + \tilde{A}(2y+w) + \tilde{B}_0x^2 + \tilde{B}_1(2y^2+w^2) + \tilde{B}_2(w-y)^2 + \tilde{B}_X(w-y)^2 \\ M_{\Xi^*} &= M_0 + \tilde{A}(y+2w) + \tilde{B}_0x^2 + \tilde{B}_1(y^2+2w^2) + \tilde{B}_2(w-y)^2 + 2\tilde{B}_X(w-y)^2 \\ M_\Omega &= M_0 + 3\tilde{A}w + \tilde{B}_0x^2 + 3\tilde{B}_1w^2 + 3\tilde{B}_X(w-y)^2\,, \end{aligned} \tag{159}$$

with $\tilde{A}, \tilde{B}_0, \tilde{B}_1, \tilde{B}_2$ defined as in eq. (157), but with an extra curvature coefficient

$$\tilde{B}_X = -\frac{A\beta_2}{4\alpha^3}\,, \tag{160}$$

so one fit constraint is lost (or deeply hidden) if we use the kaon mass to represent the strange mass.

Finally, we want to relate the partially quenched fit to the unitary results, on our trajectory $\frac{1}{3}(2m_l+m_s) = m_0$. If we use bare quark masses as our coordinates, we do this by using the substitutions

$$\delta\mu_l \to \delta m_l\,, \qquad \delta\mu_s \to -2\delta m_l\,, \tag{161}$$

giving

$$\begin{aligned} M_\Delta &= M_0 + 3A\delta m_l + [B_0 + 3B_1]\delta m_l^2 \\ M_{\Sigma^*} &= M_0 \qquad\qquad + [B_0 + 6B_1 + 9B_2]\delta m_l^2 \\ M_{\Xi^*} &= M_0 - 3A\delta m_l + [B_0 + 9B_1 + 9B_2]\delta m_l^2 \\ M_\Omega &= M_0 - 6A\delta m_l + [B_0 + 12B_1]\delta m_l^2\,. \end{aligned} \tag{162}$$

However, if we use meson-based coordinates, such as eq. (155), the mapping back to the unitary result is more complicated,

$$\begin{aligned} y &\to x \\ z &\to -2x + \frac{3(\beta_0 + 4\beta_1)}{4\alpha^2}x^2\,. \end{aligned} \tag{163}$$

The mapping from z, our measure of the strange quark mass, back to x is complicated by a second order term. The reason is clear. On our trajectory, the relation $2\delta m_l + \delta m_s = 0$ is made exactly true for bare lattice quark masses, while the meson mass relations $2M_\pi^2 + M_{\eta_s}^2 \approx$ constant or $2M_K^2 + M_\pi^2 \approx$ constant are only true to leading order. Thus in conclusion if we are considering the curvature terms it is definitely better to use (bare) lattice quark masses as the coordinates.

D The action

The particular clover action used here has a single iterated mild stout smearing, [43] for the hopping terms together with thin links for the clover term (this ensures that the fermion matrix does not become too extended). Together with the (tree level) Symanzik improved gluon action this gives

$$S = S_G + S_{Fu} + S_{Fd} + S_{Fs}\,, \tag{164}$$

with the gluon action

$$S_G = \frac{6}{g_0^2}\left\{c_0 \sum_{Plaquette} \frac{1}{3}\mathrm{Re}\,\mathrm{Tr}(1 - U_{Plaquette}) + c_1 \sum_{Rectangle} \frac{1}{3}\mathrm{Re}\,\mathrm{Tr}(1 - U_{Rectangle})\right\}\,, \tag{165}$$

and

$$\beta = \frac{6c_0}{g_0^2} = \frac{10}{g_0^2} \qquad \text{and} \quad c_0 = \frac{20}{12}\,,\ c_1 = -\frac{1}{12}\,. \tag{166}$$

For each flavour the Wilson–Dirac fermion action is

$$S_{Fq} = \sum_x \left\{ \frac{1}{2}\sum_\mu [\overline{q}(x)(\gamma_\mu - 1)\tilde{U}_\mu(x)q(x+a\hat{\mu}) - \overline{q}(x)(\gamma_\mu+1)\tilde{U}_\mu^\dagger(x-a\hat{\mu})q(x-a\hat{\mu})] \right.$$
$$\left. + \frac{1}{2\kappa_q}\overline{q}(x)q(x) - \frac{1}{4}ac_{sw}\sum_{\mu\nu}\overline{q}(x)\sigma_{\mu\nu}F_{\mu\nu}(x)q(x) \right\}\,, \tag{167}$$

where F is the 'clover' field strength, necessary for $O(a)$-improvement. As the up and down quarks are always taken here as mass degenerate we have $\kappa_u = \kappa_d \equiv \kappa_l$.

To keep the action highly local, the hopping terms use a stout smeared link ('fat link') with $\alpha = 0.1$ 'mild smearing' for the Dirac kinetic term and Wilson mass term,

$$\begin{aligned} \tilde{U}_\mu(x) &= \exp\{iQ_\mu(x)\}\,U_\mu(x) \\ Q_\mu &= \frac{\alpha}{2i}\left[V_\mu U_\mu^\dagger - U_\mu V_\mu^\dagger - \tfrac{1}{3}\mathrm{Tr}(V_\mu U_\mu^\dagger - U_\mu V_\mu^\dagger)\right]\,, \end{aligned} \tag{168}$$

where $V_\mu(x)$ is the sum of all staples around $U_\mu(x)$. The clover term is built from thin links as it is already of length $4a$ and, as previously mentioned, we do not want the fermion matrix to become too extended. Stout smearing is analytic and so a derivative can be taken (so the HMC force is well defined) and also allows for perturbative expansions [44].

The clover coefficient, c_{sw}, has recently been non-perturbatively fixed, [24], by requiring that the axial Ward identity (WI) quark mass determined in several different ways is the same. A sensitive way of achieving this is the Schrödinger functional formalism. Further details of our results may be found in [24]. c_{sw} is determined for 3 mass degenerate or $SU(3)$ flavour symmetric quarks (where $\kappa_l = \kappa_s \equiv \kappa_0$) in the chiral limit. A 5th order polynomial in g_0^2 interpolating between the numerically determined $c_{sw}(g_0)$ points was found to be [24]

$$c_{sw}^*(g_0) = 1 + 0.269041\,g_0^2 + 0.29910\,g_0^4 - 0.11491\,g_0^6 - 0.20003\,g_0^8 + 0.15359\,g_0^{10}\,. \tag{169}$$

(This interpolation function is constrained to reproduce the $O(g_0^2)$ perturbative results, [44], in the $\beta \to \infty$ limit and therefore has four free fit parameters.) We take this result to define c_{sw} for a given β.

Improving one on-shell quantity to $O(a^2)$ (here the axial WI quark mass) fixes $c_{sw}(g_0^2)$ and then all masses are automatically improved to $O(a^2)$,

$$\frac{M_H}{M_{H'}}(a) = \frac{M_H}{M_{H'}}(0) + O(a^2)\,, \tag{170}$$

rather than just to $O(a)$. Operators in general require further $O(a)$ operators together with associated improvement coefficients to ensure $O(a)$–improvement for physical on-shell quantities.

This determination of c_{sw} via the Schrödinger functional formalism also provides an estimate for the critical κ_0, [24], of

$$\kappa_{0;c}(g_0) = \frac{1}{8}\left[1 + 0.002391\, g_0^2 + 0.0122470\, g_0^4 - 0.0525676\, g_0^6 + 0.0668197\, g_0^8 - 0.0242800\, g_0^{10}\right] . \quad (171)$$

(Again this interpolation function is constrained to reproduce the $O(g_0^2)$ perturbative results, [44], in the $\beta \to \infty$ limit. The errors for c_{sw}^* from the fit are estimated to be about 0.4% while for κ_c^* we have 0.02% at $\beta = 14.0$ rising to 0.15% at $\beta = 5.10$.)

The simulations only need knowledge of c_{sw} to proceed; however it is useful to check consistency between different determinations of $\kappa_{0;c}$ (via the Schrödinger functional or the pseudoscalar mass). For $\beta = 5.50$ then using eq. (171) we find $\kappa_{0;c} = 0.120996$ (the direct simulation result is $\kappa_{0;c} = 0.121125(330)$, [24]). This is to be compared with the estimation in section 8.2 which is quite close. (It should also be noted that different determinations should only agree up to $O(a^2)$ effects.)

E Hadron masses

We collect here in Tables 19 – 27 values of the pseudoscalar octet, vector octet, baryon octet and baryon decuplet masses. In Table 19 we give values along the flavour symmetric line ($\kappa_l = \kappa_s = \kappa_0$), while in Tables 20 – 23 and in Tables 24 – 27 we give results for $\kappa_0 = 0.12090$ and $\kappa_0 = 0.12092$ respectively, while keeping $\overline{m}$ = constant, eq. (85).

In Tables 28 – 30 we give the ratios (i.e. hadron octet or decuplet masses normalised with their centre of mass).

The data sets are roughly $\sim O(2000)$ trajectories for the $24^3 \times 48$ lattices and $O(1500)$ – $O(2000)$ trajectories for the $32^3 \times 64$ lattices (with the exception for the $\kappa_0 = 0.12095$ results which are $\sim O(500)$ trajectories). The errors are all taken from a bootstrap analysis of the ratio (which often enables a smaller error to be given for the ratios than simply using error propagation).

κ_0	$N_S^3 \times N_T$	aM_π	aM_ρ	aM_N	aM_Δ
0.12000	$16^3 \times 32$	0.4908(17)	0.6427(23)	0.9612(42)	1.048(6)
0.12030	$16^3 \times 32$	0.4026(19)	0.5635(38)	0.8374(74)	0.9414(107)
0.12050	$24^3 \times 48$	0.3375(24)	0.4953(47)	0.7201(83)	0.8216(89)
0.12080	$24^3 \times 48$	0.2260(10)	0.3903(55)	0.5417(68)	0.6415(99)
0.12090	$16^3 \times 32$	0.2209(49)	0.4192(97)	0.6298(251)	0.7811(274)
0.12090	$24^3 \times 48$	see Tables 20 – 23			
0.12090	$32^3 \times 64$	see Tables 20 – 23			
0.12092	$24^3 \times 48$	see Tables 24 – 27			
0.12095	$32^3 \times 64$	0.1508(4)	0.3209(27)	0.4329(49)	0.5541(80)
0.12099	$32^3 \times 64$	0.1297(10)	0.3154(67)	0.4127(117)	0.5476(168)

Table 19: The results for the hadrons on the symmetric line, aM_π, aM_ρ, aM_N and aM_Δ for $(\beta, c_{sw}, \alpha) = (5.50, 2.65, 0.1)$.

(κ_l, κ_s)	aM_π	aM_K	aM_{η_s}
	$16^3 \times 32$		
(0.121040, 0.120620)	0.1962(74)	0.2447(49)	0.2773(37)
	$24^3 \times 48$		
(0.120830, 0.121040)	0.1933(6)	0.1688(7)	0.1391(11)
(0.120900, 0.120900)	0.1779(6)	0.1779(6)	0.1779(6)
(0.120950, 0.120800)	0.1661(8)	0.1845(7)	0.2011(7)
(0.121000, 0.120700)	0.1515(10)	0.1898(8)	0.2209(6)
(0.121040, 0.120620)	0.1406(8)	0.1949(6)	0.2361(5)
	$32^3 \times 64$		
(0.120900, 0.120900)	0.1747(5)	0.1747(5)	0.1747(5)
(0.121040, 0.120620)	0.1349(5)	0.1897(4)	0.2321(3)
(0.121095, 0.120512)	0.1162(8)	0.1956(5)	0.2512(3)
(0.121145, 0.120413)	0.09694(88)	0.2016(4)	0.2683(3)

Table 20: The results for the pseudoscalar octet mesons: aM_π, aM_K and aM_{η_s} for $(\beta, c_{sw}, \alpha) = (5.50, 2.65, 0.1)$ where $\kappa_0 = 0.12090$.

(κ_l, κ_s)	aM_ρ	aM_{K^*}	aM_{ϕ_s}
	$16^3 \times 32$		
(0.121040, 0.120620)	0.4353(123)	0.4331(84)	0.4380(60)
	$24^3 \times 48$		
(0.120830, 0.121040)	0.3460(22)	0.3335(30)	0.3198(48)
(0.120900, 0.120900)	0.3494(25)	0.3494(25)	0.3494(25)
(0.120950, 0.120800)	0.3400(40)	0.3473(32)	0.3546(27)
(0.121000, 0.120700)	0.3364(43)	0.3517(30)	0.3663(20)
(0.121040, 0.120620)	0.3270(50)	0.3484(28)	0.3701(18)
	$32^3 \times 64$		
(0.120900, 0.120900)	0.3341(34)	0.3341(34)	0.3341(34)
(0.121040, 0.120620)	0.3127(38)	0.3380(21)	0.3632(14)
(0.121095, 0.120512)	0.3123(43)	0.3426(20)	0.3738(11)
(0.121145, 0.120413)	0.3210(63)	0.3500(24)	0.3880(11)

Table 21: The results for the vector octet mesons: aM_ρ, aM_{K^*} and aM_{ϕ_s} for $(\beta, c_{sw}, \alpha) = (5.50, 2.65, 0.1)$ where $\kappa_0 = 0.12090$.

(κ_l, κ_s)	aM_N	aM_Λ	aM_Σ	aM_Ξ
	$16^3 \times 32$			
(0.121040, 0.120620)	0.5817(214)	0.5941(182)	0.6311(128)	0.6353(121)
	$24^3 \times 48$			
(0.120830, 0.121040)	0.4976(25)	0.4859(43)	0.4791(31)	0.4679(39)
(0.120900, 0.120900)	0.4811(33)	0.4811(33)	0.4811(33)	0.4811(33)
(0.120950, 0.120800)	0.4737(68)	0.4794(58)	0.4871(55)	0.4938(48)
(0.121000, 0.120700)	0.4648(46)	0.4815(49)	0.4910(36)	0.5055(28)
(0.121040, 0.120620)	0.4466(66)	0.4810(57)	0.4843(42)	0.5068(32)
	$32^3 \times 64$			
(0.120900, 0.120900)	0.4673(27)	0.4673(27)	0.4673(27)	0.4673(27)
(0.121040, 0.120620)	0.4267(50)	0.4547(43)	0.4697(33)	0.4907(21)
(0.121095, 0.120512)	0.4140(61)	0.4510(58)	0.4690(37)	0.4971(21)
(0.121145, 0.120413)	0.4016(89)	0.4507(65)	0.4761(39)	0.5092(19)

Table 22: The results for the octet baryons: aM_N, aM_Λ, aM_Σ and aM_Ξ for $(\beta, c_{sw}, \alpha) = (5.50, 2.65, 0.1)$ where $\kappa_0 = 0.12090$.

(κ_l, κ_s)	aM_Δ	aM_{Σ^*}	aM_{Ξ^*}	aM_Ω
		$16^3 \times 32$		
(0.121040, 0.120620)	0.7437(227)	0.7490(184)	0.7537(146)	0.7595(114)
		$24^3 \times 48$		
(0.120830, 0.121040)	0.5906(73)	0.5801(89)	0.5685(114)	0.5548(151)
(0.120900, 0.120900)	0.5933(88)	0.5933(88)	0.5933(88)	0.5933(88)
(0.120950, 0.120800)	0.5817(55)	0.5895(48)	0.5973(43)	0.6050(38)
(0.121000, 0.120700)	0.5883(101)	0.6006(77)	0.6133(61)	0.6262(51)
(0.121040, 0.120620)	0.5483(137)	0.5679(90)	0.5902(64)	0.6108(48)
		$32^3 \times 64$		
(0.120900, 0.120900)	0.5675(64))	0.5675(64)	0.5675(64)	0.5675(64)
(0.121040, 0.120620)	0.5520(79)	0.5744(48)	0.5968(34)	0.6194(28)
(0.121095, 0.120512)	0.5161(185)	0.5541(98)	0.5812(52)	0.6104(33)
(0.121145, 0.120413)	0.5071(211)	0.5576(105)	0.6018(51)	0.6420(29)

Table 23: The results for the decuplet baryons: aM_Δ, aM_{Σ^*}, aM_{Ξ^*} and aM_Ω for $(\beta, c_{sw}, \alpha) = (5.50, 2.65, 0.1)$ where $\kappa_0 = 0.12090$.

(κ_l, κ_s)	aM_π	aM_K	aM_{η_s}
	$24^3 \times 48$		
(0.120920, 0.120920)	0.1694(9)	0.1694(9)	0.1694(9)
	$32^3 \times 64$		
(0.121050, 0.120661)	0.1280(6)	0.1813(5)	0.2221(4)

Table 24: The results for the pseudoscalar octet mesons: aM_π, aM_K and aM_{η_s} for $(\beta, c_{sw}, \alpha) = (5.50, 2.65, 0.1)$ where $\kappa_0 = 0.12092$.

(κ_l, κ_s)	aM_ρ	aM_{K^*}	aM_{ϕ_s}
	$24^3 \times 48$		
(0.120920, 0.120920)	0.3404(44)	0.3404(44)	0.3404(44)
	$32^3 \times 64$		
(0.121050, 0.120661)	0.3161(38)	0.3354(22)	0.3564(16)

Table 25: The results for the vector octet mesons: aM_ρ, aM_{K^*} and aM_{ϕ_s} for $(\beta, c_{sw}, \alpha) = (5.50, 2.65, 0.1)$ where $\kappa_0 = 0.12092$.

(κ_l, κ_s)	aM_N	aM_Λ	aM_Σ	aM_Ξ
$24^3 \times 48$				
(0.120920, 0.120920)	0.4725(39)	0.4725(39)	0.4725(39)	0.4725(39)
$32^3 \times 64$				
(0.121050, 0.120661)	0.4127(42)	0.4444(35)	0.4580(31)	0.4798(22)

Table 26: The results for the octet baryons: aM_N, aM_Λ, aM_Σ and aM_Ξ for $(\beta, c_{sw}, \alpha) = (5.50, 2.65, 0.1)$ where $\kappa_0 = 0.12092$.

(κ_l, κ_s)	aM_Δ	aM_{Σ^*}	aM_{Ξ^*}	aM_Ω
$24^3 \times 48$				
(0.120920, 0.120920)	0.5790(97)	0.5790(97)	0.5790(97)	0.5790(97)
$32^3 \times 64$				
(0.121050, 0.120661)	0.5457(108)	0.5607(72)	0.5800(51)	0.6005(40)

Table 27: The results for the decuplet baryons: aM_Δ, aM_{Σ^*}, aM_{Ξ^*} and aM_Ω for $(\beta, c_{sw}, \alpha) = (5.50, 2.65, 0.1)$ where $\kappa_0 = 0.12092$.

(κ_l, κ_s)	M_ρ/X_ρ	M_{K^*}/X_ρ	M_{ϕ_s}/X_ρ
$24^3 \times 48$			
(0.120830, 0.121040)	1.025(2)	0.9877(12)	0.9470(155)
(0.120900, 0.120900)	1.0	1.0	1.0
(0.120950, 0.120800)	0.9859(22)	1.007(1)	1.028(6)
(0.121000, 0.120700)	0.9706(34)	1.015(2)	1.057(12)
(0.121040, 0.120620)	0.9581(60)	1.021(3)	1.086(12)
$32^3 \times 64$			
(0.120900, 0.120900)	1.0	1.0	1.0
(0.121040, 0.120620)	0.9488(50)	1.026(3)	1.102(6)
(0.121095, 0.120512)	0.9392(63)	1.030(3)	1.124(7)
(0.121145, 0.120413)	0.9431(109)	1.028(5)	1.140(9)

Table 28: Ratio results for the vector octet mesons: M_ρ/X_ρ, M_{K^*}/X_ρ and M_{ϕ_s}/X_ρ for $(\beta, c_{sw}, \alpha) = (5.50, 2.65, 0.1)$ where $\kappa_0 = 0.12090$.

(κ_l, κ_s)	M_N/X_N	M_Λ/X_N	M_Σ/X_N	M_Ξ/X_N
$24^3 \times 48$				
(0.120830, 0.121040)	1.033(2)	1.009(6)	0.9949(13)	0.9717(26)
(0.120900, 0.120900)	1.0	1.0	1.0	1.0
(0.120950, 0.120800)	0.9769(33)	0.9887(84)	1.005(1)	1.018(3)
(0.121000, 0.120700)	0.9543(32)	0.9885(77)	1.008(2)	1.038(3)
(0.121040, 0.120620)	0.9319(56)	1.004(7)	1.011(2)	1.058(4)
$32^3 \times 64$				
(0.120900, 0.120900)	1.0	1.0	1.0	1.0
(0.121040, 0.120620)	0.9229(47)	0.9833(58)	1.016(2)	1.061(4)
(0.121095, 0.120512)	0.8999(77)	0.9804(111)	1.019(4)	1.081(8)
(0.121145, 0.120413)	0.8688(118)	0.9949(130)	1.030(5)	1.101(8)

Table 29: Ratio results for the octet baryons: M_N/X_N, M_Λ/X_N, M_Σ/X_N and M_Ξ/X_N for $(\beta, c_{sw}, \alpha) = (5.50, 2.65, 0.1)$ where $\kappa_0 = 0.12090$.

(κ_l, κ_s)	M_Δ/X_Δ	M_{Σ^*}/X_Δ	M_{Ξ^*}/X_Δ	M_Ω/X_Δ
$24^3 \times 48$				
(0.120830, 0.121040)	1.021(6)	1.003(2)	0.9824(44)	0.9588(121)
(0.120900, 0.120900)	1.0	1.0	1.0	1.0
(0.120950, 0.120800)	0.9868(14)	1.0002(3)	1.013(2)	1.026(3)
(0.121000, 0.120700)	0.9790(42)	0.9993(24)	1.020(6)	1.042(8)
(0.121040, 0.120620)	0.9634(72)	0.9978(53)	1.037(11)	1.073(14)
$32^3 \times 64$				
(0.120900, 0.120900)	1.0	1.0	1.0	1.0
(0.121040, 0.120620)	0.9609(44)	0.9999(28)	1.039(7)	1.078(9)
(0.121095, 0.120512)	0.9426(120)	1.012(10)	1.062(19)	1.115(24)
(0.121145, 0.120413)	0.9185(145)	1.010(13)	1.090(23)	1.163(29)

Table 30: Ratio results for the decuplet baryons: M_Δ/X_Δ, M_{Σ^*}/X_Δ, M_{Ξ^*}/X_Δ and M_Ω/X_Δ for $(\beta, c_{sw}, \alpha) = (5.50, 2.65, 0.1)$ where $\kappa_0 = 0.12090$.

References

[1] W. Bietenholz, V. Bornyakov, N. Cundy, M. Göckeler, R. Horsley, A. D. Kennedy, W. G. Lockhart, Y. Nakamura, H. Perlt, D. Pleiter, P. E. L. Rakow, A. Schäfer, G. Schierholz, A. Schiller, H. Stüben and J. M. Zanotti, [QCDSF–UKQCD Collaboration], *Phys. Lett.* **B690** (2010) 436 [arXiv:1003.1114[hep-lat]].

[2] M. Göckeler, R. Horsley, A. C. Irving, D. Pleiter, P. E. L. Rakow, G. Schierholz and H. Stüben, [QCDSF–UKQCD Collaboration], *Phys. Lett.* **B639** (2006) 307 [arXiv:hep-ph/0409312].

[3] P. E. L. Rakow, *Nucl. Phys. Proc. Suppl.* **140** (2005) 34 [arXiv:hep-lat/0411036].

[4] A. Skouroupathis and H. Panagopoulos, *Phys. Rev.* **D76** (2007) 094514 [arXiv:0707.2906[hep-lat]]; Erratum-ibid. **D78** (2008) 119901.

[5] A. Skouroupathis and H. Panagopoulos, *Phys. Rev.* **D79** (2009) 094508 [arXiv:0811.4264[hep-lat]].

[6] P. W. Atkins, M. S. Child and C. S. G. Phillips, *Tables for Group Theory*, Oxford University Press, 1970.

[7] M. Gell-Mann, *Phys. Rev.* **125** (1962) 1067.

[8] S. Okubo, *Prog. Theor. Phys.* **27** (1962) 949.

[9] W. Pfeifer, *The Lie Algebras su(N), An Introduction*, Birkhäuser, Basel, 2003.

[10] W. Greiner and B. Müller, *Quantum Mechanics: Symmetries*, Springer, 1989.

[11] S. Capitani, M. Göckeler, R. Horsley, P. E. L. Rakow and G. Schierholz, *Phys. Lett.* **B468** (1999) 150 [arXiv:hep-lat/9908029].

[12] T. Bhattacharya, R. Gupta, W. Lee, S. R. Sharpe and J. M. S. Wu, *Phys. Rev.* **D73** (2006) 034504 [arXiv:hep-lat/0511014].

[13] S. Coleman and S. L. Glashow, *Phys. Rev. Lett.* **6** (1961) 423.

[14] V. Fanti *et al.* [NA48 Collaboration], *Eur. Phys. J.* **C12** (2000) 69.

[15] E. E. Jenkins and R. F. Lebed, *Phys. Rev.* **D62** (2000) 077901 [arXiv:hep-ph/0005038].

[16] J. J. Dudek, R. G. Edwards, B. Joó, M. J. Peardon, D. G. Richards and C. E. Thomas, *Phys. Rev.* **D83** (2011) 111502 [arXiv:1102.4299].

[17] K. Nakamura *et al.* (Particle Data Group), *J. Phys.* **G37** (2010) 075021.

[18] QCDSF–UKQCD Collaboration, ('Partially Quenching with $2+1$ Flavours', in preparation).

[19] S. Aoki, K.-I. Ishikawa, N. Ishizuka, T. Izubuchi, D. Kadoh, K. Kanaya, Y. Kuramashi, Y. Namekawa, M. Okawa, Y. Taniguchi, A. Ukawa, N. Ukita and T. Yoshié, [PACS-CS Collaboration], *Phys. Rev.* **D79** (2009) 034503 [arXiv:0807.1661[hep-lat]].

[20] H.-W. Lin, S. D. Cohen, J. Dudek, R. G. Edwards, B. Joó, D. G. Richards, J. Bulava, J. Foley, C. Morningstar, E. Engelson, S. Wallace, K. J. Juge, N. Mathur, M. J. Peardon and S. M. Ryan, [HS Collaboration], *Phys. Rev.* **D79** (2009) 034502 [arXiv:0810.3588[hep-lat]].

[21] A. Walker-Loud, *Nucl. Phys.* **A747** (2005) 476 [arXiv:hep-lat/0405007].

[22] B. C. Tiburzi and A. Walker-Loud, *Nucl. Phys.* **A748** 513 (2005) 513 [arXiv:hep-lat/0407030].

[23] C. Allton, D. J. Antonio, Y. Aoki, T. Blum, P. A. Boyle, N. H. Christ, S. D. Cohen, M. A. Clark, C. Dawson, M. A. Donnellan, J.M. Flynn, A. Hart, T. Izubuchi, A. Jüttner, C. Jung, A. D. Kennedy, R. D. Kenway, M. Li, S. Li, M. F. Lin, R. D. Mawhinney, C. M. Maynard, S. Ohta, B. J. Pendleton, C. T. Sachrajda, S. Sasaki, E. E. Scholz, A. Soni, R. J. Tweedie, J. Wennekers, T. Yamazaki and J. M. Zanotti, [RBC–UKQCD Collaboration], *Phys. Rev.* **D78** (2008) 114509 [arXiv:0804.0473[hep-lat]].

[24] N. Cundy, M. Göckeler, R. Horsley, T. Kaltenbrunner, A. D. Kennedy, Y. Nakamura, H. Perlt, D. Pleiter, P. E. L. Rakow, A. Schäfer, G. Schierholz, A. Schiller, H. Stüben and J. M. Zanotti, [QCDSF–UKQCD Collaboration], *Phys. Rev.* **D79** (2009) 094507 [arXiv:0901.3302[hep-lat]].

[25] Y. Nakamura and H. Stüben, *PoS(Lattice 2010)* **040** arXiv:1011.0199[hep-lat].

[26] M. Lüscher, S. Sint, R. Sommer and P. Weisz, *Nucl. Phys.* **B478** (1996) 365 [arXiv:hep-lat/9605038].

[27] T. Bakeyev, M. Göckeler, R. Horsley, D. Pleiter, P. E. L. Rakow, G. Schierholz and H. Stüben, *Phys. Lett.* **B580** (2004) 197 [arXiv:hep-lat/0305014].

[28] C. R. Allton, C. T. Sachrajda, R. M. Baxter, S. P. Booth, K. C. Bowler, S. Collins, D. S. Henty, R. D. Kenway, B. J. Pendleton, D. G. Richards, J. N. Simone, A. D. Simpson and B. E. Wilkes, *Phys. Rev.* **D47** (1993) 5128, [arXiv:hep-lat/9303009].

[29] C. Best, M. Göckeler, R. Horsley, E.-M. Ilgenfritz, H. Perlt, P. Rakow, A. Schäfer, G. Schierholz, A. Schiller and S. Schramm, *Phys. Rev.* **D56** (1997) 2743, [arXiv:hep-lat/9703014].

[30] A. Billoire, E. Marinari and R. Petronzio, *Nucl. Phys.* **B251[FS13]** (1985) 141.

[31] M. Göckeler, R. Horsley, M. Ilgenfritz, H. Perlt, P. Rakow, G. Schierholz and A. Schiller, *Nucl. Phys. Proc. Suppl.* **42** (1995) 337 [arXiv:hep-lat/9412055].

[32] M. Göckeler, R. Horsley, D. Pleiter, P. E. L. Rakow and G. Schierholz, *Phys. Rev.* **D71**(2005) 114511 [arXiv:hep-ph/0410187].

[33] G. Colangelo, S. Dürr and C. Haefeli, *Nucl. Phys.* **B721** (2005) 136 [arXiv:hep-lat/0503014].

[34] A. Ali Khan, T. Bakeyev, M. Göckeler, T. R. Hemmert, R. Horsley, A. C. Irving, B. Joó, D. Pleiter, P. E. L. Rakow, G. Schierholz and H. Stüben, *Nucl. Phys.* **B689** (2004) 175 [arXiv:hep-lat/0312030].

[35] S. R. Beane, K. Orginos and M. J. Savage, [NPLQCD Collaboration], *Phys. Lett.* **B654** (2007) 20 [arXiv:hep-lat/0604013].

[36] L. Burakovsky and J. T. Goldman, arXiv:hep-ph/9708498.

[37] QCDSF–UKQCD Collaboration, ('Flavour Breaking effects in Hadronic Matrix Elements', in preparation).

[38] M. Göckeler, Ph. Hägler, R. Horsley, Y. Nakamura, D. Pleiter, P. E. L. Rakow, A. Schäfer, G. Schierholz, H. Stüben, F. Winter and J. M. Zanotti, [QCDSF–UKQCD Collaboration], *PoS(Lattice 2010)* **165** arXiv:1101.2806[hep-lat].

[39] M. Göckeler, Ph. Hägler, R. Horsley, Y. Nakamura, D. Pleiter, P. E. L. Rakow, A. Schäfer, G. Schierholz, H. Stüben, F. Winter and J. M. Zanotti, [QCDSF–UKQCD Collaboration], *PoS(Lattice 2010)* **163** arXiv:1102.3407[hep-lat].

[40] R. Horsley, Y. Nakamura, D. Pleiter, P. E. L. Rakow, G. Schierholz, H. Stüben, A. W. Thomas, F. Winter, R. D. Young and J. M. Zanotti, [CSSM and QCDSF–UKQCD Collaborations], *Phys. Rev.* **D83** (2011) 051501 [arXiv:1012.0215].

[41] P. A. Boyle, *Comp. Phys. Comm.* **180** (2009) 2739.

[42] S. Gasiorowicz, *Elementary Particle Physics*, John Wiley & Sons, New York, 1966.

[43] C. Morningstar and M. J. Peardon, *Phys. Rev.* **D69** (2004) 054501 [arXiv:hep-lat/0311018].

[44] R. Horsley, H. Perlt, P. E. L. Rakow, G. Schierholz and A. Schiller, QCDSF Collaboration, *Phys. Rev.* **D78** (2008) 054504 [arXiv:0807.0345[hep-lat]].